A Population Model of Vasopressin Secretion

Ruth Durie

Doctor of Philosophy

Institute for Adaptive and Neural Computation

School of Informatics

University of Edinburgh

2008

Abstract

Computer modelling is a powerful tool for clarifying and testing theory. In neuroscience, this often means replicating firing patterns. Models need evaluation functions to quantify the significance of features in the firing patterns, but usually the effect of firing is insufficiently understood.

The magnocellular vasopressin neurons of the hypothalamus do have an output that is both well understood and quantifiable: they secrete a hormone into the bloodstream in proportion to blood osmolarity and volume, regulating these properties within a narrow physiologically acceptable range. This response of vasopressin secretion to osmotic pressure must be maintained to defend blood pressure. The neurons display a distinctive phasic firing pattern, which a model was developed to mimic. A further, unique step was then taken of extending this model by developing a model for the effect of firing, a stimulus-secretion model. The firing pattern model and stimulus secretion model were then linked and then noisily duplicated to produce a population. This population had a measurable performance - secretion - allowing evaluation of the model in a novel fashion.

The population could replicate the secretory response to osmotic pressure observed *in vivo*. It is possible to test the effect of features by incorporating them into the model and observing the response. A demonstration of this was conducted by changing the mix of excitatory and inhibitory PSPs, showing that inhibition was necessary for an efficient response. Effective techniques may well be reused elsewhere in the brain, so exploring their significance in a simple system may allow understanding of more complex ones.

This project has constructed a model from firing to effect, offering novel possibilities for quantification and therefore evaluation. The main outcomes from this work are construction of a simple model system in which features can be benchmarked; that a integrate and fire model modified to include bistability can explain the firing of vasopressin neurons; that secretion could well also be controlled by a pool structure, similar to other secretory systems and that a population of these cells can produce a linear output. It has also confirmed that balanced excitatory and inhibitory input is necessary for the most efficient response. It shows that population performance is a trade-off between maximising efficiency, maintaining the secretory response over a wide dynamic range and maximising the maximum achievable secretion rate.

Acknowledgements

To my parents, for endless support, my supervisors Pfs Gareth Leng and David Willshaw, for endless guidance and from whom I learnt a lot and my cat for complete obliviousness. I'd also like to thank Andrea for the many cups of tea and Pat for reminding me to write.

Declaration

I declare that this thesis was composed by myself, that the work contained herein is my own except where explicitly stated otherwise in the text, and that this work has not been submitted for any other degree or professional qualification except as specified.

(*Ruth Durie*)

Table of Contents

List of Figures

List of Tables

Chapter 1

Introduction

1.1 Introduction

This is a thesis about testing models, and through them the importance of theories.

Modelling is performed to clarify theory, to rigorously explore the implications of the theory as implemented and usually then to make some predictions from the theory to stimulate experiment. Typically the predictions at neuronal level involve changes in firing pattern, and nothing further as the system under investigation usually feeds to a different region of the brain, with only a vague idea of the high level purpose of the system. This makes it very difficult to extrapolate from the neuronal firing patterns how well they do what they're doing, and to know which features are important for functioning as opposed to evolutionary fluke.

Vasopressin neurons, however, have a clearly understood, quantifiable function. It is also life-critical; they must regulate plasma osmotic pressure[1]and volume by secreting arginine vasopressin into the bloodstream. Secretion is directly stimulated by firing, and then acts on the kidneys to instruct them to retain water. They therefore present a unusual opportunity for modelling, as the cell's functioning can be linked to its purpose and evaluated. This thesis will demonstrate this.

The challenge vasopressin cells must solve is, in the abstract, a common one: homoeostatic regulation of two adversely interacting quantities. By understanding the effectiveness of the techniques vasopressin neurons use, we can hope ultimately to understand whether evolution has fine tuned the system, and which mechanisms were

[1]Osmotic pressure is the pressure due to water movement between compartments separated by a semi-permeable membrane. Water will move to equalise solute concentration, ie to higher concentration compartments. It is osmotic pressure that causes injections of water into the bloodstream to be fatal, as osmotic pressure causes red blood cells to absorb the water, swelling them to bursting point.

effective.

This thesis begins with a summary of the physiological significance of vasopressin neurons. It will then continue with an outline of the project goals. Chapter 2 covers the methods used, with chapter 3 reviewing of vasopressin neurons at a functional level: it will cover the experimental evidence available for model verification. Chapter 4 then describes the evolution of a model to meet these aims.

A model of firing pattern generation is conventional in modelling terms: extending it to mimic the effect of firing is not. A second model of stimulus-secretion coupling is presented in chapter 5: it is this that translates the activity into meaningful output. This is then duplicated in a noisy fashion to construct a population of cells (Chapter 6): the output from this population is evaluated under different conditions.

The vasopressin system is critical for life: this chapter begins by summarising some of its key properties, as this is necessary to understand the tests that could be imposed on the model.

1.2 Vasopressin and the Renal System

The kidneys are responsible for filtering waste from the bloodstream. They also control the resorption rate of water into the bloodstream, responding to levels of arginine vasopressin (AVP). Vasopressin neurons secrete AVP in response to changes in plasma osmotic pressure and volume to instruct the kidneys to retain water (AVP is therefore also referred to as anti-diuretic hormone, or ADH). This contributes a crucial feedback to the kidneys.

A brief overview of the functioning of the renal system, and the properties - blood osmolarity and volume - relevant to AVP is provided.

1.2.1 The renal system

The renal system has an extensive range of functions and regulators, and to explain its full functioning would require knowledge of several hormonal signalling systems (including the renal-angiotensin system, aldosterone and atrial natriuretic peptide). It was proposed to model the simplest possible subset of the system that captures the essence of an interesting regulatory problem - defending plasma volume and osmolarity. Plasma osmolarity is the concentration of particles osmotically sensitive - ie small enough to diffuse through a membrane and sensitive to concentration - measured in

osmoles per litre solute.

Plasma volume is affected by water balance. Water is absorbed from food and drink; it is lost through sweat and surfaces (skin and lungs), through the digestive system and also though urine. Water intake is usually controllable, but of the sources of water loss only the urinary loss can be modified by the kidney.

Oddly, the body has no water pump: the kidney controls the resorption rate of water back into the bloodstream by a combination of water channels and osmotic pressure. For purposes here, it is sufficient to know the kidney is extremely efficient. In extremis, it can reduce water loss to as little as a tablespoon an hour, and processes at a rate such that "if reabsorption of water ceased but filtration continued the total plasma water would be urinated within 30 minutes" [109]. At the opposite extreme, the kidneys can eliminate as much as 25 litres a day of water from the bloodstream.

Sodium is a major component in blood osmolarity and is the one primarily affected by food intake. Sodium pumps do exist, so the kidneys can expel sodium from the bloodstream and does so in response to aldosterone levels dropping. Intake is entirely from food, and can vary 500 fold (from 50mg to 25g a day) [109]. Loss is by excretion though sweat or urine. Sodium balance can be maintained independently by this system. Disturbances in blood sodium concentration are due to abnormalities in water balance.

This is because blood osmolarity and volume can interact adversely. Under stress conditions, a choice can be forced between defending one at the expense of another. For example, in hemorrhage conditions, blood volume and pressure drop rapidly. The kidneys will then retain water, maintaining blood volume at the cost of osmolarity.

1.2.2 Threats

Threats to the system are caused by either property - blood volume or sodium levels - being either too high or too low. They may be due to disease or abnormal function - these will be covered later - or disruption of environmental conditions.

The clinical conditions are summarised in table 1.1, with possible causes (these are by no means exhaustive). Several conditions, such as dehydration and sweating, can cause different conditions depending on relative rates of loss of sodium and water. For example, hyponatraemia is sometimes seen in marathon runners who have replaced fluid loss by drinking water, but have not replaced lost sodium. These threats can of course be intertwined due to common cause: for example often losses occur simultane-

Condition	Possible causes
hyponatraemia (low blood sodium)	Intake: salt free diet (rare), excess water intake (water intoxication): eg caused by ecstasy abuse or polydipsia (excess thirst) Output: inappropriate retention of water (pathological, eg SIADH), increased loss (hypoaldostereonism)
hypernatraemia (high blood sodium)	Intake: insufficient water due to thirst deficit or drought, high salt: salt poisoning Output: water loss (usually with insufficient intake) due to renal failure, diabetes insipidus, dehydration
hypovolaemia (low blood volume)	Intake: dehydration Output: Dehydration (sweating), Vomiting, Diarrhoea, hemorrhage
hypervolaemia (high blood volume)	Intake (unlikely) water intoxication, diabetes insipidus Output: renal failure

Table 1.1: Summary of clinical conditions and main causes

ously, such as in hemorrhage, vomiting or diarrhoea. Control of antidiuretic hormone must be appropriately sensitive to both.

1.2.3 AVP Secretion in Response to Threats

AVP is secreted into the bloodstream from the posterior pituitary and instructs the kidneys to reabsorb water into the bloodstream. AVP release increases linearly relative to plasma osmolarity over a remarkably large range [9] [2]and (less sensitively) blood volume depletion (Figure 1.1). The system is very sensitive, responding to changes in blood osmolarity of as little as 1%. See [93] for a recent review of normal and disfunctional AVP secretion.

[2]Osmolality is a measurement of solute per kg of solvent, whereas osmolarity is a measure of solvent per litre of solution. In blood plasma under most circumstances osmolality is about 6% greater than osmolarity, ie usually comparable

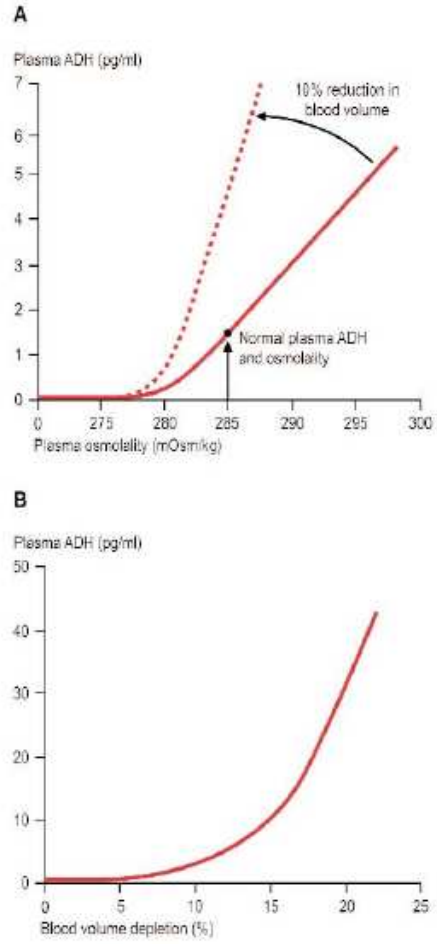

Figure 1.1: AVP secretion in response to a) osmolality b) blood volume loss (from [32])

Once in the bloodstream, AVP spreads quickly throughout the blood plasma and extracellular fluid, but is cleared or degraded quickly.

But why a proportionate response to chronic dehydration? There is a lag in the system introduced by the kidney's response time: a disproportionate response could anticipate future need. Two theories suggested [65] are that the cost of secretion is high enough for the system to attempt to conserve its resources, or that the lag in the system means a proportional response is necessary to prevent significant overshoot. Certainly conventional wisdom in control theory is that lag is a significant problem as the system has to anticipate future changes in the variables it is reacting to rather than using their current values, or it risks undoing changes still in motion. Here, lag is introduced by the digestive process (for introduction of water and sodium) and the response time of the kidneys. The system may oscillate if overcorrected: this could be wasteful of fluid and sodium, and therefore a slow correction is preferred.

The set point for the system is clearly the point where no AVP response is needed: blood osmolarity will be maintained at that level. This varies between individuals, and can be altered (eg due to pregnancy, disease or trauma), though the system is fairly robust and natural variations in thirst and AVP release occur between individuals.

Thirst is not caused by vasopressin, but shares many (although not all, and not at the same levels) of the same triggers [107]. AVP levels are too slow a feedback to inhibiting thirst; instead signals from somewhere in the throat-stomach-gut connection inhibit thirst depending on species.

1.2.3.1 Diseases and System Failures

Serious consequences can be incurred by loss of sharpness of response of AVP (see [93] for review), ie where too little vasopressin is secreted in response to osmotic pressure, either throughout a range or after a certain point. Two of the major clinical conditions are diabetes insipidus and Syndrome of Inappropriate Antidiuretic Hormone (SIADH).

Subdued vasopressin response results in the syndrome diabetes insipidus. The lack of antidiuretic hormone results in water loss in urine: thus the syndrome is characterised by large amounts of urine excretion and extraordinary thirst, as the sufferer must replenish water. The loss of response is due to destruction of the magnocellular neurons by trauma, infection, or genetic flaw. An animal model, the famed Brattleboro rat, exists with a hereditary diabetes insipidus.

Excessive vasopressin is seen in SIADH. Hyponatraemia results, as the urine is incorrectly concentrated. It is usually due to malformation of the system - either congenital, or acquired due to cancer, injury or infection.

Other conditions exist, such as primary polydipsa or excessive fluid intake. Common causes are as diverse as schizophrenia, head trauma and “irrational beliefs, usually involving the health benefits of a high water intake”! [93].

1.2.4 Anatomy

In this work, the vasopressin cells referred to are always the magnocellular vasopressin secreting cells of the paraventricular (PVN) and supraoptic nuclei (SON). These contain around half of the vasopressin neurons projecting to the pituitary: the lesser studied others are in the “accessory nuclei” [39].

The PVN and SON are located in the hypothalamus: from there, projections stretch

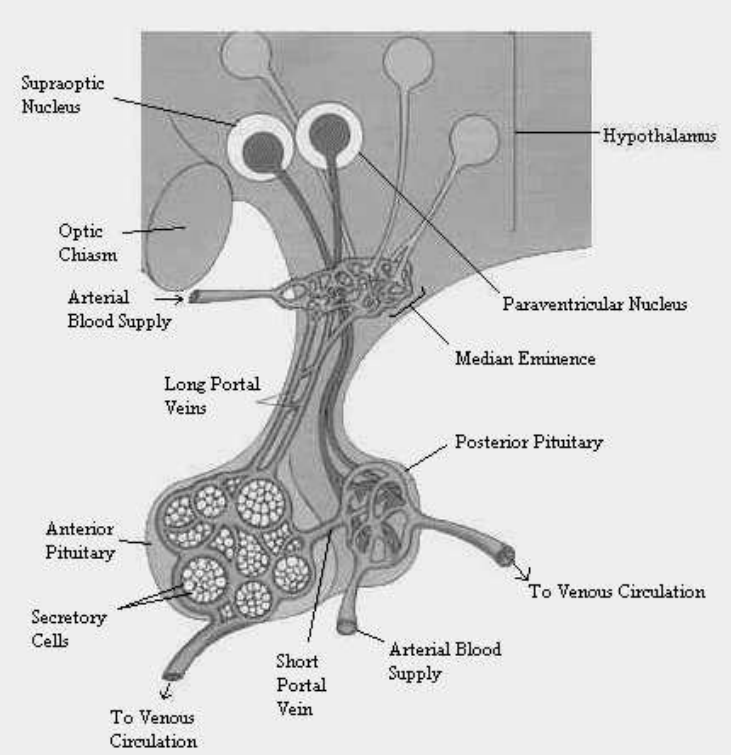

Figure 1.2: Anatomy of the hypothalamus and pituitary (from [15])

to the pituitary gland (Figure 1.2). The hypothalamus is located within the blood brain barrier, but the SON and PVN are densely vascularized. A rise in blood plasma osmolarity will cause water to drain by osmotic pressure from the extracellular fluid into these vessels. The osmolarity of the extracellular fluid increases accordingly until osmotic pressure equalises, and will therefore closely echo that of the blood plasma. Vasopressin cells are osmosensitive, and changes in the osmolarity of the compartment are detected.

Other structures feeding to the SON and PVN have been determined using anterograde and retrograde tracers in rats. Two significant areas are the organum vasculosum of the lamina terminalis (OVLT) and the subfornical organ (SFO) which lie outside the blood-brain barrier and therefore sensitive to changes of hormones in the bloodstream. Other areas, such as the nucleus medianus also show a rise in activity when osmolarity rises, leading these areas together to be labelled the osmoregulatory complex.

1.2.4.1 Experimental Identification

Magnocellular cells can be identified by antidromic stimulation of the neural stalk (evoking action potentials that return with a constant latency) or by excluding those with a resting potential below -50mV, action potential magnitude exceeding 60mV and input resistance greater than 150MΩ ([20]) and then looking for evidence of an 'A' current and spike broadening.

Techniques for identifying vasopressin neurons, particularly from magnocellular oxytocin neurons [3], have been refined since the experiments of the 1980s when either intracellular fills or functional differentiation (usually a stimulus to firing such as milk ejection which was hoped to be exclusive to oxytocin neurons) were used [6]. There is a general assumption that cells firing continuously are probably oxytocin and those firing phasically are almost certainly vasopressin ([6, 87]), but where further surety is required other stimuli, such as cholecystokinin (CCK), can be used to evoke differing responses (eg see [97]).

1.3 Modelling and Neuroscience

Since Hodgkin and Huxley, modelling has expanded to every area of neuroscience. Models force thorough examination of a hypothesis, and exposes the implications of a theory. As such, they have become a popular method for directing research although there is still no formal process for designing or evaluating models. There is informal consensus that the following traits are desirable in a model

1. Replicate the available data. If a model can replicate existing data, it confirms the underlying theory can explain the workings of the system.

2. Simplicity. The more complex the model, the harder it is to understand and analyse; it is also more difficult to avoid over-fitting the data. In general, the fewer parameters the better.

3. Robustness. The model should not be forced into unrealistic behaviour due to variations in the parameter space. Clearly, this is closely related to simplicity.

4. Make predictions. As a model with a sufficiently large number of parameters will fit any data, the test for modellers has always been to make experimental

[3] Infrequently, magnocellular neurons are found that appear to synthesise both vasopressin and oxytocin or neither.

predictions.

5. Realistic. Ideally, the mechanisms used in the model should reflect the capabilities of the underlying biology, or plausible guesses about functioning. It should be clear why the model has been designed as it has. Note that too much attention to detail can bring this into conflict with robustness.

Most of these criteria are difficult to quantify, and attempts are generally restricted to a subfield (eg cognition [83]). Different modellers may place different emphasis on the criteria, and so the idea of how good a model is remains informal.

Matters are further complicated that multiple solutions may exist in the biology. A recent excellent piece of work in the Marder lab [89] modelled the patterns generated by the simple neuronal circuit in the crustacean stomatogastric ganglion.

They used three neurons. However, instead of using a search algorithm to tune their parameters for the pattern wanted they quantised their possible synaptic strengths to 5 or 6 values and then searched all possible resulting networks. For good measure, they also allowed different neuron models to be used.

The resulting combinatorial explosion (around 20 million networks to simulate!) could only be dealt with because the network model was kept simple. The results were intriguing: they saw not only a range of behaviours to match those observed biologically, but also found that "virtually indistinguishable network activity can arise from widely disparate sets of underlying mechanisms" [89].

The novelty of this approach is the thoroughness of the exploration of the parameter space. Usually the parameter space is too large: it is possible to use a search algorithm to try and find multiple solutions but this is time consuming and modellers are usually looking for an optimum solution. This is the first attempt to quantify how much variability a circuit could potentially withstand.

Clearly homeostatic mechanisms can exploit this to compensate for variability caused by evolution and other factors. It also raises the intriguing possibility that sub-optimal solutions and extraneous factors useful in other cases are tolerable as long as the resulting solution is still good enough; thus much of the complexity seen in biological systems may not be significant all of the time. It also suggests homeostatic mechanisms can and do operate at network level.

Here, solutions were judged on their similarity to recorded *in vivo* firing patterns. The vasopressin network can be judged on the probable effectiveness of its secretory response, which raises the possibility of looking at how good 'good enough' has to be.

1.4 Aims

The physiological importance of vasopressin cells has been explained, along with some of their functioning. This project aims to provide a framework for evaluating computational theories, using the vasopressin system as an example. This will have the ability to quantify the computational effectiveness of different systems.

The main aim of this project was to replicate secretion from the system, allowing *evaluation* of the system in a way that is usually impossible in computational neuroscience. The ability to evaluate, rather than mimic and predict, increases the possibility of understanding why the system functions as it does and how mechanisms may have evolved.

The road map for this project went as follows:

1. **Create *in vivo* firing pattern model for vasopressin cells** Although previous models of *in vitro* firing exist, no *in vivo* model had been developed. Cells are damaged by the *in vitro* extraction procedure: they have fewer afferents. Experiments are also often conducted at room temperature rather than the *in vivo* range resulting in altered electrical properties.

2. **Stimulus secretion model** Secretion is stimulated by the cell firing, although this is counterbalanced by depletion of secretory resources organised into pools. After the firing of the cells has been modelled, it is necessary to link it to the secretion so the output can be evaluated. Again, no model of secretion from vasopressin cells was existent before this project.

3. **Replicate the secretory response of the system** By replicating the secretory response, we can hope to begin to understand the key influences upon it. Once a model of neuronal secretion has been constructed, it can be scaled up by duplication to form a network.

4. **Evaluate the effect of different factors** For example, how does changing the levels of inhibitory feedbacks alter the effectiveness of the system? Multiple inhibitory feedbacks such as IPSP rate and slower dendrosecretory processes exist to explore.

The next chapter deals with methods used, followed by a review of the relevant literature. The next chapters than deal with the developed models as above: the firing patterns model, stimulus secretion model and population model.

Chapter 2

Methods

2.1 Note on methods

This chapter contains all statistical definitions, classification schemes and important algorithms developed for the project, and is intended for reference.

All statistics are reported as means with standard deviations, except where otherwise noted.

2.2 Burst Processing

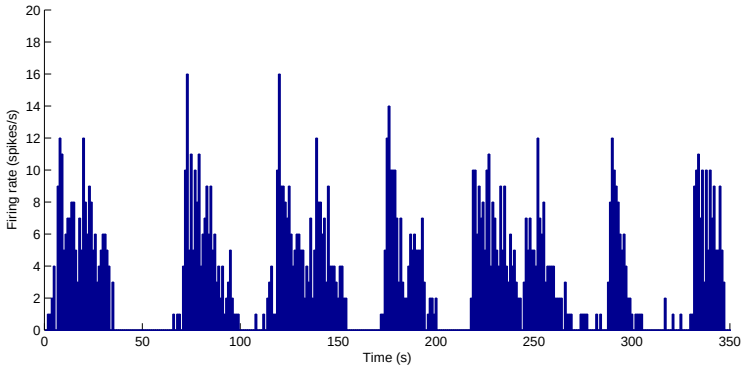

Figure 2.1: Example of a vasopressin cell firing *in vivo*: mean firing rate 3.06 $\pm$ 3.74 spikes/s (Data: personal communication from G. Leng). The cell is clearly firing phasically, it is not always clear if individual spikes should be counted as part of a burst.

Vasopressin cells display a distinctive phasic firing pattern (Figure 2.1), with a burst constituting a period of neural firing activity followed by a period of silence.

There is not an exact definition of what constitutes a burst. Firing behaviour is more of a continuum than a set of easily separable behaviours: even in a cell with a clearly distinguishable phasic pattern, short periods of firing or quiescence may occur. For example, Figure 2.1 shows fragmentation around bursts that is difficult to classify. The tail of the interspike intervals distribution can be fit with an exponential [97], so there is no clear cut-off point beyond which a spike can be considered isolated.

Early classification of patterns was subjective, depending on the description of the researcher involved. Computer processing became widespread: early algorithms for burst processing would calculate firing rates in second long blocks. For example, Wakerley et al. [112] considered a run of three non-zero blocks as marking the beginning of a burst: three zero blocks were likewise marked as a beginning of a silence. Everything between the beginning of a burst and the beginning of the following silence would be considered part of the burst: so silences under 3s could be absorbed into a burst and likewise bursts under 3s long would be absorbed into silences.

Precision has increased - ISIs are not processed as part of firing blocks - but the basic algorithm remains unchanged. The current proprietary standard is the bursts script in Spike2 (Spike2, CED Products). This was impractical for use in this project for a number of reasons, including platform availability and ease of importing and batch processing model generated data: however, a Matlab script was developed to be equivalent to Spike2 processing (see supplementary CD).

Bursts were categorised as follows: maximum intraburst interspike interval 1s, minimum burst length 3s, minimum silence length 3s, minimum spikes per burst 20. These are the same parameters used by Sabatier et al [97]. All periods were then classified into bursts and silences, with a classification rate: a high failure rate essentially indicates the behaviour is not recognisable as phasic firing, as many spikes have been classified as outside bursts. Examples of burst processing are in Figure 2.2.

2.3 Hazard Functions

The hazard function of an event is the probability of the event occurring during a time period as opposed to those succeeding it. For example, it is commonly used to calculate the probability of dying during a particular year given survival to the current age. Here, it is applied to the probability of a spike occurring. The hazard for a time period t, $h(t)$, is calculated from the histogram of the interspike intervals $n(t)$ by:

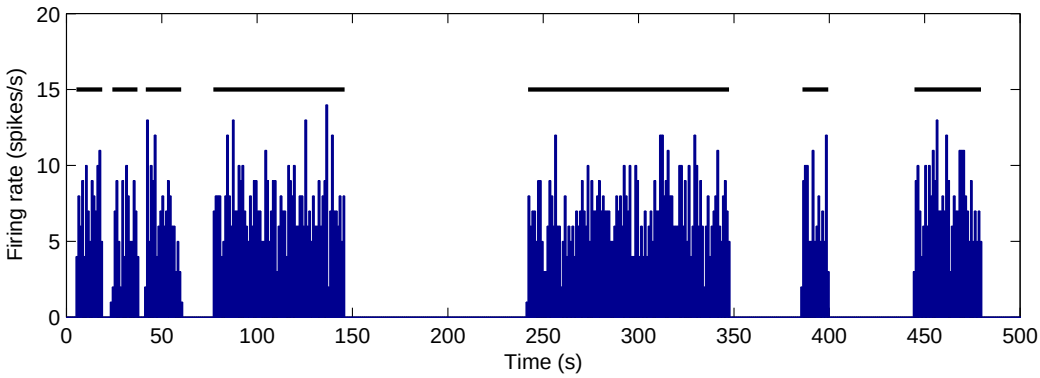

(a)

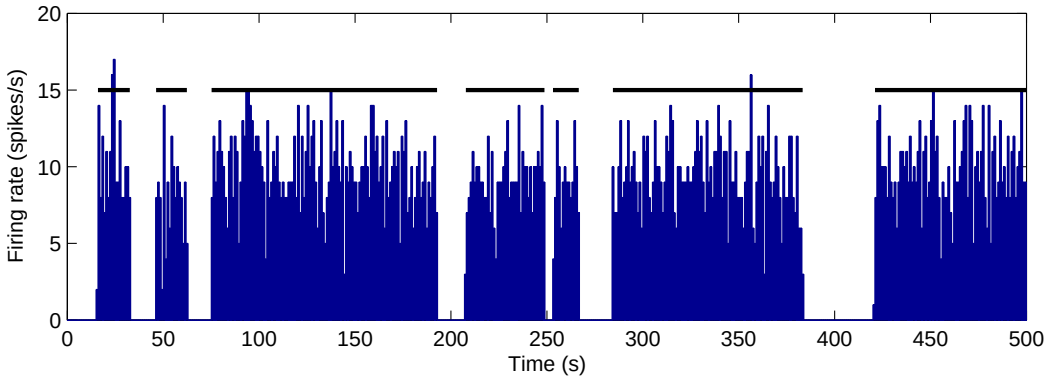

(b)

Figure 2.2: **Sample Burst processing** Two examples of generated firing patterns, with bursts marked in black after processing by the Matlab script. a) Mean firing rate here is 3.8 spikes/s. b) mean firing rate: 6.0 spikes/s

$$h(t) = \frac{n(t)}{\sum_{i=t}^{N} n(i)} \tag{2.1}$$

where N is the last bin in the histogram.

A process driven randomly by a Poisson process produces a flat hazard.

2.4 Cell Classification

Firing patterns are classified into the following firing types: silent, slow irregular, transitional, phasic and continuous. A previous scheme [86] used the variance to classify firing pattens, but was adapted here to use the activity quotient, Q, in line with most recent papers.

- Silent or very slow, mean firing rate $<$0.5spikes/sec
- Slow irregular, $<$1.5spikes/sec
- Transitional, $<$3spikes/sec and $>$1.5spikes/sec
- Phasic, $>$ 3 spikes/sec and Q$<$0.8
- Continuous, $>$3spikes/sec and Q$>$0.8

Q is the proportion of time spent in bursts, defined here as the sum of all ISIs under 2s divided by the total time.

2.5 Linear Regressions

Linear regressions are performed in Section 4.4.6. To be consistent with the original processing of the in vivo data, R^2 is calculated using Pearson's coefficients.

2.6 Curve fitting

MATLAB was used to fit multiple exponentials to hazard functions by least squares. When fitting hazard functions, the first few points tend to zero, and are therefore best ignored: the first point greater than 0.005 was usually used.

2.7 Implementation

Models were implemented in C++ on a workstation running RedHat Linux. Matlab (Version 6.5, MathWorks, Inc.) was used to interpret results. Several timesteps were usually tried to check the effect on the results (for example with the firing model, reducing the time step by a factor of 10 had no discernible effect on firing rate or phasic patterning). A gradient descent algorithm was on occasion used to search parameter space (Matlab's fminsearch function).

2.8 Significance tests: t-tests and ANOVA

When comparing two tests where the variance could reasonably be expected to be equal (eg from populations of cells generated with the same underlying parameter variations), unpaired t-tests are used or Wilcoxon ranksum test where variance may differ.

Significance for more than two groups is carried out by nonparametric ANOVA (matlab's kruskalwallis function): results are considered significant at $p < 0.05$, (or 5% significance).

2.9 Entropy

Statistical characterisations of vasopressin cells have generally focused on first order statistics (eg mean firing rate and variance, ISI histogram). This may miss higher order effects, such as the development of spike motifs in firing - repeated patterns of firing.

Entropy and mutual information have been suggested as alternative measures of information capacity in a cell by Bhumbra & Dyball [10]. Entropy will accurately measure the irregularity of a spike train; mutual information measured the information shared by neighbouring intervals, ie how much knowledge is conveyed by knowing the value of one interval about the other. Mutual information of zero means the intervals are independent, just as an entropy of zero indicates a regular, utterly predictable process.

Entropy is often used in terms of the maximum information a channel can encode; here, it could encode the maximum information an action potential could convey, although this is the *maximum* and action potentials (especially if the theory of stochastic resonance is correct) may be conveying little information in practice. However, it is

useful to have these measures available, especially when trying to divine the weight of non-deterministic factors (PSPs) to deterministic factors (depolarisation) as the authors have demonstrated [11].

Measuring entropy is itself nontrivial, as it relies on the description of the spike train. Bhumbra & Dyball suggest avoiding sensitivity to the bin size used by using a log transform of the ISIs [10]. Use of the log transform minimises influence of long intervals, which may otherwise have a disproportionate effect: they then fit the probability distribution with two Gaussians (to ensure the measure is continuous)and used that fit as the probability mass function to calculate the entropy. Measurement of the entropy was carried out using the software provided by Bhumbra and Dyball (Interlab, available from `http://www.pdn.cam.ac.uk/staff/dyball/interlab.html`).

Chapter 3

Literature Review

3.1 Introduction

Vasopressin cells have been extensively studied, due to their significance and easily located experimental location: there is therefore an extensive body of evidence to review. As the models produced must be computationally lightweight enough to be replicated to form a network, it is important to only include the minimum necessary for the desired results - but the simplifications must be as realistic as possible.

The key feature of vasopressin cells is phasic firing. The bulk of the experimental and computational work has been targeted towards this key feature. However, replicating the response to osmotic pressure required a range of firing patterns.

This section will first look at the firing patterns of the cells, and at the underlying currents. Evidence for secretory behaviour will be reviewed in Chapter 5.

3.2 Heterogeneity of patterning

Heterogeneity of firing in vasopressin cells was noted in some of the first surveys of different types of firing [112, 21]. Although there was general consensus that a range of non-phasic patterns could be seen, a formal definition of phasic was more difficult to define. Phasic patterns also varied wildly: see Figure 3.1.

The non-phasic patterns were generally classified as continuous or irregular firing. Irregular firing is seen only at low firing rates: continuous mostly at high (eg [9]). In physiological contexts, this can be seen as a continuum of behaviour: cells tend to be slow or silent initially and change into phasic and continuous firing under hyperosmotic conditions [9, 21, 112].

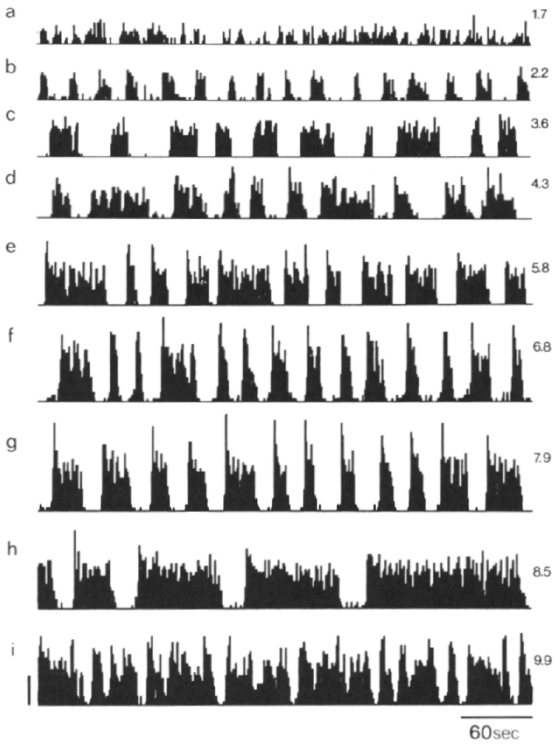

Figure 3.1: Example *in vivo* firing patterns (from [86]). Although the cell with lowest activity is firing in a slow irregular pattern, the others all fire phasically but with different periods and intraburst firing rate.

An early attempt to categorise firing patterns systematically using mean firing rate and the variance to mean ratio by Poulain *et al.* ([86]) also introduced a transitional category to further separate irregular and phasic firing. Another suggestion was to use the distribution of firing rates (measured per second): slow irregular cells have a relatively high proportion of zeros, with phasic cells having a bimodal distribution and continuous cells a unimodal distribution ([112]).

More recently, use of the activity quotient has increased (eg [47]. It is defined as the proportion of time spent bursting (to avoid problems with differing burst finding algorithms, any ISI under 2s is assumed to be in a burst). This is used instead of variance to calculate classification of cells (see Methods).

The population is heterogeneous: so are the cells themselves. In those displaying phasic patterning, firing varies within cells although less so between cells [112]. Variability is more visible during physiologically normal conditions. Cells are not stable: they may spontaneously switch between phasic and continuous firing: or between continuous and silent.

3.2.1 Phasic Firing

Phasic firing is commonly observed after osmotic stimulus: bursts are usually between 20-60s, with a silence of 20-40s. The bulk of the electrophysiological research has looked at and for this pattern, sometimes using it to differentiate the cells from their close relatives, oxytocin cells. However, this is not the only response the cells are capable of. Phasic firing is hard to recognise at firing rates less than 3 spikes/s or over 10 spikes/s. A definition of phasic generally in concordance with the literature is a cell with mean firing rate greater than 3 spikes/s and activity quotient below 0.8.

A very comprehensive survey of statistics of vasopressin cell firing was carried out in 1988 [86]. Since then the differences between *in vivo* and *in vitro* work have been further quantified in a thorough analysis by Sabatier *et al.* [97], and an information theory approach has been developed [10].

The 1988 Poulain *et al.* [86] work was one of the first attempts to formalise cell categorisation and systematically analyse firing patterns: previous researchers tended to select a few measures by guesswork. It analysed, by computer, recordings made from 68 vasopressin neurones recorded during a 24 period of dehydration (to ensure a range of patterns). The contribution to reminding researchers that phasic firing was part of a continuum of behaviour was valuable. This was an extensive analysis, confirming

the wide variability in firing patterns the cells were capable of manifesting. Variability in firing pattern was unpredicatable, ie has not yet been tied to any particular cell property.

They analysed correlations between burst and silence durations, and found no long or short term correlations between burst durations and silences: they noted only intraburst firing rate is stable. Mean burst duration increased with firing rate and mean silence duration decreased: ie, an increase in firing rate was not solely due to changes in intraburst firing but also in burst patterning.

However, this trend was clearest when the cells were approaching continuous firing: in the 'classic' phasic range it was more difficult to distinguish: this was confirmed by Sabatier *et al.*, who found only a weak correlation between burst length and intraburst firing rate, and no correlation between silence length and intraburst firing rate.

This was further elucidated in a recent work by Brown *et al.* [25], which has shown burst and silence termination is largely stochastic after around 20s. They analysed the hazard functions for burst and silence initiation by analysing 324 bursts from 28 SON cells). The probability of a burst initiating increased from a low base until around 20s, at which point it stabilised. In the case of burst termination, they used a κ-opioid antagonist to show build up of dynorphin during the first 20s is probably responsible for the influence seen in the hazard function. After 20s, levels of dynorphin are probably static, leading to the flat hazard.

The probability of burst initiation within 20s of the last burst was not altered by the antagonist, suggesting that dynorphin was not responsible for inhibition of the plateau. Other activity dependent forms of inhibition exist and are covered later.

Poulain *et al.* also noted clustering of firing rates (using only cells showing stationary firing, ie with stable mean firing rate), but only at high firing rates (greater than 10 spikes/s: most cells are firing continuously to sustain this mean firing rate). This was not observed by Sabatier *et al.*, but they were concerned with cells firing clearly phasically, and had only a few firing that intensively.

The condition of the animal also affects recording: anaesthetised rats may have longer burst/silence durations than their conscious counterparts, with a higher intraburst firing rate [113].

3.2.2 Other firing patterns

Non-phasic patterns are prevalent under normal conditions [112]; cells fire in a slow irregular fashion.

3.3 Firing during raised osmotic pressure

There are different experimental protocols for altering osmotic pressure, with slightly differing results. The methods mainly relevant for this thesis are:

- **Water Deprivation** Water deprivation is used to induce dehydration: a chronic challenge imposed over many days.
- **NaCl Solution Injection** NaCl solution is injected. Injection can produce a spike in blood pressure, so this must be adjusted for.
- **Salt Loading** Rats are given only a salt solution to drink. Dehydration probably results in more hypovolemia and less hypernatremia than salt loading [72].

Other methods such as mannitol infusion [11] and hypertonic urea infusion also exist.

3.3.1 Dehydration

During dehydration, an increase in cells firing phasically and continuously at the expense of those firing irregularly was observed in both rats (Wakerley *et al.* [112]) and monkeys (Arnauld *et al.* [9]). Arnauld *et al.* suggested this was one cell type altering its behaviour, rather than different populations.

After six hours of dehydration in rats, more than 80% of cells are firing phasically, with slow irregular firing disappearing by 18 hours and some fast continuous firing seen. A similar shift was observed over days in the monkeys.

Dehydration results in an increase in intraburst firing rate, although no change in mean silence duration or mean burst duration is seen until the late stages [112]. Unfortunately, Wakerley *et al.* report only means, not standard deviations and ranges for their burst and silence durations, although they did report informally that the variability of the patterning reduced throughout dehydration. They also mention that the variation in burst patterning was very large, and that units from the same rat “might differ 10-fold in their burst durations”. This large variation caused the difference in mean burst

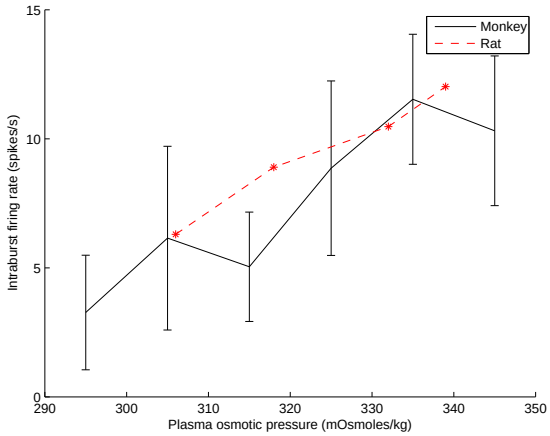

Figure 3.2: Intraburst firing rate under osmotic pressure in rats and monkeys. Data from Arnauld *et al.*. (Monkeys, [9]), and Wakerley *et al.*. (rats, [112]). Intraburst firing rate rises under osmotic pressure linearly.

duration to be non-significant. They also did not report burst and silence durations for the normally hydrated rats, presumably because of the eight cells they measured before beginning dehydration only one could be described as phasic.

Arnauld *et al.* generally concur, although they did find four phasic cells under initial conditions (of 26) with cycle times about double those under dehydrated conditions. They did not see any increase in burst/silence duration during late stage conditions, but their intraburst firing rate was also less and they were of course using a different animal.

Intraburst firing rate is more straightforward: both papers agree that it increases in steady fashion (Figure 3.2). Wakerley *et al.* also note a correlation between osmotic pressure and median ISI, reflective a trend towards shorter intervals as the intraburst firing rate increases.

Dehydration progressively increases secretion of vasopressin into the bloodstream [8].

3.3.2 NaCl injection

Intraperitoneal injection was the method used by Brimble & Dyball [21]: injection into the abdomen causes fluctuations in blood pressure that subside within about 10 minutes.

In the response to injection, cells that were firing slowly showed a period of contin-

uous firing and then adopted phasic firing after 10-15 minutes. Those firing phasically beforehand continued to fire phasically, but with longer bursts and shorter silences (unfortunately not quantified).

The continuous firing could be due to the disruption of the injection; it could also reflect the time necessary for inhibitory feedbacks (such as dynorphin) to build up sufficient to enforce phasic firing.

Interestingly, the cells showed a decrease in firing rate after the initial increase, although plasma osmotic pressure remained constant. This could reflect dampening of the system response to prevent overexertion, but dendritic vasopressin or other agents.

A similar, more recent experiment, again with hypertonic saline and carried out in Dyball's lab [11] did not group responses, and note a far greater range of response than was clear in the earlier results. Although an overall increase in firing rate was again observed, individual cells shows responses ranging from excitation to a few actually decreasing firing rate! This study also recorded more cells than the original (51 versus 22).

3.3.3 Salt loading

Dyball and Pountney [38] found rats given NaCl solution to drink for several days had increased activity. Cells in the SON had increased intraburst firing rate (interestingly, this was not true in the PVN although they only measured 6 cells). They saw an *increase* in silence duration, although not a significant change in burst duration. Again, no information other than the mean is recorded.

Their total cell sample in the SON and PVN after salt loading was 21 cells; in light of recent evidence about the variety of response under acute pressure from Bhumbra and Dyball [11], it may be more cell recordings are required to get a fuller picture here as well.

3.3.4 Summary

Vasopressin cells are highly variable, both in terms of original patterning and in response to osmotic pressure. The use of different experimental protocols, designed to induce chronic or acute strain, provides a variety of challenges. In all cases a population of vasopressin cells will respond to osmotic pressure with an overall rise in mean firing rate, and most cells will be excited. The excitation generally includes a rise in intraburst firing rate: beyond that it is hard to say much about the phasic patterning.

3.4 Evidence on Functioning

Key to the modelling are two theories, and the evidence is easier to review in this context. The first is a theory initially proposed by Andrews and Dudek [3]: that the cells fire phasically because a Depolarising AfterPotential (DAP) which peaks after the hyperpolarising afterpotential (HAP) facilitates further firing: more DAPs can then be created and will summate to create a plateau potential, from which burst firing can be sustained (Figure 3.3). This theory has dominated the field since its inception 30 years ago.

The second was proposed in 1997 by Leng & Brown [64]. They proposed a simple bistable oscillator: fluctuation in the input then would cause the state to flip periodically, thus controlling burst initiation and termination. It may be that only the EPSP/IPSP rate is significant: a faster arrival rate of both EPSPs and IPSPs would causes more transitions: bursts become shorter and more closely spaced, as is seen during increases in osmotic pressure. This would also suggest the cells could act as stochastic resonators [63]: an increase in noise (the input) is sufficient to boost a small signal over a threshold.

Both these models, together with the others developed thus far will be reviewed in section 3.7.

First I will summarise the evidence for the functioning of the cells, as opposed to their effect. A particularly good review of cell workings can be found in [22].

3.4.1 Interconnections between cells

Evidence in the SON has tended to indicate vasopressin cells are probably not synaptically coupled: stimulating the neural stalk at maximal subthreshold levels did not produce any extra activity, whereas if the cells were interconnected one would expect the activity to be amplified [41].

3.4.2 EPSPs and IPSPs

Transmission in the hypothalamus is primarily driven by glutamate and GABA. PSPs are not patterned: during hyperpolarisation of phasic cells, Andrew and Dudek observed only one of eight with patterned synaptic input [4]. Hatton observed phasic firing *in vitro* when synatpic input was blocked [50]. Bursting instead relies upon the DAP [4]. They are generally assumed to arrive randomly with a Poisson distribution:

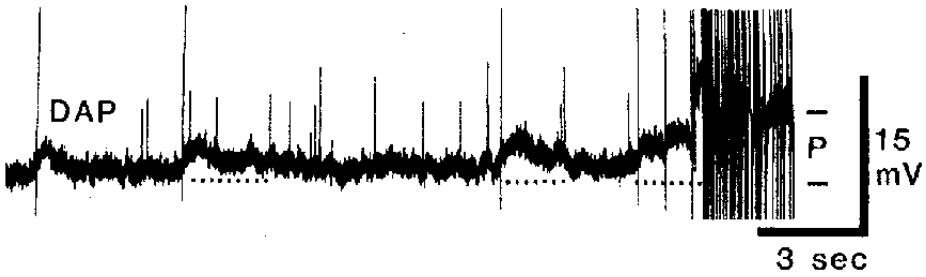

(a)

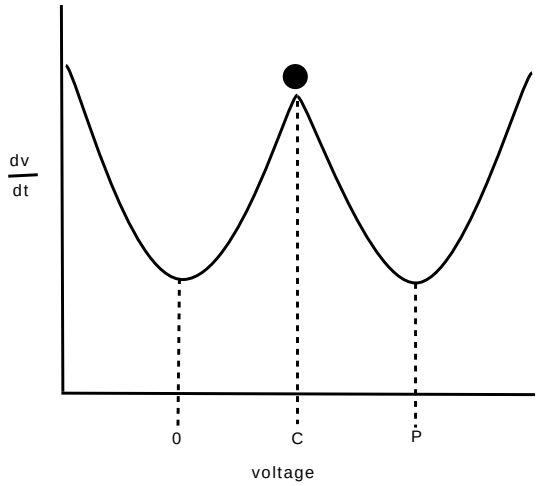

(b)

Figure 3.3: Illustation of theories on phasic firing from a) Andrew & Dudek [3] and b) Leng & Brown [64]. a) A DAP is caused by firing, which in turns faciltates further firing, which can in turn create a plateau potential.Shows DAP summation to a plateau potential as recorded *in vitro*, from [3]. b) Illustration of model proposed by Leng and Brown [64]. This model is a bistable oscillator: there are two stable states at 0 and P. C is an unstable equilibrium seperating the two. As the black ball (the voltage) is perturbed, it will roll, but return to the nearest stable equiliria until it passes the critical point, C.

this is supported by statistical analysis of intraburst firing [97]. Rates of IPSPs are above 100/s [20]: it is unlikely this a vast disparity between EPSP and IPSP rates, as this would inhibit oscillation although this is not confirmed *in vivo*.

3.4.3 The Hyperpolarising afterpotential

The hyperpolarising afterpotential (HAP) is visible after each firing instance: it lasts around 50ms and prevents firing during that time [5]. The primary component, I_c, is carried by BK channels [48]. It has a weak effect on frequency adaptation [48]: probably by forcing a refractory period.

3.4.4 The Depolarising Afterpotential

The Depolarising Afterpotential (DAP) is a slower, smaller current than the HAP and partly masked by it: *in vivo* it peaks around 45ms after firing, facilitating further firing. *In vitro* the dynamics of both the HAP and the DAP are slower: it has a time constant of around 294ms opposed to 69ms *in vivo* [97].

Andrews and Dudek [3] were the first to observe the DAP and theorised that the DAP could create a positive feedback to initiate and support burst firing. For a time window after firing, the DAP facilitates further firing: if this occurs, the DAP created will summate with the first one, and so on, creating a plateau potential to sustain firing. Use of tetrodotoxin to block spikes revealed the mechanism underlying phasic firing was endogenous, as the plateau potential persisted.

Ghamari-Langroudi and Bourque [42] tried blocking DAPs with caesium. This abolished phasic firing: cells would fire either irregularly, or continuously if depolarised.

In vitro, a suprathreshold plateau potential can form, leading to regenerative firing [3, 2]. *In vivo*, the plateau is subthreshold and EPSPs are required to trigger firing [24].

The DAP is calcium sensitive [2]: it was blocked in hypothalamic slices placed in low Ca2+ saline, and increased when the Ca2+ agonist Sr2+ was used. It was also voltage dependent, progressively activating at more depolarised levels until about 10mV below spike threshold [2, 16]: it may then be restrained by an increased outward rectification [17]. Cells *in vitro* current clamped by Li and Hatton [67] and depolarised showed DAP amplitude increases up to -50mV: they also claimed an increase in duration but this is unquantified, and they did not calculate the time constant.

The currents underlying the DAP are poorly understood, especially *in vivo*. Recent theories attribute it to either a resting K+ conductance inhibited by Ca2+ influx during action potentials [67] or non-selective cation channels [43]. As pointed out by [43], differences in experimental setup (voltage clamp or sharp microelectrode) and protocol (DAPs evoked by several action potentials, trains of action potentials, depolarising steps) have produced entirely different answers.

The calcium dynamics required for the DAP are complicated: calcium comes from multiple sources, external and internal ([66], for review, see [51]). Externally, multiple channels including T-,N-,L- and P-Type channels admit calcium ([40]). The higher levels of external calcium exist, the larger the DAP [66]. Internally, Ca2+ dependent Ca2+ internal stores provide a positive feedback which boosts the DAP magnitude [51]. Calcium imaging has been used *in vitro* to show that internal Ca rises rapidly after a burst has begun, stabilises and then decays when the burst ends [95]; although useful to know, calcium imaging is too low resolution to account for any compartmentalisation occurring.

3.4.5 The Plateau Potential

The theory proposed by Andrew and Dudek [3] is still used today: that the DAP summates to create the plateau potential. But is the DAP both necessary and sufficient to generate the plateau potential?

In vitro, experiments that alter the DAP generally find the effect on the plateau potential is consistent with the summation hypothesis. For example, if the DAP is blocked with caesium, phasic firing is abolished and no plateau potential is observed [42], and increasing the DAP increases the plateau as well [25] (at least until the summation of DAPs is outweighed by summation of slow AHPs). However, there is no proof that plateau potentials form *in vivo* [22], and caution must be taken in extrapolating from the slower dynamics seen *in vitro*.

There is also evidence that the plateau potential could be sustained by currents other than the DAP. When vasopressin cells are depolarised from their normal resting potentials of around -70mV, they can stabilise at around -60mV [64].

3.4.6 The slow Afterhyperpolarisation

One further component of post-spike behaviour has been observed, although it requires a high frequency spike train to observe it clearly ($>$20Hz *in vitro*) [5, 19]: the slow af-

terhyperpolarisation (slow AHP). Its intensity increases with duration and intensity: it can outweigh the plateau *in vitro* [5]. It is voltage independent, but calcium dependent requiring calcium release from intracellular stores [5], and Ca2+ influx through voltage gated Ca2+ channels. It is sensitive to apamin.

The magnitude of the slow AHP may vary with the frequency of stimulating train, but it requires only around 15-20 spikes to establish that magnitude [58]. Spike trains in the normal steady state firing range (5-10Hz) can generate a slow AHP [58], but this may be masked by the plateau potential. Under normal conditions, the slow AHP functions to prevent more intense stimulation than is useful for the cell. It is the slow AHP that is mostly responsible for frequency adaptation after the beginning of bursts [48]: when blocked with apamin, the intraburst firing rate does not decrease after the beginning of the burst and the burst length decreases [58].

Confusingly, an even slower hyperpolarisation has been found that is not blocked by apamin, but is inhibited by muscarine [44] suggesting the involvement of muscarinic cholinergic receptors. This accumulates far more slowly over a burst, requiring $\sim$70-100 spikes to maximise. Its time course is around 1-2s [49, 44], and it may continue to rise even after firing ceases. When inhibited using muscarine, burst durations and firing rates rise, suggesting this current may play a role in phasic firing. They note that the muscarine caused a small depolarisation, which may have increased DAP magnitude. However, this effect was observed even in silent cells and so is not part of the sHAP.

If a hyperpolarisation is caused by muscarinic sholinergic receptors, one would expect an increase in silence duration as reaching the firing threshold would be harder. Phasic firing may cease if the hyperpolarisation was large: the DAP and possibly the plateau would be weaker with hyperpolarisation. A depolarisation cause by muscarine and consequent increase in burst frequency is consistent with this.

3.5 Osmosensitivity

The vasopressin cells themselves are osmosensitive [75, 74], as well as being fed by areas that are osmosensitive. When osmotic pressure rises, they depolarise, and a rise in EPSP rate is observed [74]. Likewise, hyposmotic stimuli will result in hyperpolarisation, and overall the change in membrane potential can be fit well linearly throughout the physiological range [80]. The bulk of the response is therefore probably mediated by a single current (mediated by stretch inactivated cation (SIC) channels), although

other currents may also be osmosensitive (eg [68]).

As osmotic pressure rises, water is drawn through the blood brain barrier to equalise osmotic pressure on both sides of the barrier: thus the extracellular spaces loses water, causing the cells to shrink. As they contract, SIC channels activate and depolarise the cells. Likewise, hypotonic stimuli cause swelling of the cells and deactivation of the SICs, hyperpolarising the cell [111, 80].

Apart from depolarisation, calcium influx through stretch inhibited calcium channels also occurs [114], although this doesn't appear to influence the DAP [18].

The Organum Vasculosum Laminae Terminalis (OVLT), a major provider of synaptic inputs to the SON and PVN (although not the only: see [76]) and located outside the blood-brain barrier is highly osmosensitive. When the OVLT is osmotically stimulated, EPSP rates to vasopressin cells increase while IPSP rates remain constant [92] (although nitric oxide or similar feedbacks may upregulated IPSP rates to match: rates were only monitored for 30s after a stimulus had been applied only to the OVLT). EPSP rates increase 2-3 fold up to the range usually seen during osmotic pressure (up to 325mosmol/kg), with indications that the rate continued to increase beyond this. However, this experiment was in explants, so connectivity may not accurately reflect that *in vivo*.

Under hyposmotic conditions exerted on the OVLT, EPSP rates fell to around 50% of set point conditions, although IPSP rates remained unaffected [92].

A further problem is the majority of the experimental data is *in vitro*: extrapolating to *in vivo* is difficult, although one would generally expect currents to be smaller and input rates to be higher.

3.6 Inhibitory feedbacks

Vasopressin cells have a multitude of inhibitory mechanisms: apart from the slow AHP and IPSPs, there are at least four other forms of feedbacks involved in these cells. Unusually, some of these are mediated through peptide release from the dendrites (vasopressin and dynorphin).

3.6.1 Nitric Oxide

Nitric oxide (NO) is synthesised and released from the vasopressin neurons: it acts on GABAergic inputs to increase IPSC size and frequency. The changes in mIPSC fre-

quency are probably due to presynaptic action, where amplitude alterations are more probably postsynaptic [106]. Other effects have been reported, including possibly depolarisation and increased coupling of cells, but its effect upon vasopressin neurons is generally agreed to be inhibitory. In phasically firing vasopressin neurons, the firing rate is reduced, caused more by a reduction in their firing quotient than intraburst firing rate. [106].

Consistent with the inhibitory actions reported, inhibiting nitric oxide during salt loading in rats increases depletion of AVP stores; the same paper demonstrates nitric oxide production is upregulated [57].

3.6.2 Dynorphin

Dynorphin is one of the peptides released in neurosecretory granules from the dendrites [88], along with the κ-opioid receptors it activates [102]. Dynorphin activates κ-opioid receptors in vasopressin cells: this inhibits the cells by reducing the DAP and the plateau [25], although other effects have also been reported [28] (including reduction of PSP magnitudes, [54]).

Unlike vasopressin, κ-opioid inhibition activates progressively though a burst: this indicates it is a fast acting, localised effect [27]. Analysis of the probabilities of a burst terminating shows there is a strong random component: dynorphin increases the probability of a burst ending, acting in concert with a more stochastic mechanism (fluctuations in the membrane voltage due to EPSPs/IPSPs). It has no effect on burst initiation: when blocked with antagonists, bursts are terminated by a slowly acting but more deterministic mechanism [25], although sometimes this is insufficient and continuous firing results [26, 25]

3.6.3 Adenosine

Adenosine is another inhibitor, relatively recently researched. Unlike vasopressin and dynorphin it is probably not directly packaged in dendritically secreted granules. The source is likely to be ATP, converted to adenosine in the synaptic cleft, although it may also emanate from glia or other sources [29].

Although adenosine is inhibitory by A1 receptors, it exercises excitatory effects via A2 receptors [84]. The A1 receptors seem to prevail under basal conditions. The excitatory effects reported with an A2A receptor agonist include depolarisation and slightly increased clustering of EPSCs [85].

Interestingly, Bull *et al.* [29] note the A1 antagonist they used increased intra-burst firing rate and burst duration by more than V1 and kappa-opioid antagonists and suggest that adenosine may predominate in inhibition of the cells.

The mechanism by which adenosine inhibits cells is uncertain: it may effect the DAP, on calcium components (it reduces calcium spike broadening [84]) or AHP, or combinations thereof. There is also the frequently reported reduction of IPSC and EPSC frequency [82].

3.6.4 Vasopressin

Vasopressin is released dendritically, independently of axonal release (see [69] for summary of evidence). This feature isn't unique to vasopressin cells, but it was one of the first systems it was identified in. The soma and dendrites can be separated easily from their distant axon terminals, allowing for easy distinction between axonal and dendritic release, but definite proof came with examination by the electron microscope [88].

Vasopressin is tonically present, and is the longest lasting of the peptides mentioned with a half life of minutes. It could then act as a 'population' signal [78], providing an indication of the total activity over the population rather than only to a neuron's nearest neighbours. Its effects are visible throughout bursts, supported this hypothesis and also indicating a rapid effect [27].

The effects of vasopressin have caused controversy: both inhibitory and excitatory effects on firing pattern have been observed. Inenaga & Yamashita [56] saw an increase in firing rate in 64 of 97 cells from the PVN in slice preparation, after application of vasopressin. Responses occurred within minutes, and ceased within 5-15mins of wash out. However, they did not separate vasopressin and oxytocin cells or even determine whether the cells were magnocellular. Abe *et al.* [1] report a decrease in firing rate accompanied by a *depolarisation* in SON cells, although these were not identified as vasopressin cells.

Like adenosine, two receptors are implicated: the inhibitory V1a and another excitatory one. The inhibitory effects may dominate [71], but an alternate theory [47] is that vasopressin acts according to the state of the cell: it is excitatory to a quiet cell and inhibitory to a excited cells, essentially regularising the population. Unfortunately, calcium is heavily implicated in the chain reaction triggered by vasopressin [46, 99]: given the number of signalling chains calcium is implicated in, it is difficult to trace

the effect.

Dendritic release can be elevated by osmotic pressure. After a hyperosmotic stimulus is given, plasma vasopressin peaks first at around 30 minutes and then returns to basal levels: after this internuclear vasopressin levels peak (at around 2.5 hours) and are sustained [70]. This is consistent with the inhibitory theory: the systems responds, and then requires inhibition, although to return to previous activity levels, although plasma sodium levels were still elevated at the end of the experiment.The delay in internuclear release may also reflect the time for morphological changes to take place, or the need for 'priming' before release.

3.6.5 Other

The above constitute a selection of the major feedbacks so far explored: others exist, both independently and interacting with the other signalling pathways [103]: for example ATP, apelin [33], galanin and histamine.

3.7 Previous Models

3.7.1 The oxytocin model

Oxytocin cells are also magnocellular secretory cells: they are not bistable, but are otherwise close relatives of vasopressin cells.

An integrate and fire model was modified [62] to include a HAP and then driven by different proportions of inhibitory and excitation input, generated randomly with a Poissonian distribution. The model was deliberately simple: the HAP was an exponentially decaying voltage, and no other intrinsic currents (apart from the leak) were included.

This model could replicate basic features of oxytocin cells, including the ISI distribution and translating a linear rise in input rate to a proportional output rate. The responsiveness of the model depended on the mix of EPSPs to IPSPs: IPSPs were necessary to increase the linear range of the model. This resulting in other benefits, such as the response being independent of the initial firing rate.

A key conclusion from the model was then that inhibition used to balance excitation was beneficial. This model was simple, allowing solid conclusions to be drawn - more complex models may include more features but inevitably increase the risk of unexpected behaviour.

3.7.2 *in vivo*

A full *in vivo* model has yet to be implemented. However, Leng & Brown [64] suggested a variation of the FitzHugh-Nagumo model for producing bistable behaviour (Figure 3.3). Two equations, controlling the membrane voltage and the inhibition were used.

That model used the formulation:

$$\frac{dv}{dt} = s[-v(v-C)(v-P) - k_1 w] \tag{3.1}$$

where s and k_1 are scaling factors, v is the activity, 0 and P (for plateau) are the stable states in the absence of inhibition, C is the "critical point" (an unstable equilibrium between 0 and P) and w is an inhibitory term.

Inhibition increased as a constant proportion of activity, and decayed exponentially:

$$\frac{dw}{dt} = b(k_4 v - k_5 w) \tag{3.2}$$

where k_4 and k_5 are constants, and b is a scaling factor.

Large fluctuations in the input would cause transitions between states. A rapid succession of EPSPs would force the model into an upward transition: likewise a sequence of IPSPs could cause return to the resting voltage. An inhibitory term ensured that after a burst of activity, silence was enforced, and that bursts would eventually stop. This model should successfully be able to mimic phasic firing, with a range of burst and silence durations. However, it did not include the HAP or the DAP, and v is somewhat ambiguous: it represents the firing rate when v is above the firing threshold, and the probability of firing when below the firing threshold.

This idea was implemented by Milne and Chalabi [77], using a Rose-Hindmarsh model (an extension of the FitzHugh-Nagumo equations used by Leng and Brown).These are third degree differential equations, with variables for membrane potential, recovery and inhibition. Somewhat oddly, they do not explicitly include input (it indirectly alters a constant), presumably to allow analysis. The model did display a range of behaviours, including phasic firing and frequency adaptation. Unfortunately, inhibition continued throughout the burst, so firing always slows steadily throughout the burst, contradictory to most observations *in vivo*.

The main goal of this work was not really to produce realistic replicas of cell firing as it was to analyse (in simplified form) how the system may rotate through different behaviours, and in this respect it was successful. They showed that although it was

always possible to force the system into a particular type of behaviour (including silence), but not to control precisely the behaviour. they also confirmed the bistability of the cells could be expressed as an oscillation between two stable states (silence and activity).

The original model by Leng and Brown contains some useful ideas, especially that of oscillation between stable attractor (being the plateau and resting voltage) controlled by randomised input. This could be expected to produce realistic burst and silence distributions. This idea will be further developed later to produce a model which can also replicate intraburst firing statistics by including the HAP and DAP.

3.7.3 *in vitro*

One major model of *in vitro* behaviour exists, published by Roper *et al.* [96] in 2003. This model is designed for biological plausibility: thus it incorporates as much as possible of known currents.

The advantage of this approach is that one may, with luck, discover phenomena emerging from the interplay of currents, and can thus become more certain about which currents may be responsible for behaviour. Prediction can also be made which are directly (and easily) testable with experimental blockers.

The disadvantage of this approach is that one rarely has all the information required to fully specify currents: thus models necessary incorporate a fair amount of guesswork. Conclusions may become unreliable if many parameters have had to be estimated. It is also very difficult to extend models like this to *in vivo*, where there is even less information about currents.

The case in vasopressin cells is also complicated by the number of transactions involving calcium. Calcium arrives from multiple sources, both internal and external: compartmentalisation also makes modelling calcium alone difficult, although it has been attempted.

Roper *et al.* based their calcium modelling upon calcium imaging experiments they also carried out. Fluorescent imaging may itself alter calcium dynamics (personal communication: D Sterratt), but at least this provided some experimental basis for the resulting equations which take some account of local dynamics.

The model is a Hodgkin Huxley model, with the membrane potential modified by eight currents, each of which was of one of two forms depending on whether it was voltage dependent inactivating or activating. Each required a conductance, reversal

potential and time constant. This is a considerable number of parameters, and while experimental data can be used to narrow the ranges the authors did have to adjust many parameters.

This is a process followed with all models, but it would have been useful to know the model's sensitivity to parameters. Could it cope with biological levels of variation? However, this is certainly not a problem unique to Roper *et al.* - with many published models it is difficult to ascertain robustness. The field is increasingly aware of the problem and some effort is being made to quantify how well designed models are: in the meantime, it is assumed more complex models are less robust.

The model does provide a useful picture of how the system might fit together, and contains the crucial features of firing. It will also hopefully encourage experimentalists to refine the data available (for example, how exactly is the DAP voltage dependent). The main flaw is the complexity of the model - while it can be somewhat constrained by the *in vitro* data, there are still many assumptions and little likelihood of gaining equivalent levels of *in vivo* data.

There are several useful points arising from their work, apart from the general framework. The first is that the cells may act as filters: they carry low frequency signals up to a point, at which point feedback limits the effect of higher frequency signals (probably as a self-protective mechanism). The calcium in particular contributes to this effect as too low frequency signals will fail to stimulate Ca2+ levels and too high will exhaust them.

They also showed that DAP summation, together with calcium accumulation could account for the plateau computationally (at least *in vitro*) [95].

Chapter 4

Cell Firing Model

4.1 Introduction

When building a model, it is better to start with the simplest model possible for the stated purpose. Complex models have more chance of including unforeseen and undesirable results. Here the goal is to understand the linear secretion of vasopressin from a network of vasopressin cells: a first step is replicating the steady state firing patterns of the cells, then producing an unconnected population of cells and finally incorporating interactions between cells such as dendritic secretion. Vasopressin cells also have interesting potential for network properties, given the diffusion of substances from the dendrites of one cell to its neighbours [69]. With a view to this, the aim here is to devise a model computationally tractable enough to be networked. This constrains both memory and processing limits.

A simple and experimentally supported hypothesis proposed by Andrew and Dudek [3] has already been mentioned: that the DAP summates to create a plateau which supports phasic firing. It is already known that the oxytocin cells, close relatives of vasopressin cells, can have key statistical features replicated by an integrate and fire model modified to include the HAP [62]. Could this model, modified to include the DAP, mimic vasopressin cells?

A statistical characterisation of these cells *in vivo* has recently been conducted by Sabatier *et al.* [97]. The crucial features this model must display are a clear phasic pattern, with burst and silence durations of plausible length. The interspike interval distributions should match those seen *in vivo*, and statistics such as mean firing rate and intraburst firing rate should also be within accepted ranges.

One distinctive feature will be omitted: that of frequency adaptation or the rapid fir-

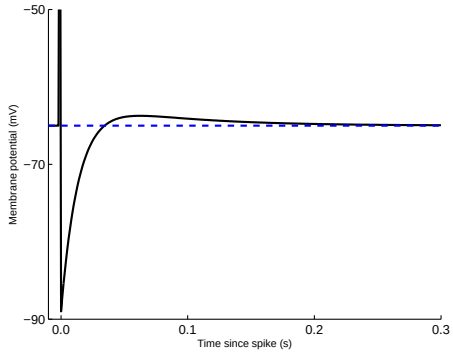

Figure 4.1: Model afterpolarisation of vasopressin cell: this shows the HAP and DAP after a firing instance at 0ms. The hyperpolarising afterpotential (HAP) here has a magnitude of -30mV and time constant 14ms. The depolarising afterpotential (DAP) has a magnitude of 4mV and time constant 69ms[97]. Resting membrane potential is -65mV (blue dashed line).

ing seen at the start of a burst. The steady state of the cells is assumed to be of far more importance to secretion, particularly when considering a network, as high frequency stimulation accounts for relatively few spikes comparatively and is also inefficient at stimulating secretion per spike (see Figure 5.12). All other identifiable statistics and relations should be comparable to those measured.

A secondary concern after demonstrating a stereotypical phasic cell can be mimicked is to explore the range of expression: vasopressin cells display a wide range of firing ranges and patterns, some aphasic, although phasic firing is prevalent under hyperosmotic conditions ([112]).

This section begins by examining an integrate and fire model modified to include a DAP. This model can not demonstrate plateaux under *in vivo* circumstances, so an explicitly bistable model is introduced. The behaviour of this model under different conditions will be explored; it will be shown it can match both the intraburst firing statistics of the cells and the range of phasic patterning. The model's performance under different parameter schemes will then be shown, enabling an evaluation of its robustness.

4.2 Simple Integrate and Fire

In the oxytocin model [62], the HAP was modelled by increasing the firing threshold by an exponentially decaying amount, calculated as in Equation 4.1. The DAP can

likewise be modelled with an exponential decay. This is the only modification to the oxytocin model. As in the oxytocin model, this model uses voltages rather than currents: many of the concepts are already stated in terms of voltages (eg the DAP and the HAP). The model is deliberately simplistic to minimise computational load. The HAP and DAP are stereotyped, although factors such as the membrane potential they are invoked at almost certainly alter their shape. Quite how this might affect firing is an interesting research question, but unfortunately the changes, particularly *in vivo* are very poorly understood, both in terms of current and because results have been grouped, with no attempt made to relate indicators such as spike shape to the firing pattern.

To try and quantify the effect of this somewhat, the resulting hazard functions for different time constants and magnitudes of HAP and DAP have been calculated later (see Figure 4.7).

The magnitude of the *s*th HAP is:

$$v_{H_s}(t) = A_H exp(\frac{-(t-t_i)}{\tau_H}) \tag{4.1}$$

where A_H is the HAP magnitude, t_i the time it was initiated, and τ_H the HAP time constant. DAPs are generated in similar fashion replacing A_H with A_D and τ_H with τ_D, ie:

$$v_{D_s}(t) = A_D exp(\frac{-(t-t_i)}{\tau_D}) \tag{4.2}$$

A sample afterhyperpolarisation is displayed in Figure 4.1. The DAP time constant is as stated in Sabatier *et al.*. [97], although the HAP time constant is slightly shorter (14ms instead of 17ms), as this produced a better match to the hazard function (Figure 4.8).

Analysis of summation of HAPs and DAPs is difficult, the plateau can be examined assuming a steady rate of stimulated action potentials (Fig 4.2). DAP summation with a steady rate of firing can produce a sustained, although small depolarisation: at typical intraburst firing rates (around 10 spikes/s), it is less than 50% of DAP magnitude.

This analysis ignores the positive feedback loop by which firing creates more firing. Can a plateau be created with the irregular stimulation seen *in vivo*?

The oxytocin model was modified to include a DAP in the same fashion as the HAP. Input is modelled by generating EPSPs and IPSPs with a Poisson distribution and of equal magnitude and rate. EPSP arrival times, $E(t)$ are generated iteratively at rate R_E

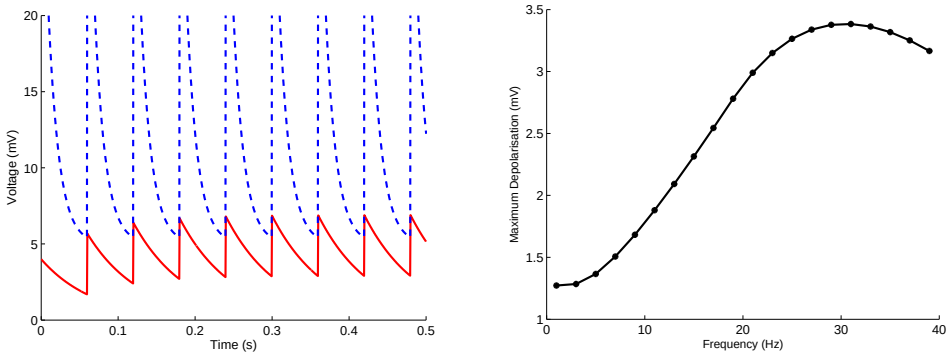

(a) (b)

Figure 4.2: DAP summation to a plateau level. Here, a spike is invoked every 60ms (ie, mean firing rate of 16.7Hz), and the resulting HAPs and DAPs summated (parameters: HAP time constant 14ms and magnitude 30mV, DAP time constant 69ms and magnitude 4mV). a) Here the DAP is unmasked (red lower trace) as the HAP summation is displaced by 5mV and reversed to to form a firing threshold, as implemented in the oxytocin model (blue upper trace). It can clearly seen that the DAP summation would cause a constant depolarisation of around 2.5mV when considered separately from the HAP. Depending how often postsynaptic spikes occur, the final level of summation is different: b records the maximum depolarisation (this time, including the HAP) reached for different firing rates: maximal depolarisation occurs around 30Hz, as above this summation of the HAP outweighs summation of the DAP. At 1Hz, the HAP and DAP from the previous spike have decayed to a negligible amount by the next spike: thus the maximum is the peak of one afterpolarisation (see Figure 4.1). Initial firing rates in vasopressin cells are around 20-30Hz, so this suggests DAP summation could establish the plateau, but not sustain it.

$$E(t) = E(t - \Delta t) - log(\frac{r}{R_E}) \tag{4.3}$$

where r is a uniformly generated random number between 0 and 1 and the $E(t)$ are the arrival times.

IPSP times are generated in the same fashion, at rate R_I. The EPSP and IPSP rates are identical, so the rate of both will be referred to at $R_{E(I)}$. In each timestep, the number of EPSPs and IPSPs arriving is calculated. Rather than calculate the decay of each individual PSP, an IPSP arriving in the same timestep as an EPSP is assumed to cancel it: the surplus is then multiplied by the PSP magnitude to form the input voltage, v_i: this will cause an instantaneous jump in the membrane voltage, which then decays according to the membrane time constant.

The membrane voltage is calculated using the standard leaky integrate and fire equation:

$$\Delta v_m(t) = v_i(t) - \frac{v_m(t - \Delta t) - v_r}{t_m}\Delta t \tag{4.4}$$

Unlike the standard integrate and fire model, the membrane voltage does not reset after firing: the HAP will force a refractory period.

The firing threshold incorporates the summed HAPs and DAPs:

$$\Delta v_t(t) = V_t - \sum_s v_{H_s} + \sum_s v_{D_s} \tag{4.5}$$

where V_t is the unmodified firing threshold, and v_{Ds} is the sth DAP.

Integration here is by the Euler method, rather than Runge-Kutta, as accuracy is not considered a priority: there is almost certainly considerable noise in the biological system.

The model uses a DAP time constant of 69ms [97], and HAP time constant of 14ms. While the HAP time constant is shorter than the one derived by Sabatier *et al.*, this matches the ISI distribution closely: it has a mode of 40ms (the discrepancy could be accounted for by considering other factors, for example spike duration, that may disrupt the analysis slightly). Mean firing rate is 4.6 spikes/s. But there is no long lasting plateau potential: although sometimes DAPs do summate, any nascent plateau collapses quickly.

Channel dynamics, including those underpinning the HAP and DAP, *in vivo* are faster than *in vitro* [97], so time constants /it in vitro are larger: using these longer time constants (77ms for the HAP, 294ms for the DAP) produces an unmistakable plateau

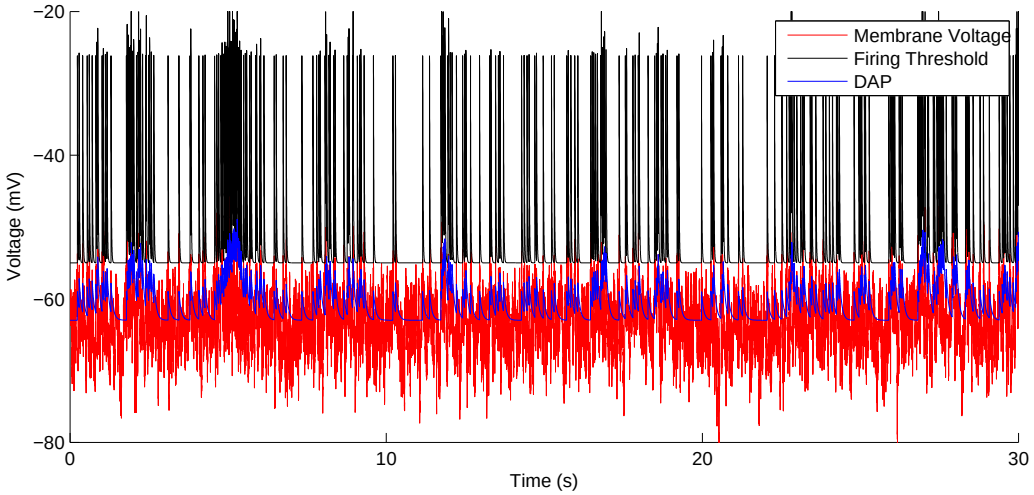

Figure 4.3: Firing in a modified integrate and fire model using *in vivo* parameters. Input is randomly generated with a Poisson distribution. Instead of adding the HAPs and DAPs to the membrane voltage, they are subtracted from the firing threshold (in black): they have magnitude -30mV and 4mV, and time constants 14ms and 69ms respectively [97]. The DAP with a baseline of the resting potential for clarity. Parameters: membrane time constant 8.3ms, $R_{E(I)}$ 200 PSPs/s, PSP magnitude 2.5mV, resting potential -64mV, firing threshold -55mV. Firing rate is 8.3 spikes/s, higher than the average intraburst rate in vasopressin neurons. Although summation of DAPs can be seen, collapse soon follows, on a time scale much too short to account for a plateau.

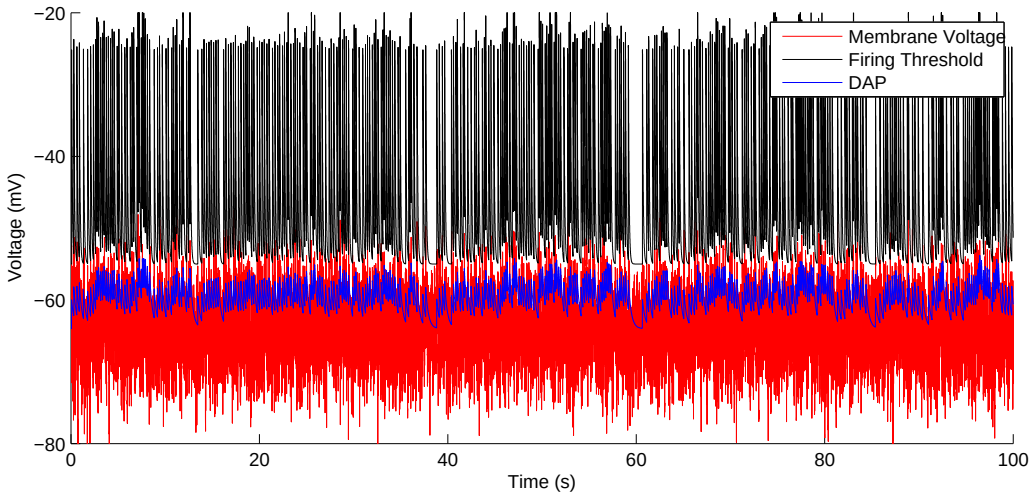

Figure 4.4: Modified integrate and fire model with *in vitro* parameters. The HAP time constant is 77ms, and the DAP time constant 294ms [97]. Other parameters as in Figure 4.3. Plateaux are successfully formed for tens of seconds: for example, there is a continual displacement of at least 2mV from 40s to 55s. This model has no inhibitory influences to enforce the silences necessary for phasic firing and so fires continuously, consistent with cells in which dynorphin is blocked [23]. Clearly a phasic model could be developed from this. Firing rate is 3.5 spikes/s, with the ISI mode at 175ms.

potential, sustained at around 4mV above resting potential for $\sim$10s. This is still not phasic firing: there are no silent periods. However, this is unsurprising in the light of recent experimental work demonstrating inhibitory feedback is necessary for phasic firing [23]. However, plateaux cannot be sustained at realistic intraburst firing rates with the *in vivo* time constants.

An attempt could have been made to further adapt the above integrate and fire model to include inhibition, DAP scaling, maintenance current and other nonlinearities, until a sustainable plateau was seen. The shape of the HAP and DAP may change depending on V_r and the ISI: there is a danger in assuming the typical values used here. The complex subtleties of the biology are not yet quantified sufficiently for confident modelling: this would also increase the computational complexity of the model.

4.3 Forcing Bistability

An alternative is to further abstract from the underlying currents and consider instead their effect: a higher level model, by considering results of the DAP separately. The DAP has two proposed purposes: it creates and sustains a plateau potential to support burst firing, and it transiently increases the probability of firing after a previous spike.

One simplifying assumption is that the cells are successful in creating and maintaining a robust plateau potential. Without using the DAP to create stable plateau potential, bistability could be forced in the model by allowing two resting voltages, one corresponding to an 'up' state, providing maintenance for the plateau. Changes between the states is governed by the input, DAP and inhibitory feedback.

The plateau can then be modelled by a constant level the DAP is assumed to maintain and occasionally exceed. However, the HAP should not be artificially curtailed by such a plateau. One alternative is to add the HAP to the firing threshold instead. This forces a refractory period and simplifies the plateau design.

There is some evidence to support this: when depolarised by about 10mV, vasopressin cells tend to maintain this depolarisation [64].

Figure 4.2 shows summation of DAPs and HAPs when the HAP is added to a 5mV threshold. In this case, summation of the DAP to form a plateau potential can be clearly seen, although the firing rate here is high (16.7Hz).

Once a separate plateau is modelled, inspiration can be taken from a previous model by Leng and Brown [64] to create bistability in the model without explicitly using summation of DAPs. The model explicitly created two attractors: the input caused the

membrane voltage to oscillate between the two.

The idea of enforcing stable states was used for this model, as the idea of generating burst and silence durations as a function of the input caught between attractors seemed good. Both states are not active simultaneously, as in the previous model, with the membrane voltage pulled towards both: only one is active. This allows for a more explicit tipping point to be included. It is also important to clarify the activity term used in the original model, where it was used as the membrane voltage in some circumstances and the probability of firing in others.

One potential criticism of this approach is that the plateau is not proven to exist *in vivo*; *in vitro*, the DAP is could be entirely responsible for plateau formation and thus extrapolation to *in vivo* is dangerous. One alternative is that inhibitory feedback could be responsible for the phasic firing.

But to model this requires inhibition that does not slow firing progressively throughout a burst, yet suddenly terminates a burst. This is very difficult to model without having something that underpins phasic firing that suddenly terminates. Here, we have assumed a plateau and made it voltage based, but it could be a current that ceases, a desensitisation, an accumulation of calcium suddenly cleared during a pause in firing. Nevertheless, the model is sufficiently abstracted to provide a useful description of what features the underlying process must have without being too precise about what it is. This is a top-down form of modelling.

The classical integrate-and-fire model integrates input voltage to form a membrane voltage that decays to a unique resting potential. Here there is an alternate equilibrium, a plateau potential V_p, making the model bistable [64]; this is equivalent to postulating a non-inactivating or slowly-inactivating voltage-dependent depolarisation. Only one equilibrium is 'active' at any time, either V_p, or the 'normal' resting potential (the 'rest potential', V_r), and the rules for which is active define burst initiation and termination. The membrane voltage $v_m(t)$ (all times are in brackets) is an integral of the input $v_i(t)$, and decays with time constant τ_m towards the active equilibrium v_a (either V_r or V_p):

$$\Delta v_m(t) = v_i(t) - \frac{v_m(t-\delta t) - v_a(t-\delta t)}{\tau_m}\Delta t \tag{4.6}$$

It is assumed that v_i is a mix of IPSPs and EPSPs generated randomly. EPSP arrivals are generated at mean rate R_E, and IPSP times at mean rate R_I as in the integrate and fire model (Equation 4.3); for the results here, EPSP and IPSP rates were identical. PSP scaling was not incorporated as it was not expected to have much effect.

The firing rates of vasopressin cells *in vivo* do not generally slow until the last few

spikes of a burst, so activity-dependent inhibition should increase the probability of a burst ending but not affect the probability of firing within bursts. Certainly a model in which firing progressively slowed throughout the burst would be wrong: the cells themselves are capable of both increases and decreases in firing rate before the end of a burst [98]. We included a variable $w(t)$ to model the effects of the medium term dendrosecretory influences (such as dynorphin). w_t that increases by a constant I_w at every spike, and decays with decay constant λ_w:

$$\Delta w(t) = \begin{cases} I_w - \lambda_w w(t-\Delta t)\Delta t & \text{After a spike} \\ -\lambda_w w(t-\Delta t)\Delta t & \text{Otherwise} \end{cases} \tag{4.7}$$

w_t is referred to as autosecretory inhibition hereafter, to avoid confusion with the other forms of inhibition is the system (the HAP and IPSP rate).

The HAP forces a refractory period after spikes by modifying the firing threshold, v_t:

$$v_t(t) = V_t + v_H(t) \tag{4.8}$$

where V_t is the unmodified firing threshold, and $v_H(t)$ is the post-spike hypoexcitability that corresponds to the HAP. Unlike traditional integrate and fire, v_m is not reset after firing as this would upset the bistability of the model: the HAP is therefore responsible for enforcing a refractory period. The DAP both sustains the plateau and transiently facilitates firing after a spike. V_p is the DC component of the plateau, and to incorporate the transient effects, v_m is transiently increased after a spike by a facilitation voltage. The cell fires a spike when

$$v_m(t) + A_F exp(\frac{(-(t-t_n))}{t_D}) > v_i(t) \tag{4.9}$$

where t_n is the time of the most recent spike, τ_D is the DAP decay constant and A_F is the initial magnitude of the facilitation voltage. The facilitation voltage increases the probability of firing transiently after firing has occurred: it exists to fulfil that part of the DAP's function and to ensure the intraburst firing statistics are correct (see Figures 4.7 and 4.8). It represents the last DAP to exceed plateau level and transiently increase the probability of firing.

A valid question is why the DAP voltage $V_D(t)$ is not used instead. Without more information about how the plateau and DAPs interact, it is difficult to know whether DAPs should be allowed to accumulate from the plateau potential. It was felt best to

explore this possibility by depolarising the plateau directly in the model. The DAP voltage also tends to be too large to use: experimentation soon revealed the best fit to the ISI statistics was with a smaller voltage.

There is a state transition when v_a changes from V_p to V_r or vice versa. Vasopressin cells can switch from silence to bursting after just one spike, so the 'tipping point' p for a switch from V_r to V_p at the end of a silent period is the firing threshold, V_t. A burst stops if the ISI is too long, so the tipping point from V_p to V_r is a voltage which will trigger the state change when v_m falls below it. For symmetry, the voltage change needed to stop a burst is the same as that needed to start one, i.e. $V_t - V_r$ above or below v_a. However, transitions are not determined only by fluctuations in input: the DAP makes the plateau less likely to collapse, but autosecretory inhibition progressively makes collapse more likely (Figure 4.5).

At low input rates ($R_{E(I)}$), fluctuations in v_m are unlikely to cause state changes, and more deterministic mechanisms dominate. Vasopressin cells also often show a slow depolarising drift during the silent period [3, 2], so a slow drift was introduced $u(t)$ to modify the tipping point.

The tipping point and conditions for state transition depend on v_a, ie which of V_p and V_r are currently being used as the active resting potential. If V_r, firing has not yet started. The tipping point will then be the firing threshold, modified by any autosecretory inhibition left from the last burst (thus it is possible for the model to fire isolated spikes, as the tipping point will be higher than the firing threshold until the autosecretory inhibition decays). The tipping point also includes the DAP, although this decays far more quickly than autosecretory inhibition: nevertheless, this makes it technically possible for a inhibitory stimulus to fail to end a burst. If it is V_p, a burst is in progress: the tipping point then represents the probability of the plateau collapsing.

$$
\begin{array}{lll}
\text{If } v_a(t-delta) = V_r & p(t) = V_t - v_D(t) - u(t) + w(t) & \\
& \text{And if } v_m(t) > p(t) & v_a(t) = V_p \\
& \text{Otherwise} & v_a(t) = v_a(t-delta) \\
\text{If } v_a(t-delta) = V_p & p(t) = V_p - (V_t - V_r) - v_D(t) - u(t) + w(t) & \\
& \text{And if } v_m(t) < p(t) & v_a(t) = V_r \\
& \text{Otherwise} & v_a(t) = v_a(t-delta)
\end{array}
\tag{4.10}
$$

where $v_D(t)$ is the cumulative DAP:

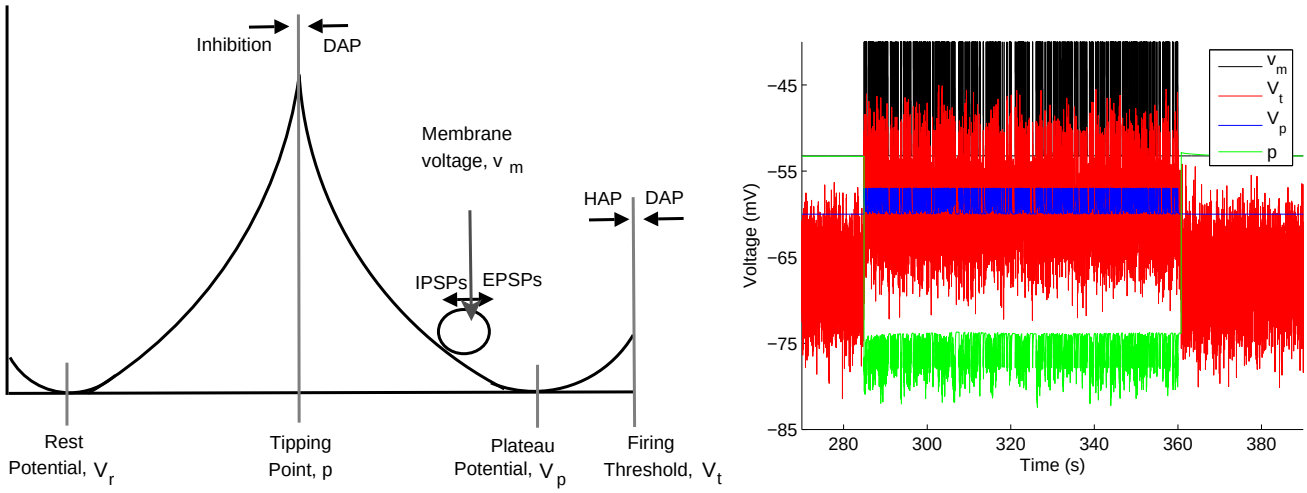

Figure 4.5: Cell Firing Model Schematic and Sample Run. a) The stable states can be imagined as local equilibria of membrane voltage v_m, which the input perturbs. The tipping point can then be shifted to change the probability of transitions from a state to occur. The DAP and autosecretory inhibition influence burst and silence duration, something modelled by moving the tipping point. The DAP also facilitates firing: this is modelled by including a voltage which decreases firing threshold. V_t, with the same time course and similar magnitude to the DAP, referred to as the facilitation voltage. The HAP raises the firing threshold. b) Section of a run for a model cell firing at $\sim$4spikes/s with V_t -53.25mV, V_p -60.0mV and V_r -67.5mV (all parameters as in Table 4.1). Initially V_r is the active equilibrium, and the tipping point is V_t, as firing should be necessary to trigger a burst. When EPSPs elevate v_m above V_t, a spike occurs, and V_p becomes active. The reverse tipping point is now 14.25mV below V_p, minus the DAP for the spike that just occurred, plus the autosecretory inhibition. v_m now decays to V_p, and firing continues, here at $\sim$10spikes/sec. Each spike creates a DAP, which cumulatively decreases the chance of the active equilibrium reverting to V_r by lowering the tipping point. Autosecretory inhibition, however, raises the tipping point until v_m falls below it and V_r becomes active. The burst ends, and the new tipping point is V_t modified by the DAP and autosecretory inhibition. Autosecretory Inhibition still affects the tipping point for some time after a burst has ended, reducing the chance of another burst starting soon after. Even if some spikes occur while the autosecretory inhibition lasts, another burst might not start, as the tipping part is $> V_t$. The facilitation voltage is shown added to V_p, to indicate its influence on further firing: in practise it is subtracted from V_t but this would be difficult to see.

$$v_D(t) = \Sigma A_D exp \frac{-(t-t_s)\Delta t}{\tau_D} \tag{4.11}$$

$u(t)$ is calculated depending on whether a state transition has occurred:

$$\begin{cases} v_a(t) \neq v_a(t-\Delta t) & u(t) = 0.01 \\ v_a(t) = v_a(t-\Delta t) & u(t) = u(t-delta)(1+(1-\frac{u(t-delta)}{D(V_p-V_r)}))\Delta t \end{cases} \tag{4.12}$$

where D is the drift time constant. $u(t)$ thus slowly drags v_m towards the inactive equilibrium.

4.4 Phasic Firing

4.4.1 *in vivo* firing model: statistical characterisation

The aim was to produce a model capable of generating firing patterns that reflected the characteristics important for secretion *in vivo*, and so needed both the spike distribution within bursts and the phasic patterning to be realistic. The HAP and DAP parameters are critical for spike distribution within bursts, and so these parameters were based on matches to the hazard functions in [97]. Hazard functions show the probability of an event as a function of time elapsed since a previous event; for ISIs, they display the probability of a spike as a function of time since the last spike. Thus, a constant hazard indicates that the probability of a spike is independent of time since the last spike, i.e. that there are no post-spike effects on excitability, and that spikes are generated randomly.

4.4.2 The HAP, the DAP and the hazard function

For oxytocin cells [62], the hazard rises slowly from zero after a spike (reflecting relative refractoriness because of a HAP) and is constant from $\sim$50ms onwards (Fig 4.6). For vasopressin cells, the hazard also starts from zero, increases to a maximum at $\sim$45ms, and then declines to a constant level, reflecting a sequence of hyperpolarisation and depolarisation as a HAP is succeeded by a DAP.

The HAP's main effect is on the intraburst firing frequency and the mode: this is reflected in the hazard as an increased depression in the early firing probability. The mode decreased from 47 $\pm$ 3ms to 64 $\pm$ 5ms when the HAP was increase to 17ms

Symbol	Description	Value
Parameters		Default Value
V_p	Plateau potential	-60 (0.2)mV
V_r	Rest potential	-67.25 (0.5)mV
I_w	Increase in autosecretory inhibition	0.015 mV/spike
λ_w	Autosecretory Inhibition decay constant	0.000189
R_E	EPSP rate	190(15) Hz
R_I	IPSP rate	equal to R_E
A_F	Facilitation voltage	3mV
Constants (Fixed for all runs)		Value
	Drift start value	0.01
D	Drift time constant	1min
A_D	DAP magnitude	4mV
τ_D	DAP time constant	69ms
A_H	HAP magnitude	30mV
τ_H	HAP time constant	12.5ms
τ_m	Membrane time constant	8.3ms
V_t	Unmodified firing threshold	53.25mV
Δ_t	time step	0.5ms
A_P	PSP magnitude	2.45mV
A_F	Facilitation voltage	3mV

Table 4.1: Values used with cell firing model, except when otherwise stated

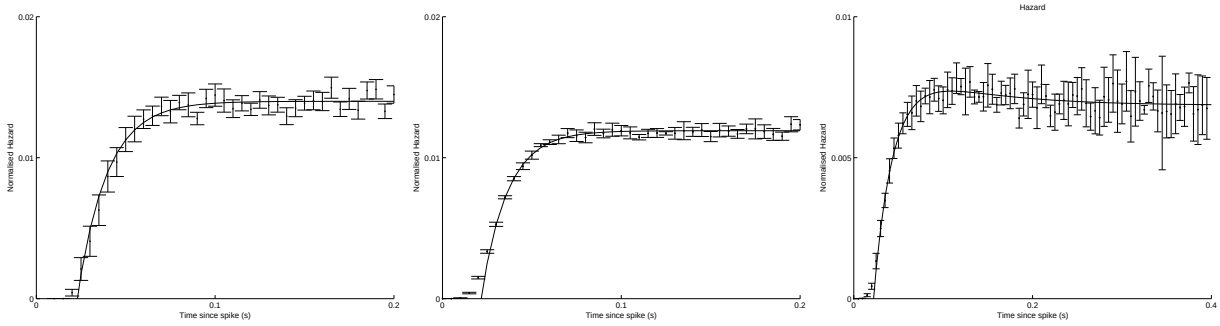

(a) (b) (c)

Figure 4.6: Effect of bistability and depolarising afterpotential (DAP) on hazard. Fits here were done as in methods, but a single exponentials fitted from the first non zero point was found to be sufficient rather than a double. a) Oxytocin hazard function, from [97]. b) With no DAP or plateau, the model resembles an oxytocin cell (Runs of 60 mins, 5 cells). The mean EPSP and IPSP arrival rates are 260/s each, resting potential is -60mV, other parameters as in Table 4.1. Mean Firing rate 8 spikes/s. c) Adding bistability to the model does not produce the distinctive hyperexcitement seen with vasopressin cells: here the plateau potential exists and all parameters are as in Table 4.1, except for the DAP magnitude set to zero. For the firing statistics to be correct, the DAP must influence the chance of firing as well as the probability of state change: the facilitation voltage was designed and added to the model to incorporate this.

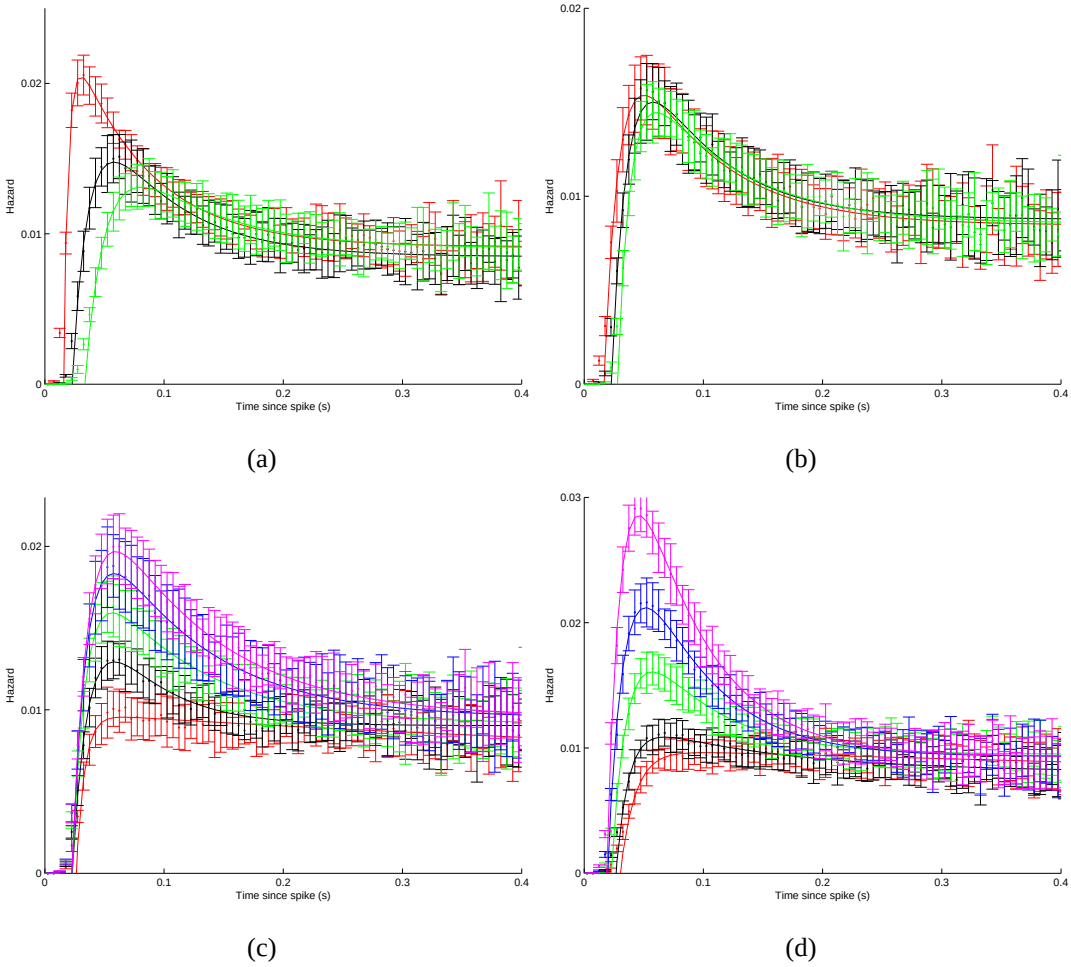

Figure 4.7: HAP and DAP parameters: effect on hazard function. Hazards normalised to first 500ms. Input rate alters the shape of the hazard and thus was kept a constant for 10 model cells run for 60 mins: all other parameters as in Table 4.1. a) The HAP time constants tried were 8ms (red), 12.5ms(black) and 17ms(green). Fits shown are double exponentials, with HAP time constants derived 4.5ms, 13.9ms and 17.3ms, so fitting was generally accurate. b) HAP size altered: from top to bottom -40mv, -30mV, -20mV. c) DAP time constant altered: from top to bottom 110ms to 30ms in steps of 20ms. Duration of the hyperexcitement caused by the DAP increases with the time constant. 30ms cannot be fit properly with a double exponential, but the other times derived from the fit were 49.75ms (for 50ms), 82ms (for 70ms), 85ms (for 90ms) and 91ms (for 110ms). d) DAP size 0-8mv, lowest to highest in steps of 2mv. Fits consistently fitted the DAP $>$ 2mV with a time constant of around -17.5.

from 12.5ms (significant, ANOVA between all 3 groups, p = 1.6e-6). Although input rates up to 400 PSP/s were tried with the longer time constant, the mode could not be reduced below 50ms. Shorting the HAP to 8ms reduced the mode to 26.5ms $\pm$ 2.1ms,. The HAP affects the minimum refractory time, and also the mode.

The intraburst firing firing rose to 5.1 $\pm$ 0.66 from 4.05 $\pm$ 0.4 when the HAP time constant was reduced (significant, p = 0.002), and when increased to 17ms the intraburst firing decreased to 3.5$\pm$ 0.5 (significant vs 12.5ms, p =0.03). There was no significant change in burst duration or silence duration.

As DAP time constant increases, the mode reduces slightly (from 52.5 at 30ms to 46.5 at 110ms: ANOVA p = 0.04). There was no significant change in mean silence duration (p=0.262), but mean burst duration and intraburst firing rate both increased; the intraburst firing rate from 5.7spikes/s at 30ms to 8.7spikes/s at 110ms and burst duration from 39s $\pm$ 13s to 129s $\pm$ 41s (this will be discussed further in section 4.6.4.2). For purposes of matching the ISI distribution, the HAP clearly has a larger effect on mode for less change, and so this was altered to match the distribution.

4.4.3 Choice of parameters

Where possible, values in the literature were used to estimate a range for a parameter, then MATLAB's fminsearch function was used to find an optimal parameter set. The absolute values of V_t, V_p and V_r are not important, only their values relative to each other. In vasopressin cells, the firing threshold is around -50mV [20], and rest potentials are 8-16mV below this [20].

The plateau potential is around -60mV [91]. IPSP rates exceed100Hz [20]: it was assumed that R_E=R_I(=$R_{E(I)}$) *in vivo*. PSP magnitudes are assumed to be 2 to 5mV (as assumed for oxytocin cells, [62]). For the DAP, a time constant of 69ms was used (after [97]). The best match to the ISI mode was with a HAP time constant of 12.5 ms, shorter than the 17ms reported by Sabatier *et al.*. for oxytocin cells; with this, a HAP magnitude of 30mV matched the ISI distribution, and the model was robust to relatively large variations in this. DAP magnitude varies with voltage and [Ca2+] ([4, 16]), but is generally $<$5mV; 4mV was used. The ability to sustain a plateau potential after the end of a burst recovers in 10 to 20s with a time constant of around 5s ([22]).

The parameters are summarised in Table 4.1.

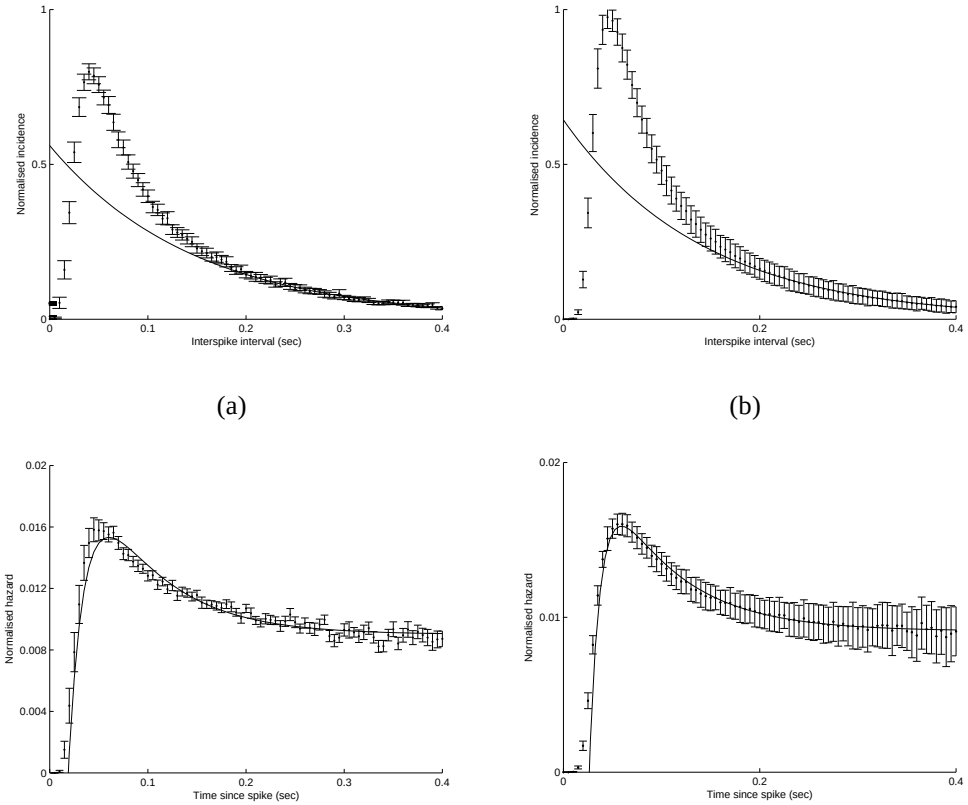

Figure 4.8: ISI distributions and Hazards from experimental and model vasopressin cells, showing inhibition (the HAP) and then facilitation (the DAP) of further firing after a spike. 77 phasic cells recorded from the SON *in vivo*, from [97]. 100 model cells with parameters as in Table 4.1 generated 60 mins of ISIs each. a: Vasopressin cells *in vivo* ISI histogram, shown $\pm$ SEM. Mode is at 45ms. b) model ISI, generated for cell with $R_{E(I)}$, V_p and V_r are randomised, other parameters fixed as in Table1). The model generates a narrower range of modes, and so has a greater normalised maximum at 47ms. c) consensus hazard function ($\pm$ SEM), fitted by $0.009 - 0.075exp(-60t) + 0.02exp(-14.5t)$. d) Model hazard function fitted by $0.009 - 0.207exp(-85.9t) + 0.018exp(-13.8t)$. Thus the model cells have a similar ISI distributions to phasic cells *in vivo*.

4.4.4 Statistical characterisation

100 cells were generated with parameters randomised as in Table 4.1 and run times of 1h, of which all had 95% or more of spikes classified into bursts and were used for analysis. The parameters were set to match closely the observed ISI distributions and hazard functions (Fig.4.8). For both real cells and model cells, the distribution of ISIs $>$200ms is fit well by a single exponential, reflecting the underlying Poisson process. This indicates the firing process is well matched after the first 200ms for intraburst firing (the maximum intraburst period for burst processing is 1s, so the distribution of intervals longer than this is better considered by looking at the burst/silence distribution).

The average mode is nearly the same, in the model population (at 47ms) as in cells *in vivo* (45ms), but the model population has a narrower range of modes. *in vivo*, $\sim$1.6% of ISIs are $<$20msec, and only 22% are shorter than the mode [97]. In the model, 0.2% of ISIs are $<$20ms and 20% are shorter than the mode. This is an inevitable result of excluding frequency adaptation: the bulk of secretion probably occurs during the steady state, as the frequency adaptation occurs at inefficent rate for stimulating secretion and covers a relatively small number of spikes.

4.4.5 Phasic patterning

While many vasopressin cells fire phasically when stimulated, burst and silence durations are very variable *in vivo* [112]. The model population is similar to cells *in vivo* (Table 4.2), but more homogeneous; median and antilog durations are closer to the mean, and the range of burst and silence durations is narrower than observed. Fewer cells have very long bursts and silences, but such cells are relatively rare and so their omission is unlikely to distort the results. State changes in the model are a function of a Poisson process (the input), influenced over short time scales by the DAP and autosecretory inhibition and over the longer term by drift. The coefficient of variation (COV) is a measure of regularity, calculated by standard deviation/mean: here it is smaller than *in vivo*, indicating that model cells fire more regularly (though less regularly than vasopressin cells *in vitro*). This may be due to the absence of frequency adaptation.

This is a subset of the full range available, but demonstrates a range of phasic ability. The range of modes is less in seen *in vivo*, as is the firing range, but this population is initially intended to reflect typical cells rather than those borderline phasic (as those with firing rates under 2 spikes/s and therefore long modes and those firing with very

Measurement, means (SD)	*In vivo*	Model
Number of cells	83	100
Firing rate, spikes/s		
Mean	4.2(1.8)	4.3(0.9)
Range	0.9 - 10.7	2.3 - 6.9
Mean intraburst rate	7.1(2.3)	7.3(1.0)
Range of mean intraburst rates	2.3 - 13.3	4.8 - 10.1
Coefficient of variation	100.6(16.6)%	90.4(2.3)%
ISI distributions		
Mean mode, ms	45(13.4)	47(4.1)
Range modes, ms	10 - 80	40 - 60
ISIs <20ms	1.6%	0.3%
ISIs <mode	22(1)%	17(3)%
Burst durations, s		
Mean, s	62(54)	54(26)
Range of means of different cells	10 - 360	21 - 136
Median of mean duration	42	50
Antilog of mean log duration	48	49
Silence durations, s		
Mean	37(36)	39(23)
Range of means of different cells	4 - 216	14 - 110
Median of mean durations	28	31
Antilog of mean duration	28	34

Table 4.2: *in vivo* statistics: experimental data from [97], compared with 100 model cells with parameters as in Table 4.1.

short modes probably are). In later sections more variable types of firing including non phasic will be considered.

Using a model allows an almost limitless quantity of data to be gathered under identical conditions - a longer recording than is possible with cell recordings. A more precise description of the distribution is therefore possible: the burst and silence length histograms are in Figure 4.9. The histograms can be fitted by an exponential, indicating termination of burst/silences greater than 20s could occurs randomly as the result of a Poisson process. However, during the first 20s of a burst or silence the model and the experimental data differ, something more easily visualised by looking at the hazard (Figure 4.10).

In the model, changes of state are governed by the position of the tipping point and PSP arrival. Factors affecting the tipping point are mostly on too short a scale to be visible here (for example, the autosecretory inhibition has a half life of only 5s: any DAP summation is even shorter). So, state changes are fundamentally a function of a Poisson process (the input), influenced over short timescales by DAP and autosecretory inhibition and over very long time scales by the drift (if the drift is eliminated, it makes no difference to the burst/silence hazards within the first 60s). By comparing the hazards, it is obvious there is an influence missing during the first 20s of the hazard.

To investigate the effect of autosecretory inhibition upon the phasic patterning, different levels of autosecretory inhibition were tried: the autosecretory inhibition per spike I_w was raised from 0.0150 to 0.03 and then 0.05 (parameters otherwise as means in table 4.1, 4800 mins of data, Figure 4.11).This had no effect on the silence hazard or mean silence duration, but it did cause mean burst duration to fall from 49s to 33s and 21s respectively: unsurprisingly, as the number of spikes in a burst required to reach a set level of autosecretory inhibition drops.

The inhibitory half life was extended from 3.6s to 5s and 10s. The mean burst duration fell from to 50s to 43s and then 30s, but silence duration was reasonably constant (34, 35, 36s respectively) Figure 4.11. The longer inhibitory time constant clearly produces a hazard more akin to the biologically derived, however, this conflicts with reports that the plateau recovers within 10-20s [22]. It may seem surprising that the inhibitory time constant has relatively little effect on the silence duration: once autosecretory inhibition passes a certain level it tends to terminate the burst, thus levels at the beginning of silences are fairly consistent. That in both cases altering the autosecretory inhibition affected burst termination but not initiation is consistent with the evidence on dynorphin [25]. This suggest there may be a missing slow inhibitory feedback, or

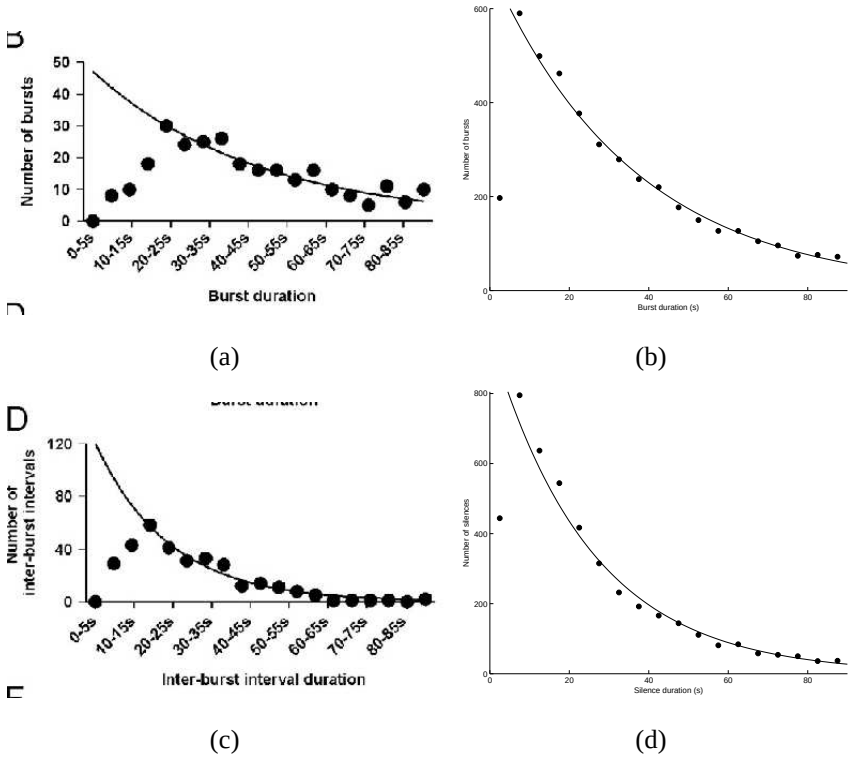

Figure 4.9: Burst and Silence Distributions *in vivo* and in the model differ. Experimental data in a and c is from [26]: consists of 324 bursts from 28 SON cells recorded *in vivo*. Bin size 5s. Model data is in b (burst durations) and d (silences), 4767 bursts from 100 cells. Data fitted between 7.5-87.5ms. In all cases tails of the distributions can be fit by a exponential. For the bursts, the fits over time,t, are $47.111exp(-0.224t)$ (*in vivo* data, a, $R^2 = 0.9$) and $690.249exp(-0.028t)$ (model data, b,,$R^2 = 0.99$). For silences, the fits are $20.08exp(-0.0498t)$ (c, *in vivo*, $R^2 = 0.96$) and $964.308exp(-0.040t)$ (d, model data, $R^2 = 0.98$). The model has a greater proportion of short bursts (10-15s) than seen experimentally, but the distribution of bursts after this point is consistent with the experimental data. The exponential fit indicates initiation and termination could be the result of a Poisson process.

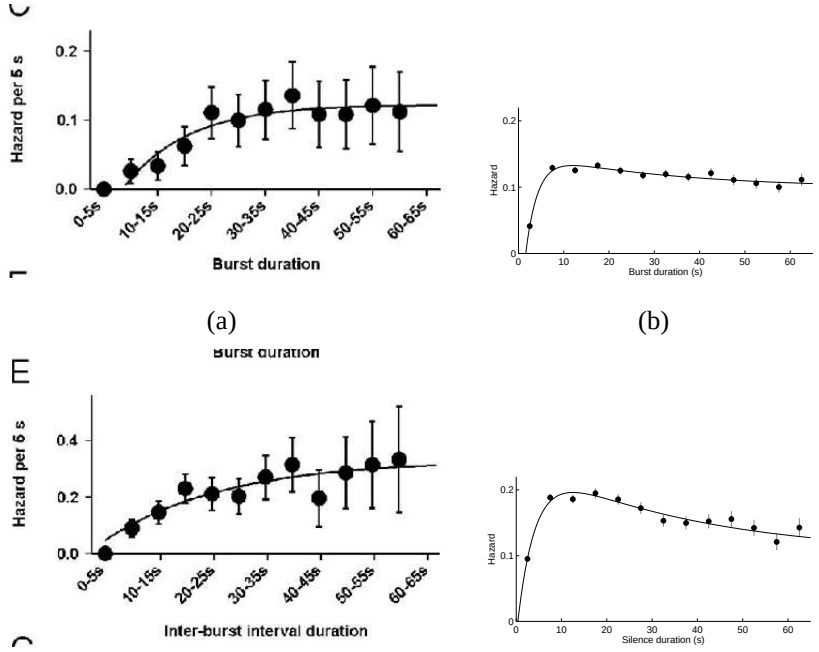

Figure 4.10: Burst and silence hazard functions, showing burst initiation and termination takes longer to recover *in vivo* than in the model. For both burst (a) and silence (c) durations *in vivo* from [25], the hazard indicates termination is initially unlikely due to some stabilising factor, and then ($>$20-30s) random, probably due to fluctuations in the input. The model also indicates burst duration is a function of the input, but the early influence preventing bursts ceasing within the first 20s is absent. This also could be due to autosecretory inhibition increasing and then stabilising. The model lacks this: the DAP is too short term an influence and so burst durations (c) are simply a function of the input after the autosecretory inhibition stabilises, in the first 5s or so (c). Silence duration (d) is also a function of the input. The silence duration does not fall to a constant, but this is because the data is not normalised to be consistent with the original processing.

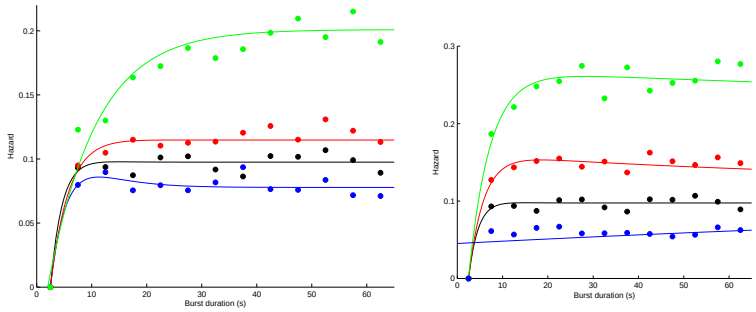

(a) (b)

Figure 4.11: Burst hazards for different levels of inhibitory time constant. This corresponds to the probability of a burst ending. One model cell, run for 80 hours. a) Altering the inhibitory time constant λ_w does not alter the hazard for silence duration (not shown), but it does lead to differing levels of hazard for burst duration. Half lives are 2s (blue), 3.6s (black), 5s (red) 10s (green). The mean burst duration is falling due to the extra autosecretory inhibition, but even the largest half life tried does not impact upon the recovery of the system. b) Different levels of autosecretory inhibition per spike I_w: 0 (blue), 0.015 (black) 0.03 (red) and 0.05 (green). The distribution of bursts alters with increased autosecretory inhibition: bursts become on average shorter. The slope of the highest level of autosecretory inhibition would suggest this is the right distribution, with the wrong mean burst rate. There was no significant effect on the silence hazard function(not shown).

possibly that autosecretory inhibition should be lagged or subject to secretory restraints [94].

4.4.6 Order effects

There should be no relationship between mean burst duration, mean silence duration and intraburst firing rate, except for a weak relation between intraburst firing rate and burst length. The model shows only weak correlations between intraburst firing rates and mean burst or silence length, but it does show a strong correlation between burst and silence length (Figure 4.12).

This is due to the symmetry of the tipping point. There are number of possibilities to break this correlation, all of which involve varying the influences on the tipping point. The most obvious is to break the symmetry of the tipping point directly by randomising the position the tipping point lies below the firing threshold when in a burst. However, it's unclear what this would correspond to biologically (some plateaux are less naturally stable?), so it would be better to alter a parameter more obviously linked to the biology.

The tipping point is influenced by the DAP and the autosecretory inhibition, so these are the obvious candidates for alteration. Varying the autosecretory inhibition per spike introduces an unwelcome correlation between intraburst firing rate and burst length (not shown) as autosecretory inhibition builds up more rapidly over a burst. Varying the inhibitory time constant also failed to break the correlation, probably because autosecretory inhibition in the model is not strong enough (see Figure 4.10 on burst/silence hazards). It should be noticed that the model is still missing a crucial inhibitory feedback (vasopressin),

The DAP time constant has a small effect on burst duration and could break the correlation. Another possibility is to alter $R_E : R_I$:perhaps a more likely possibility, as rates are unlikely to be exactly matched. The next section will look at this, but a brief look will be taken at what happens if the HAP and DAP time constant are altered.

One indication that the HAP should be distributed comes from the small range of modes in the model (Figure 4.13). The coefficient of variation is also considerably less variable than in the biology. The lower the coefficient of variation, the more deterministic the underlying generative process. A value of 100% is consistent a random, Poisson process: the wide range observed *in vivo* (76% to 155%) suggests factors other than IPSPs/EPSPs coming into play, sucha s dynorphin and other inhibitory feedbacks.

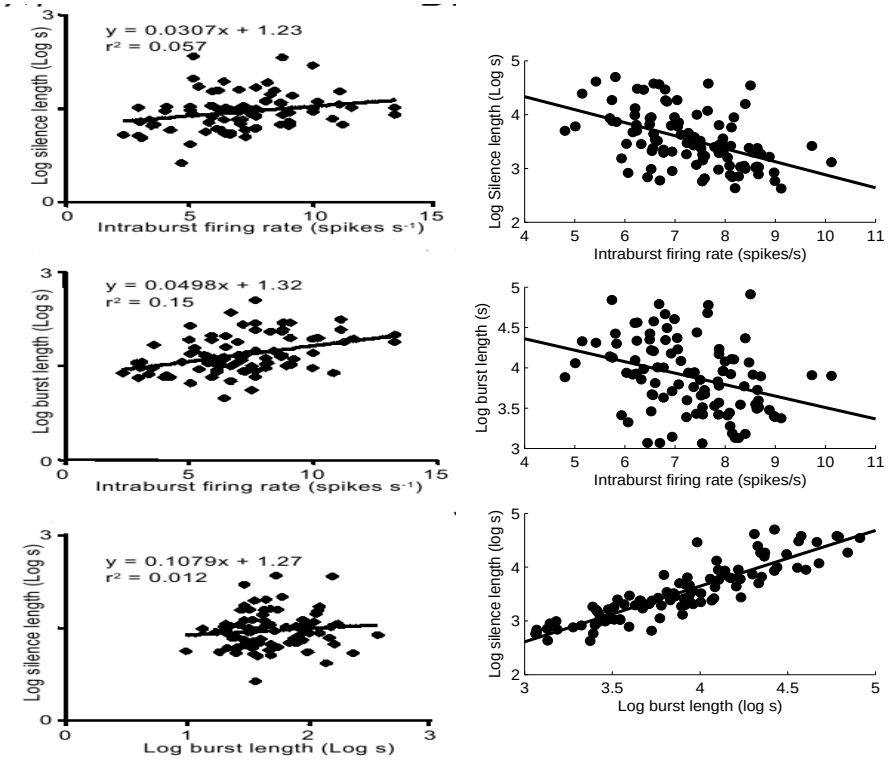

(a) (b)

Figure 4.12: Relationships between intraburst firing rate, mean burst and mean silence lengths, for all cells. Left: *in vivo* data from [97]: only the correlation between intraburst firing rate and burst length is significant, although weak. Right: data from 100 model cells used previously. From top to bottom, there is a weak negative correlation between silence length and intraburst firing rate ($y = -0.24x + 5.30$, $R^2 = 0.24$) , and an even weaker negative correlation between burst length and intraburst firing rate ($y = -0.14x + 4.93$, $R^2 = 0.11$). The most significant relationship is between mean burst length and mean silence length ($1.04x - 0.50$, $R^2 = 0.80$): this reflects that cycle period in the model is a property of the distance between v_a and p, and the input rate, and is the same for both bursts and silences, thus the model contains an unwanted correlation that does not exist in the biology. See text for discussion on how to remove this. R^2 calculated using Pearson's coefficients to match *in vivo* data processing. Intraburst firing rate, log mean burst length and log mean silence length all pass a Bera-Jarque test for normality.

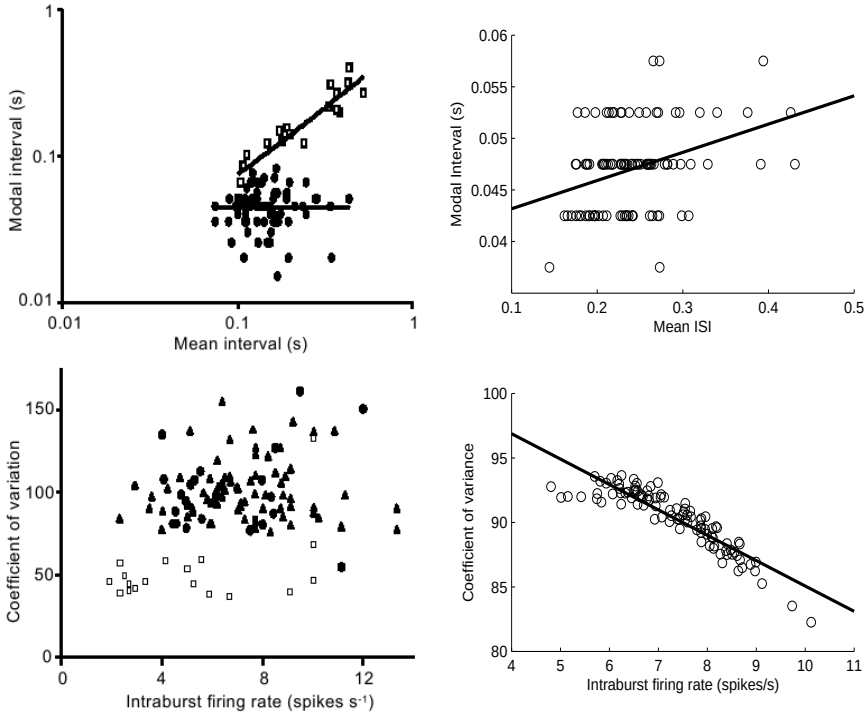

(a) (b)

Figure 4.13: Intraburst firing rate versus mode and coefficient of variation (COV). Left: *in vivo* (solid) data and *in vitro* (clear) data from [97]. Right: model data. There is no significant relationship in the model between mean interval and model interval, although a lower range is observed (line fitted $y = 0.03x + 0.04$, $R^2 = 0.13$). Bottom: COV and Intraburst firing rate are related in the model $y = -1.97x + 104.75$, $R^2 = 0.81$, a correlation not seen *in vivo*. As intraburst firing rate increase, the COV drops. The range of COV seen is also smaller than *in vivo*.

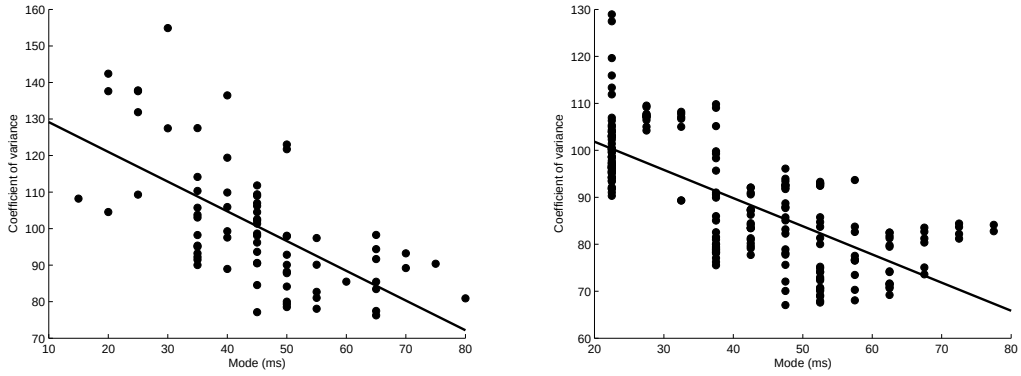

(a) (b)

Figure 4.14: Coefficient Of Variation versus mode: both are affected by the skew of the data and thus it worth knowing whether the model's lack of range of COV is related to the HAP parameters being fixed. a) *in vivo* data for 76 cells provided by G. Leng, same data as that used in [97]. Line fitted is $-0.81x+137.29$, $R^2=0.4$ (R^2 calculated using Pearson's coefficients). The shorter the mode, the larger the coefficient of variation. The coefficient of variation is affected by the skew: a short mode indicates the refractory period enforced by the HAP is shorter, allowing for shorter intervals and increasing the variance. b) The same thing can be achieved in the model by varying the HAP time constant, here to 8ms, 12.5ms and 17ms. This shows a range of modes gained by varying the HAP, against the coefficient of variation: line fit is $-0.60x+113.82$, R^2 is 0.5.

It is known coefficient of variation is affected by skew in the distribution: skew in the model is also related to the mode, which is heavily influenced by the HAP (see Figure 4.7). To investigate this, the HAP time constant was altered to 8ms, 12.5ms and 17ms and data generated at a wide range of input rates (10 cells at input rates of 70 to 390 in steps of 40 PSPs/s).

With a HAP time constant of 8ms, the COV increases: there is less of a refractory period By distributing the HAP time constant, a range of COV values can be attained: this is probably due to the skew of the distribution altering, something best examined by looking at the relationship between mode and COV (Figure 4.14). Altering the DAP time constant had relatively little effect on COV (not shown), and also failed to alter the burst/silence duration significantly.

One difficulty is the ease of disguising correlations in a model by varying sufficient parameters: this may reflect genuine biological variability, but it is difficult to

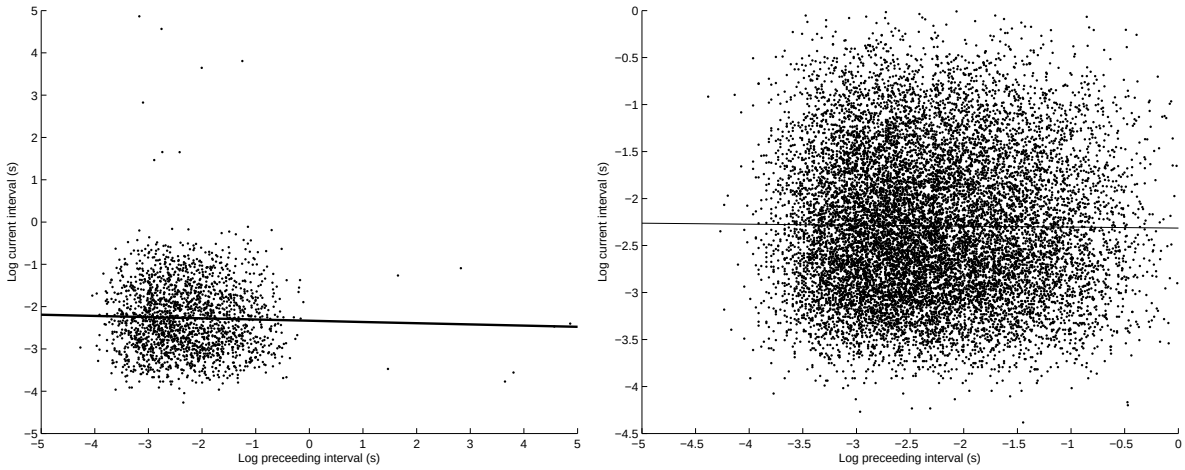

(a) (b)

Figure 4.15: There are no correlations between adjacent interspike intervals in the model. Linear regression calculated as in Sabatier *et al.*. There is no correlation between adjacent ISI intervals in the model: sample cells with firing rate 3.8 spikes/s. a) Using first 2000 intervals: line fitted is $-0.03x + -2.33$, R^2=0.00 b) Using intervals under 1s, to pick out intraburst firing. Line $-0.01x + -2.31$, $R^2 = 0.00$

determine this.

Finally, there should be no correlation between adjacent intervals in steady state firing ($r^2 = 0.02$) [97], and none was observed (Figure 4.15).

4.4.7 What if $R_E \neq R_I$?

This project has assumed that the input rate is balanced, ie $R_E = R_I$. However, it is worth exploring modest violations of this assumption as physiological data on the correspondence of EPSP and IPSP rates *in vivo* is sparse, particularly to see if continuous firing results.

100 cells were generated with parameters as in Table 4.1, except with a wider variation of input rate (std dev 30 PSP/s) and R_I at 100% (20%) of R_E.

In general, regardless of the value of R_E, the greater relatively R_I was the more Q fell (Figure 4.16). The main contributor was a reduction in burst duration - although silence duration also increased. It could be expected that the altering the input balance would have an equal effect on both burst and silence duration, yet clearly increasing the IPSP rate is more influential on terminating bursts than on prolonging silences.

This could be because one only requires a cluster of IPSPs to finish a burst versus a fairly constant stream to maintain a silence, but as the IPSP rate drops EPSP clustering should increase (less IPSP interference). It is therefore more likely to be down to the longer term influences having a disproportionate effect on transitions in one direction. For example, autosecretory inhibition builds up during a burst, moving the tipping point: inhibitory input will then find it easier to cause a transition than EPSPs will once autosecretory inhibition has worn off in the resulting silence.

If R_I is 90% or less of R_E, continuous firing is produced. From then on, firing progressing through phasic patterning to something more irregular (Figure 4.17). The range of modes was 35ms-85s in the sample suggesting this is not the only explanation for continuous firing in the cells where the mode is shorter.

Altering R_E:R_I changes excitatory/inhibitory balance in the model: thus the correlation between burst duration and silence duration is destroyed.

4.4.8 *In vitro* behaviour

In vitro, dynamics are slower: the HAP and DAP are of greater duration. Firing is more regular than *in vivo*, and is not dependent on external excitement to the cell. Afferents to the cells are destroyed to varying degrees, depending on experimental procedure. Cells are often slightly depolarised compared to *in vivo*. Firing can become regenerative.

The HAP and DAP time constants were changed to 77ms and 294ms [97], and the membrane time constant to 12.6ms as the average of various recordings [75, 105, 7].

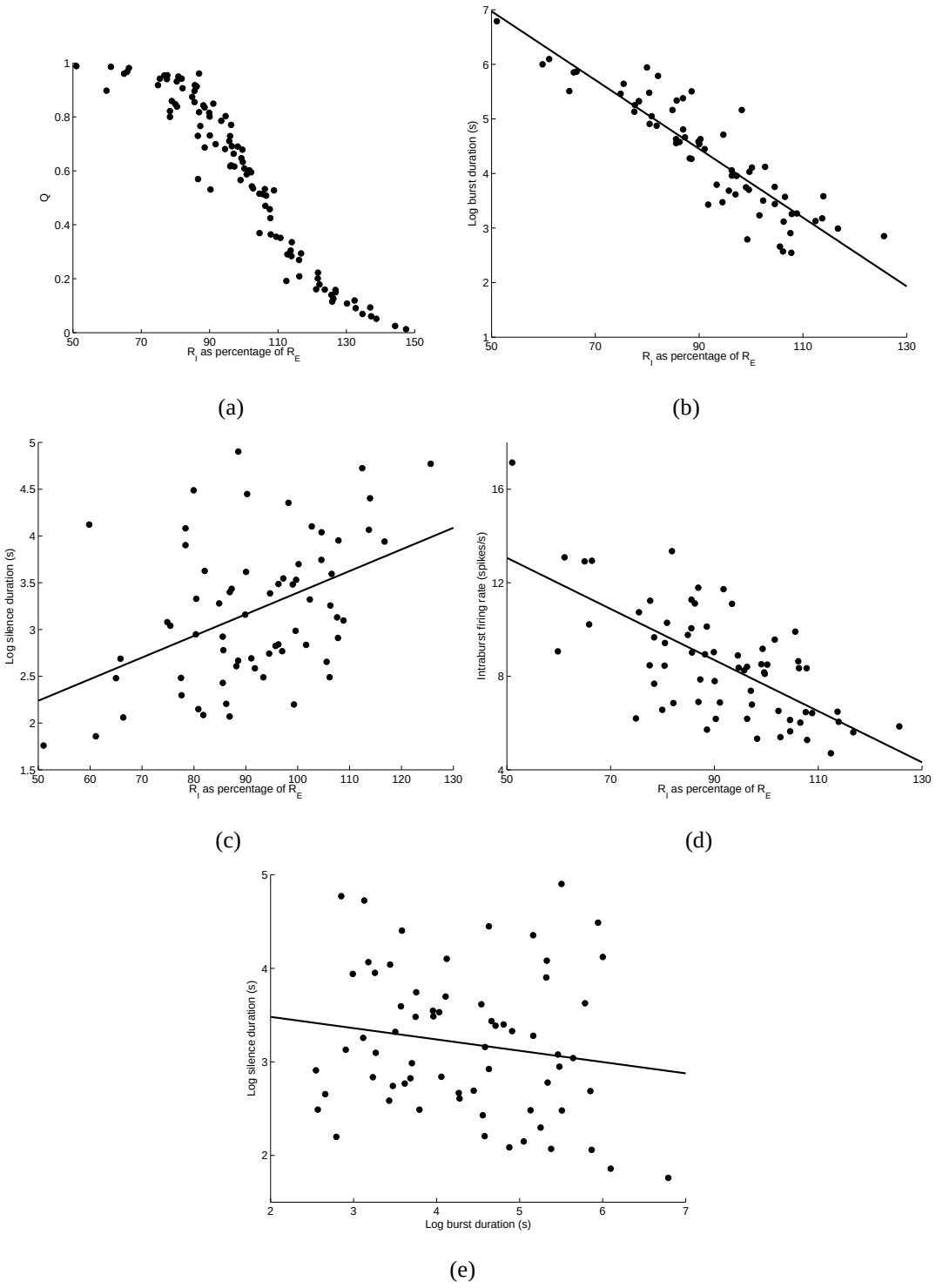

Figure 4.16: Changing the mix of EPSP(R_E):IPSP(R_I). 100 cells, with R_E = 190 (30) EPSPs/s and R_I = 100% (20%) of R_E. a) Increasing the proportion of inhibitory input quietens the cell. Firing is continious when $R_I <$ 80% of R_E. The reduction in Q is mostly due to a reduction in burst duration, b), ($10.125 - 0.063x$, R^2=0.81), although silence duration also increases, c ($1.08 + 0.023x$, R^2=0.20). Intraburst firing rate also decreases, d, ($18.54 - 0.109x$, R^2=0.45). Randomising the EPSP:IPSP ratio does destroy the correlation between burst duration and silence duration, e, ($3.73 - 0.121x$, R^2=0.03), although not between intraburst firing rate and burst duration or silence duration (not shown).

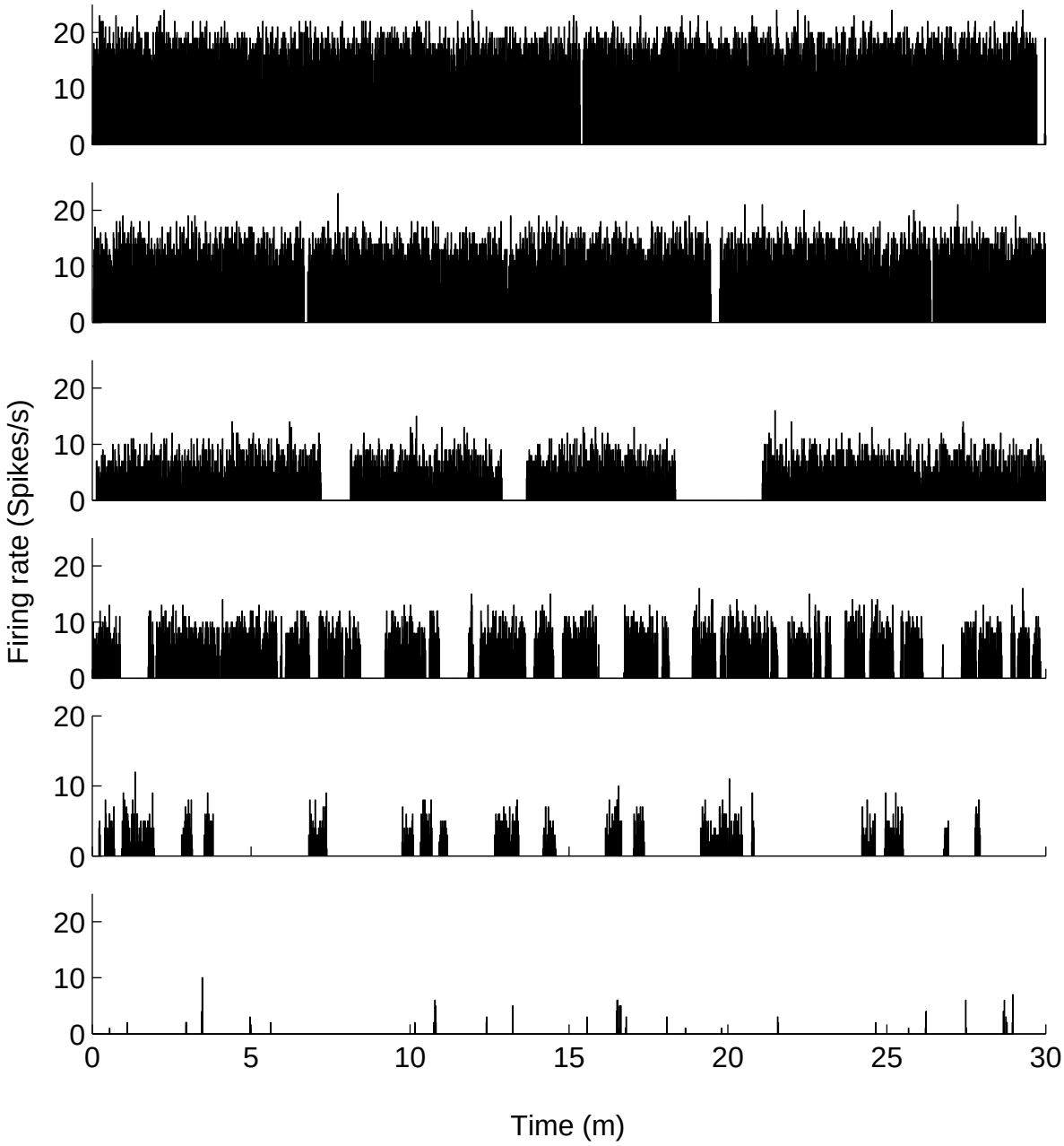

Figure 4.17: Evolution of firing as R_I increases as proportion of R_E: from top to bottom, the percentages are 50%, 66.5%, 80%, 100%, 113% and 148%. R_E itself varies from 240 PSP/s (first cell)to 151 PSP/s (cell 5). Nevertheless, it can clearly be seen that increasing the inhibitory input alters the phasic patterning: at the extremes, firing is not phasic at all and does not resemble the phasic patterns seen *in vivo* (eg Fig 3.1), adding credance to the assumption that EPSP and IPSP rates are closely matched *in vivo*.

$R_{E(I)}$ was reduced to 170 (25)PSP/s and the resting potential depolarised to -65.5mV. Other parameters were as in table 4.1.

This project is unconcerned with *in vitro* behaviour, but whether the model can match the *in vitro* statistics may reveal flaws in the model design.

The shape of the hazard function for the model resembles that seen *in vitro* (Figure 4.18), despite the crude change in parameters (for example, the HAP has both fast and slow components *in vitro*). The hazard function for the model has a later peak and longer tail that those measured *in vitro*: the HAP and DAP should probably be shorter to match the hazard function exactly. However, the shape is generally correct.

The phasic patterning is not so convincing (Table 4.3). Burst durations are excessive and silences brief. This may reflect the lack of longer term powerful feedbacks to counterbalance the improved DAP.

Experiments with raising $R_{E(I)}$ indicated the intraburst firing rate cannot be raised as even a relatively high input rate does not overcome the augmented HAP. This is consistent with the theory that maximal firing is dictated by the HAP.

4.5 Heterogeneity

Heterogeneous behaviour tends to occur as part of a spectrum: continuous cells are normally observed with high firing rates relative to the other types. Cells can also spontaneously change between phasic and continuous firing. There is less analysis available of their behaviour as research has focused on the phasic firing due to its physiological significance, and the difficulty of definitively identifying non-phasic cells as vasopressin has also deterred exploration.

4.5.1 Continuous firing

Phasic firing is considered unique to vasopressin cells: while continuously firing cells are considered oxytocin cells (eg [11]), there are a few vasopressin cells in the group (identified by using CCK [97]). They may have a shorter HAP than the other cells, as the mode of the ISI is shorter [97].

When osmotically challenged, cells may adopt a continuous pattern but this may be a distinct behaviour from the cells that have never demonstrated a phasic behaviour. Wakerley *et al.* saw very few continuous cells during dehydration [112]: continuous firing is seen during injections of NaCl solution [21] at high plasma osmotic pressure.

Measurement, mean (SD)	*In vitro*	**Model**
Number of cells	19	79
Firing rates, spikes/s		
Mean		3.11 (0.35)
Range		2.2 - 3.8
Mean intraburst rate	5.3(3.0)	3.46 (0.3)
Range of mean intraburst rates	1.9 - 10	2.8 - 4.0
Coefficient of variation	54 (22%)	41 (1.6)
ISI distributions		
Mean mode, ms	174(98)	228 (2)
Median mode	177	225
Range modes, ms	30 - 395	185 - 300
ISIs <mode, %		31.65
Burst durations, s		
Mean, s	41(48)	70 (19)
Range of means of different cells	7 - 207	35 -151
Median of mean duration	25.5	64.7
Antilog of mean log duration		64.6
Silence durations, s		
Mean	35(22)	8.5 (2.6)
Range of means of different cells	8 - 67	5 - 20
Median of mean durations	36	8.2
Antilog of mean duration		8.8

Table 4.3: *In vitro* statistics: experimental data from Sabatier *et al.*. [97]. The model has been altered to use the longer *in vitro* HAP and DAP time constants derived in that paper (77 and 294ms respectively), and a slightly longer membrane time constant than *in vivo*. Although not designed to replicate *in vitro* behaviour, the model shows several keys characteristics, such as lower coefficient of variation and longer mode. The model fires almost continuously and at lower rate than observed *in vitro*.

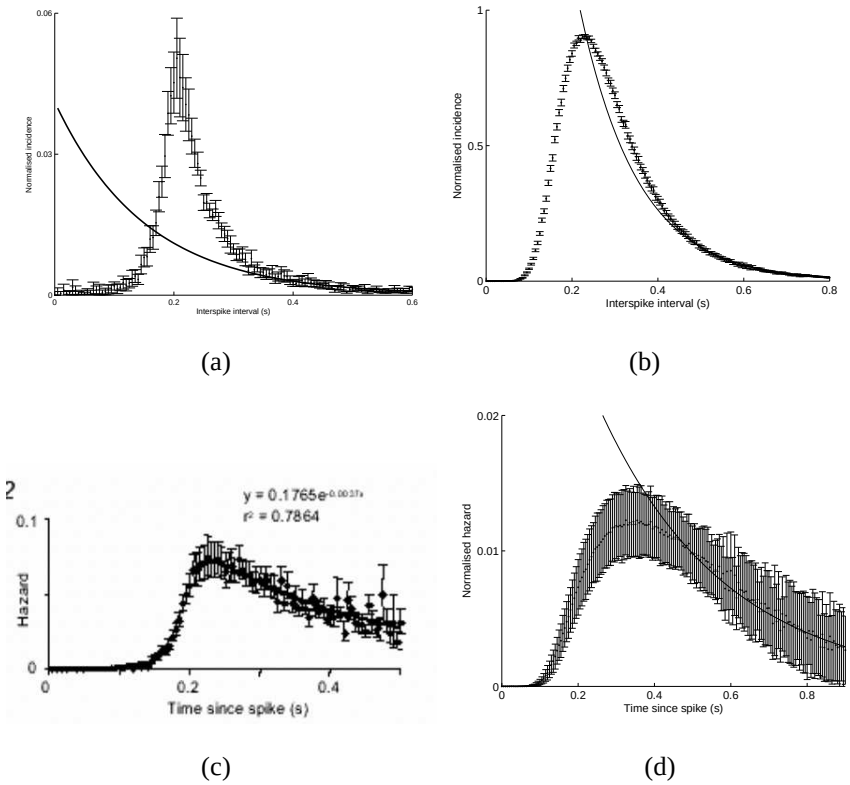

Figure 4.18: *in vitro* ISI and Hazard. Parameters are as in table 4.1, except that HAP and DAP duration are lengthened to the estimated *in vitro* durations (77ms and 294ms respectively), membrane time constant is 12.6ms, mean V_r is -65.5, $R_{E(I)}$ is 170 $\pm$ 25 PSPs/s. 100 cells, 1 hour data. Hazard and ISI distributions are of similar shapes although shifted, suggesting a closer match could be obtained with further alteration to the HAP/DAP. The purpose here was to validate the model by trying a different regime. a) ISI distribution, data from [97] b) Model data: Line fitted from 400ms onwards: again an exponential fits the tail of the data. Note that the peak is shifted compared to the *in vitro* data. c) *in vitro* hazard function, Mean $\pm$ SEM. d) Model hazard function: again, an exponential is fitted to the tail from 0.4s onwards ($R^2 = 0.97$). The tail is longer than with the *in vitro* data, and the peak is shifted. These reflect that the DAP and the HAP respectively may be too large in the model.

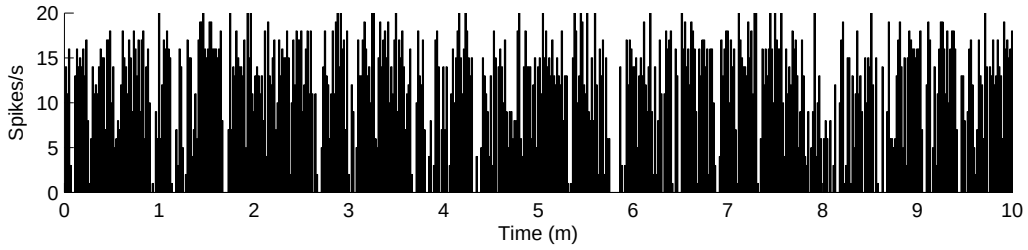

Figure 4.19: Continuous firing due to a high input rate and depolarised resting potential in the model. How frequently transitions between silence and firing occur in the model is a function of the input rate and the difference between V_r and V_t. Increasing the input rate and depolarising V_r as happens under osmotic pressure can cause transitions to occur so frequently bistability has essentially collapsed and continuous firing results. Here, the firing rate is 11.5 $\pm$ 6.1 spikes/s, COV 105.5, and Q 0.89 from a cell with parameters $R_{E(I)}$ 390 PSPs/s, V_r -66.8, V_p -59/9, others as default. The high Q value categorises this cell as continuous as per the scheme defined in methods.

In the model, osmotic pressure is simulated by raising the input rate and depolarising the cell: both of these contribute to increase frequency of transition between V_p and V_r. Continuous firing may then result, as transitions happen so frequently the bistability essentially collapses (Figure 4.19).

This may account for the continuous firing seen during saline injection. However, this results in a high firing rate - consistent with measurement under osmotic pressure [21], but not with the continuous cells seen firing at lower firing rates under physiological normal conditions [97].

How does one generate continuous firing at relatively low firing rate? The likeliest possibilities are either depolarisation of the resting potential to the extent that bistability collapses, or failure of the inhibitory feedback mechanisms. Blockage of the k-opioid receptors can cause continuous firing, probably by elevating the DAP and the plateau [27, 25]. The HAP may also be diminished: while this accounts for a higher firing rate due to shorter refractory period, it is unlikely to cause continuous firing as this will cause more inhibitory feedback, not less. The DAP is also shortened, suggesting an *in vitro* like accumulation to a perpetual plateau is unlikely: however, if both of these are reduced, it's possible that other calcium dependent processes like the sAHP and even the plateau are also affected.

Just reducing the HAP and DAP time constants would have little effect on the model's behaviour: reducing the DAP time constant to the 29ms suggested by Sabatier

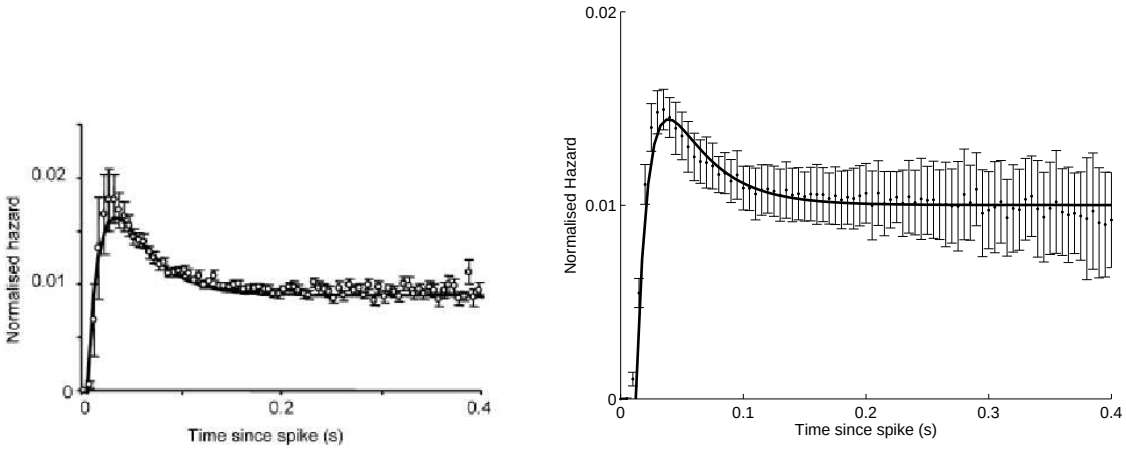

(a) (b)

Figure 4.20: Hazard functions of continuous cells *in vivo* and in the model. a) Data from vasopressin non-phasic cells *in vivo*, Sabatier *et al.* [97]. Line fit is $0.009 - 0.075exp(-60t) + 0.02exp(-14.5t)$ b) Data from 50 cells with DAP time constant 29ms and HAP time constant 8ms. The average mode was 29(4.6)ms, range 25-45ms. Line fit is $0.010 - 0.075exp(-94.5t) + 0.019exp(-28.1t)$, fit from 3rd point $R^2 = 0.84$. This is a reasonable fit to the hazard function, but the model cells are not firing continuously.

et al.. and then adjusting the HAP to 8ms moved the average mode to 30ms over 50 cells run for 30mins. The hazard also resembled that found *in vivo* (Figure 4.20). However, none of the cells fired continuously and coefficients of variation were 91% to 97%. This is unsurprisingly: the model's bistability is largely unaffected by changes in the HAP and DAP.

A further complication is the drift. This is separate from the kappa-opioid feedback: it will force state changes unless the bistability of the model has collapsed.

To adumbrate on the methods of causing continuous firing:

1. $R_E > R_I$: input rate unbalanced: an excess of EPSPs will tip the model towards continuous firing. At $R_{E(I)}$ of 190 spikes/s, Qs of above 0.8 appear at a 90% IPSP:EPSP mix. This could be due to a failure of the nitric oxide feedback. It does not explain changes in the HAP or DAP, especially as the AHP probably saturates under continuous firing.

2. V_r too close to V_p, causing the bistability to collapse. This is however unlikely: if the plateau is still in existence the gaps in firing caused by falls to the resting

potential reveals an almost cyclic appearance to firing. Biologically, this corresponds to a weak plateau mechanism.

3. Inhibitory feedback failure: at the moment, this doesn't affect phasic firing model, but in future with more powerful lagged autosecretory inhibition it may be possible to push the states closer together. However, inhibitory failure would not explain why the DAP and HAP shorten, especially as dynorphin appears to inhibit the DAP [25].

4. Failure of plateau to form. The DAP appears to be curtailed in continuous firing: this may also reflect a disruption of the processes underlying the plateau as well.

Figure 4.21 illustrates each of these.

There is no way to know which of these is responsible for the continuous firing observed, especially without a description of how the DAP and plateau are linked, so modelling of the continuously firing vasopressin cells will not be attempted, especially as their response to osmotic pressure is unknown.

Nevertheless, the model could replicate continuous firing of the type seen under osmotic pressure if required, and it occurs under physiologically critical conditions (osmotic pressure) without alteration to parameters other than input rate or resting potential.

4.5.2 Slow Irregular and Transitional firing

Slow irregular firing occurs in the model with low input rates, and therefore low firing rates, as is consistent with observations. With low input rates, state changes in the model due to fluctuations in the input are rare: the drift is the main mechanism for state change, over a timescale of minutes.

Whether this is realistic is difficult to ascertain: breaks in firing or changes in state of cells are certainly seen biologically. It may be that the plateau does not form until a trigger, such as depolarisation of the cell, occurs. Fortunately, in terms of population performance this is irrelevant: the firing rate is not high enough for cells to deplete secretion seriously, so there are no memory effects. One cell firing for a period of minutes only to be replaced by another beginning to fire may be secretionally equivalent to a silent cell and a slow continuous cell.

As far I can determine, the sole attempt at applying burst recognition software at low firing rates is by Poulain *et al.* [86]. They found sequences of firing tend to be

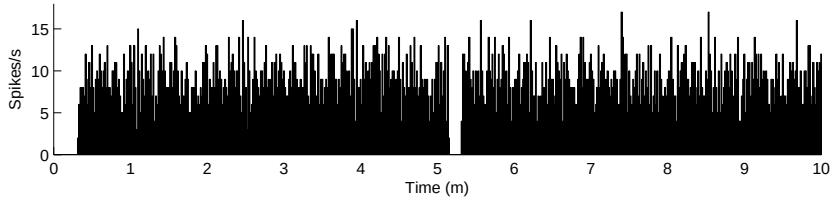

(a)

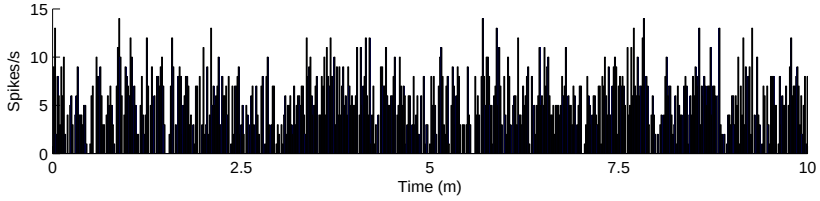

(b)

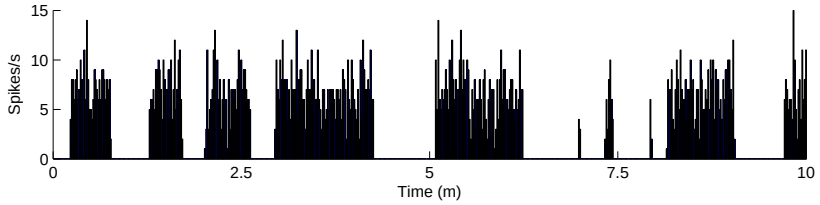

(c)

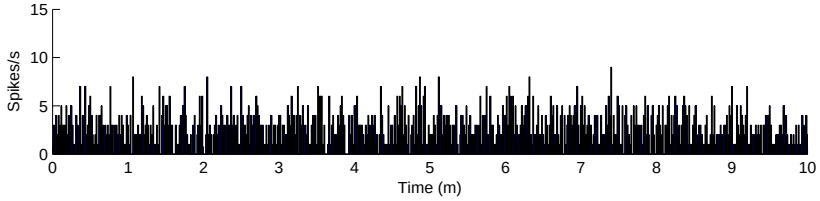

(d)

Figure 4.21: Different methods of inducing continuous firing. a) R_I rate dropped to 80% of $R_{E(I)}$ (= 190EPSPs/s): firing rate is 8.5 $\pm$ 3.5 Q:0.92. Breaks in firing occur, probably due to the drift. b) V_r=-62.25mV V_p=-60mV :with the plateau and the resting potential close together, phasic firing collapses. However, patterns in firing are still visible (firing rate 5.4 $\pm$ 3.2, COV 103, Q 0.93) c: Turning the inhibitory feedback off, $\lambda_w = 0$, does not prevent phasic firing. d: Plateau collapsed: $V_r = V_p$=-63.25mV. Q=0.98, COV = 85.7. firing is continuous: however, the result of destroying V_p is a a lower firing rate for the same input rate, which would imply either continuous cells receive greater EPSP rates than phasic cells or tend to have lower firing rates, which seems unlikely.

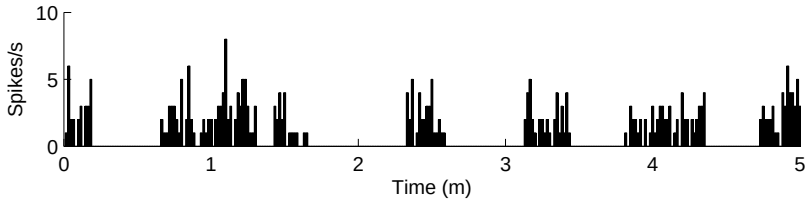

Figure 4.22: Slow Irregular firing: sample cell with parameters V_r=-64mV and $R_{E(I)}$ = 100 PSPs/s, other parameters as default. Mean firing rate is 0.98 $\pm$ 1.45 spikes/s, with Q=0.42. The low firing rate is sufficient to class this cell as slow: however it retains a semi phasic appearance suggesting with higher input rates it will jump to the transitional stage.

very small ($\sim$5s), and separated by small silences at low firing rates. Phasic firing could then be seen as an evolution of patterning from very small bursts, whereas here it is more an evolution from long bursts. However gaps in firing 'within bursts' can be of considerable duration, so it is difficult to process these firing patterns consistently.

4.6 Osmotic Pressure Response

4.6.1 Design

There are numerous experimental protocols for inducing abnormal osmotic pressure (see literature review). As dehydration is the best characterised and understood, it will be simulated. The most useful paper in terms of statistics and number of measurements taken is Wakerley *et al.* [112].

It is known that the cells experience an increase in input rate and depolarise in response to heightened osmotic pressure. It is unclear whether the plateau potential is sensitive to the depolarisation caused by osmotic pressure, so experiments will be done with both the plateau fixed or susceptible to depolarisation. There is also the question of how the component responses to osmotic pressure should be weighted, so each parameter will be varied individually before constructing the protocol.

4.6.2 Input Rate

Raising the input rate results in a linear rise in mean firing rate, mostly accounted for by increases in intraburst firing rates, although silence duration also falls (Figure 4.23). Burst and silence durations are initially large, then falls as the input drives

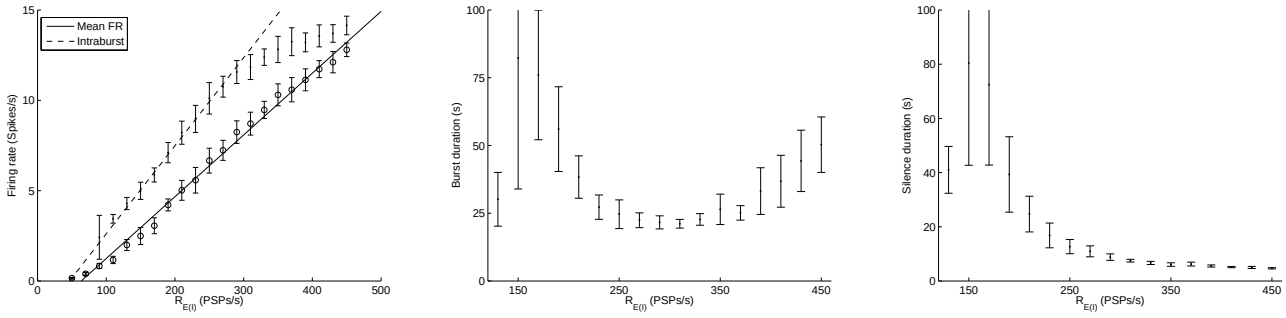

(a) (b) (c)

Figure 4.23: Response to rises in input rate ($R_{E(I)}$). a) Increasing $R_{E(I)}$ results in a linear increase in mean firing rate (open circles, line fit: $0.0342x - 2.17$, $R^2 = 0.99$), partly accounted for by a rise in intraburst firing rate (closed circles, line fit: $0.049x - 2.27$, $R^2 = 0.99$), fit between $R_{E(I)}$ = 70 to 290. The rise in intraburst firing rate cannot be sustained, as it converges with firing rate as continuous firing begins. It will equal the mean firing rate when no gaps in firing can be located. b) Burst durations are initially wildly variable as phasic firing begins to form, then decrease with $R_{E(I)}$ to a constant level and then begin to increase as firing begins to become continuous. That burst durations are relatively constant for a while suggests the autosecretory inhibition is successfully balancing the extra excitation. c) Silence durations fall to a level probably dictated by the autosecretory inhibitory feedback. The autosecretory inhibitory feedback increases the probability of a burst ending by altering the tipping point: the minimum silence duration will be a function of how quickly it clears.

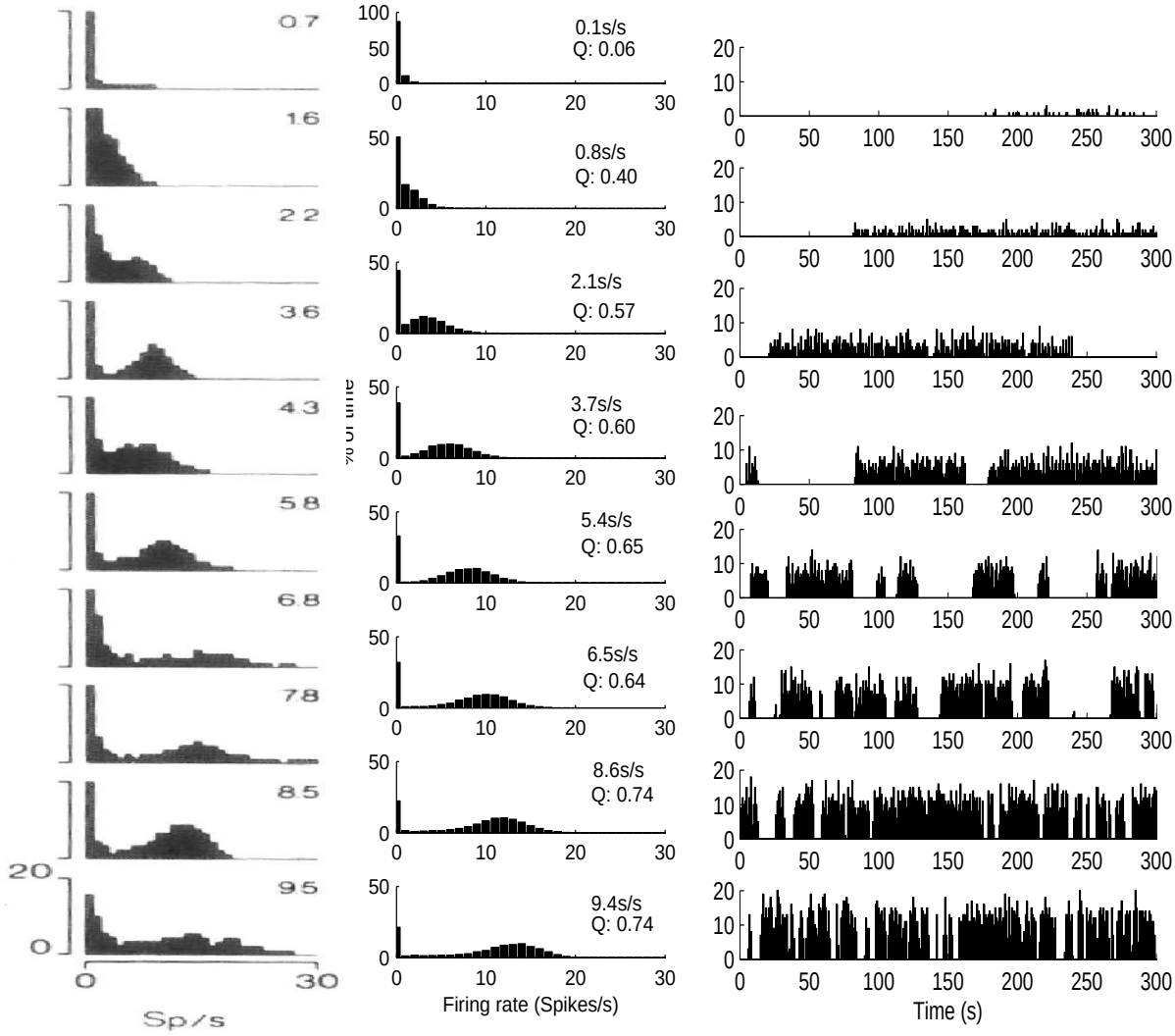

Figure 4.24: Input rate and firing rate distribution. a) Figure from [86]: histograms of firing rates in vasopressin cells. Data was from a pool of 68 vasopressin cells in various stages of dehydration *in vivo*. Phasic cells would appear bimodal as individuals as well. b) Model data: from 120 mins of data from one cell with parameters as as default, but escalating $R_{E(I)}$ (top is $R_{E(I)}$= 50PSPs/s, $R_{E(I)}$ increased by 40 PSPs/s per graph, so 90PSP/s in second row, 130PSP/s in third, etc). The separation of two bumps in the firing rate distribution is a key feature of phasic firing, and it can be seen that this evolves smoothly in both the model and *in vivo*. In both cases the bump is a Gaussian, although the model shows a smoother progression in the centring. Note the differing y-axis: the model has a larger proportion of zeros than *in vivo*, as it tends to have less isolated firing. c) Sample firing from model cells

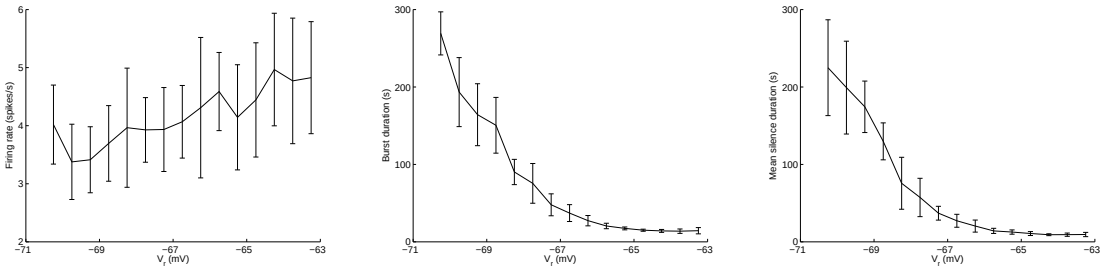

(a) (b) (c)

Figure 4.25: Resting potential, V_r, affects phasic patterning but not intraburst firing rate. a) V_r has no significant effect on firing rate. b) Burst durations decrease, as do silence durations (c) as V_r depolarises. The tipping point depends on the distance between V_r and V_t, so decreasing this distance increases transitions in an even handed fashion. Data from ten runs of 60 mins per V_r with other parameters as default.

more frequent state changes. In the mid-range, burst and silence durations are reasonably constant suggesting that autosecretory inhibition and excitation are fairly evenly balanced. As $R_{E(I)}$ is increased further the inhibitory feedbacks cannot prevent burst duration increasing and a swing into continuous firing. Burst and silence durations eventually fall to a minimum level.

The behaviour produced by changes in input rate is quite realistic: for example, in Figure 4.24 a comparison between the distribution of firing rates shows the formations of a bimodal distribution. This suggests varying input rate is a viable method of forming a range of behaviour.

4.6.3 Effect of depolarising V_r and V_p

During osmotic stimulation, the cells depolarise. In the model it is unclear if V_r, V_p or both should depolarise. This section looks at the effect of altering each individually, while later sections look at the combined effect.

4.6.3.1 Resting Potential, V_r

V_r has no significant effect on the intraburst firing rate as all firing occurs from V_p: it does alter the patterning on firing (Figure 4.25). As V_r depolarises in a model cell, the distance to the tipping point decreases and transition frequency increases: the range of firing then runs from long period firing through shorter to continuous although firing rate itself does not alter significantly.

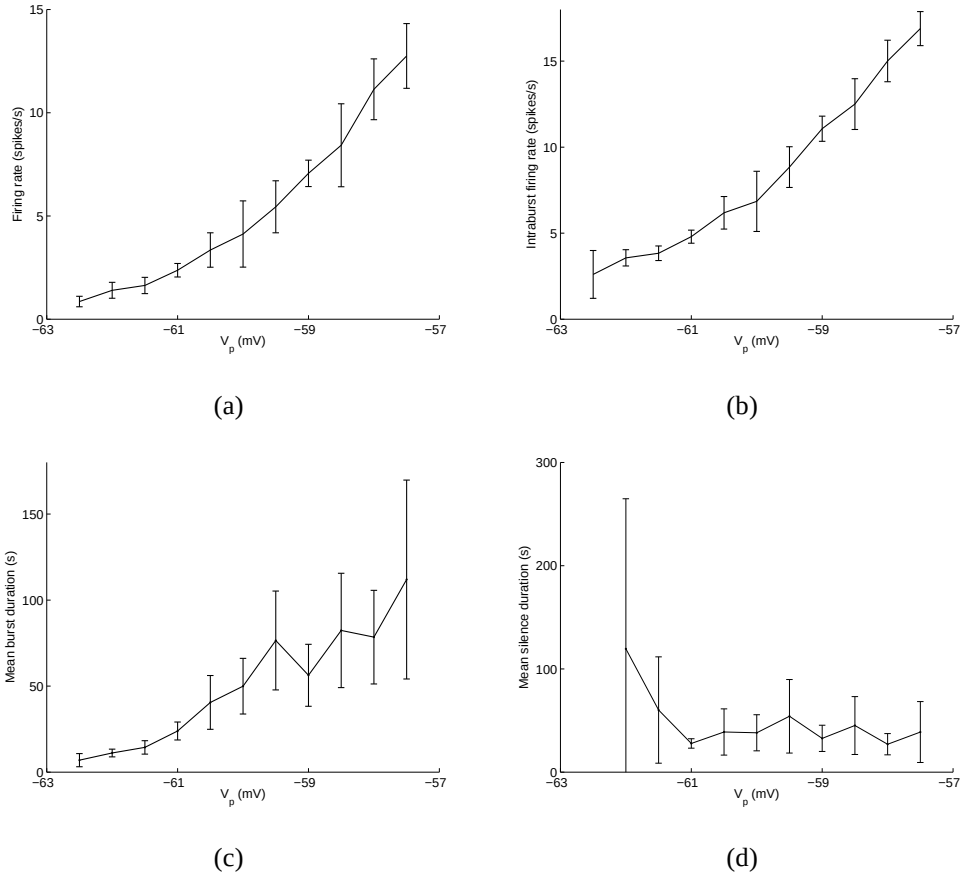

Figure 4.26: Depolarising the plateau potential, V_p, increases firing rate (a) by raising the intraburst firing rate (b). Burst duration also increases (c), although silence duration remains fairly constant (d). The increase in burst duration must be due to the extra DAPs created by the increased firing rate: see text. Data from ten runs of 60 mins per V_p with other parameters as default.

4.6.3.2 Plateau Potential, V_p

Raising the plateau (Figure 4.26) increases firing rate by boosting intraburst firing rate and burst duration. The transitive between states in the model is dependent on the input rate, difference between V_t and V_r, autosecretory inhibition, DAP and drift. The first two factors do not change when the plateau is altered: the changes in burst duration are too short scale for the drift to be an influence. This therefore suggests that the intraburst firing rates creates more DAPs which help to sustain the plateau further, something that doesn't happen when the intraburst firing rate is increased by boosting $R_{E(I)}$.

Raising the plateau gives EPSPs proportionally more effect than IPSPs: they are more likely to create firing and therefore a DAP and a positive influence, whereas

IPSPs have the same chance of forcing a silence as previously. There is more autosecretory inhibition, but this in counteracted by the greater influence of DAPs.

4.6.4 Protocol for simulating raised osmotic pressure

Dehydration can be simulated by a combination of depolarisation and rises in input rate (see literature review). It is unclear whether the plateau is affected by osmotic stimulation or not.

4.6.4.1 Depolarisation of resting potential, with and without plateau depolarisation

The response to dehydration should be [112]:

- A linear increase in firing rate, caused by a linear increase in intraburst firing rate
- mean burst duration of around 20s until the last 24 hours of dehydration, then a rise to around 45s
- mean silence duration constant around 15s
- a linear relationship between osmotic pressure and the reciprocal of the median interval

Rises in osmotic pressure were simulated in a typical neuron by increasing input rates over a wide range and depolarising the resting potential. The plateau was either fixed (Figure 4.27) or depolarised in sync with the resting potential (Figure 4.28). This allows interpolation of different degrees of depolarisation applied at different points.

Either fixing or depolarising the plateau could account for a linear increase in intraburst firing rate. The main difference was depolarising the plateau meant the realistic intraburst firing rate range was covered with a smaller change in input rate. In the key range (5-12 spikes/s), burst durations tended to be larger when depolarised when the plateau could 'move': this reflects that in the hyperpolarised states the plateau is also hyperpolarised, and firing may have gaps in it due to this.

In both cases, increasing input rate reduced burst duration, although this effect was less pronounced with a fixed plateau. Depolarisation shortens bursts - a consequence of a smaller difference between V_t and v_a. The main difference between the protocols - which showed a similar range of burst and silence durations - was the increase in

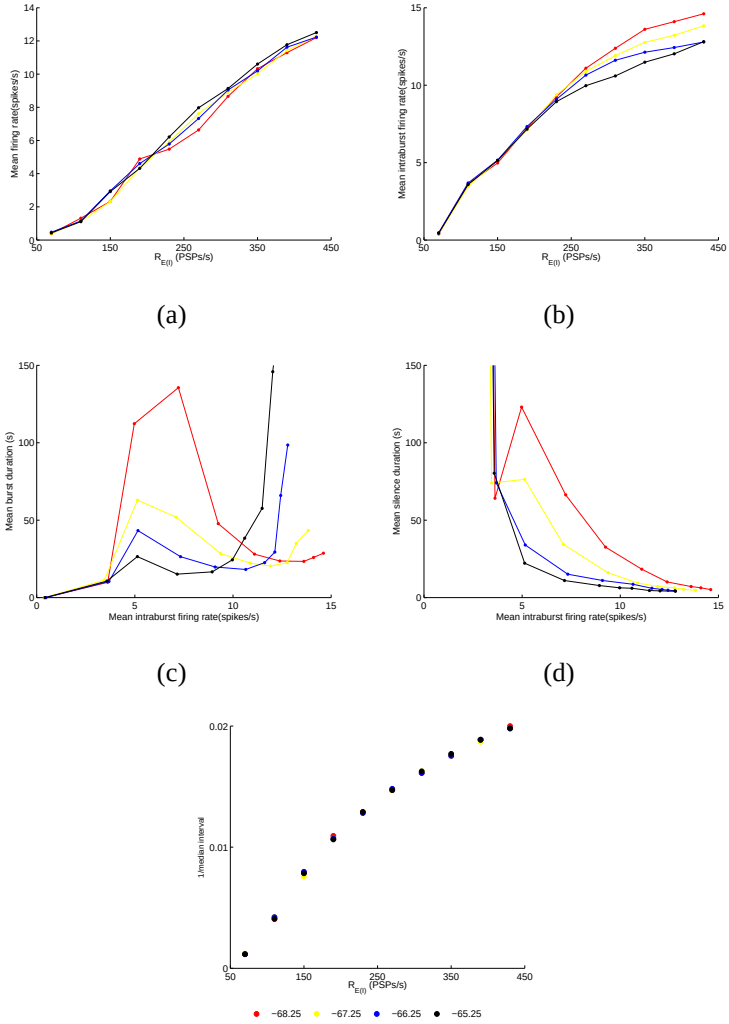

Figure 4.27: Osmotic Pressure, simulated by increase $R_{E(I)}$ and depolarising V_r, with V_p fixed. Firing rate from a neuron over 60mins with rest potential varied from -68.25mV to -64.25mV in steps of 1mV (legend at bottom). V_p was fixed at -60mV. a) Firing rate increases linearly (as observed *in vivo* during infusion of NaCL [62]) b) as does intraburst firing rate regardless of the value of V_r c) Burst duration: plotted against intraburst firing rate. The key range is 6-12 spikes/s, during which burst duration should be around 20s, then rise. Depolarising V_r shortens the point at which burst duration begins increasing. d) Silence duration is within the range observed for most depolarisations and increases with hyperpolarisation e) Reciprocal of median interval should be directly proportional to osmotic pressure. Here, depolarisation has no effect on it and it is linear in the phasic range ($R_{E(I)}$) between around 70-250PSP/s), corresponding to intraburst firing rates of under 10 spikes/s - the range of interest.

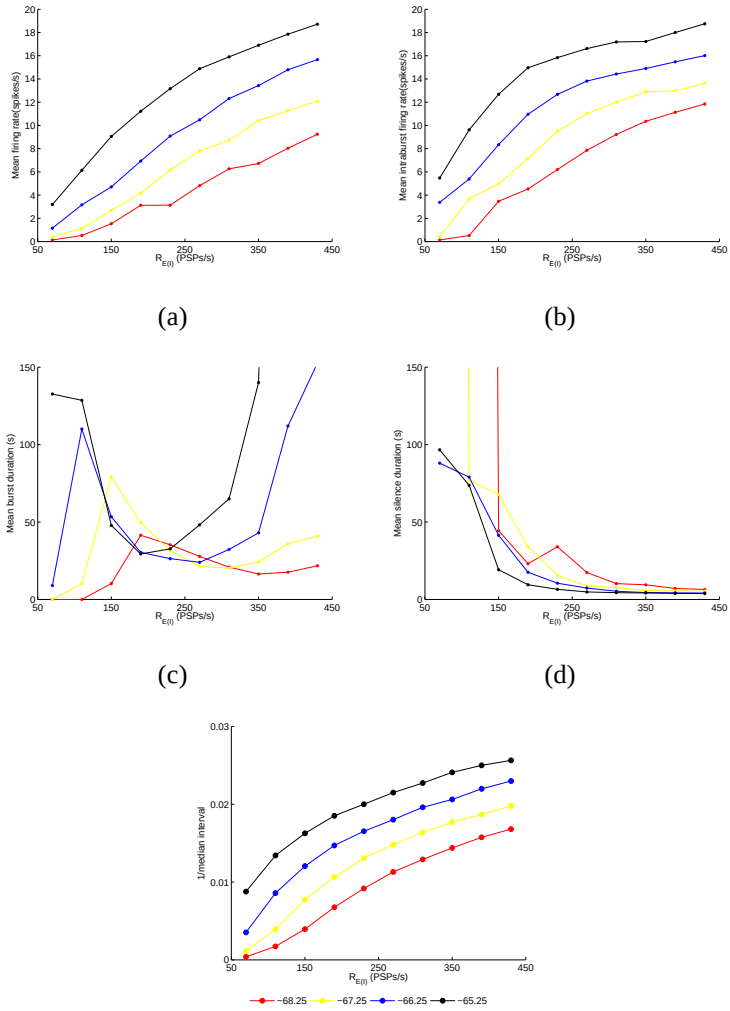

(a) (b)

(c) (d)

(e)

Figure 4.28: Osmotic Pressure: plateau depolarised (V_p) and resting potential (V_R) depolarised during rises in osmotic pressure. Firing rate from a neuron over 60mins with rest potential varied from -68.25mV to -66.25mV in steps of 1mV, with plateau potential always 7.25mV above rest potential. a) Response to increased stimulation is linear regardless of depolarisation: however, steady depolarisation and input rate could also be linear. b) Intraburst firing rate increases until around 15 spikes/s, consistent with the evidence which only noted intraburst firing rates of up to 12 spikes/s. c Burst duration (c) and silence duration (d) Hyperpolarisation increases silence duration, but reduces burst duration (as there is less firing from the plateau) e) Reciprocal of median interval is once again linear when plotted against intraburst firing rate.

input rate required to raise intraburst firing rate. The depolarised plateaux covered the realistic intraburst firing rates with changes in the input within a 100 PSP/s range, which seems small given rates are reported to increase several fold even *in vitro* [92]. This indicates depolarisation of the plateau is limited, and that the plateau may start from a low base.

4.6.4.2 Are longer bursts possible?

Under some circumstances - for example, after 24 hours of dehydration - bursts are reported as having increased duration. This does not happen in the model, where bursts become shorter under stimulation.

Increased intraburst firing is noted during acute stimulation. For bursts to become longer, the DAP must exert more influence than the IPSP rate. Although the DAP has been fixed, there is probably a range of DAP durations, and it could alter during stimulation.

Increasing the input rate increases the intraburst firing rate and consequently the number of DAPs produced: do these DAPs ever outweigh the fluctuations caused by the extra input?

Figure 4.29 illustrates the effect of changing DAP duration. Only with τ_D greater than 80ms was an increase in burst duration seen, and then at the expense of silence duration - more a change into continuous firing. Silence durations do stabilise, at just below 8s. Around 13Hz, burst durations do begin to rise for DAP time constants greater than 70ms. Were there some feedback mechanisms ensuring longer recovery periods, this suggests an increase in burst duration could occur with a sufficiently high intraburst firing rate.

Below 13Hz, burst durations are either steady or even falling slightly, consistent with Wakerley *et al.*'s observations.

4.7 Conclusion

The aim here was to build a computationally lightweight model that could simulate phasic firing, with the characteristics important for network secretion.

This process started with the simplest possible model: a modification of the integrate and fire model developed for oxytocin cells to include the DAP. However the DAP in this simple form could not form a plateau potential.

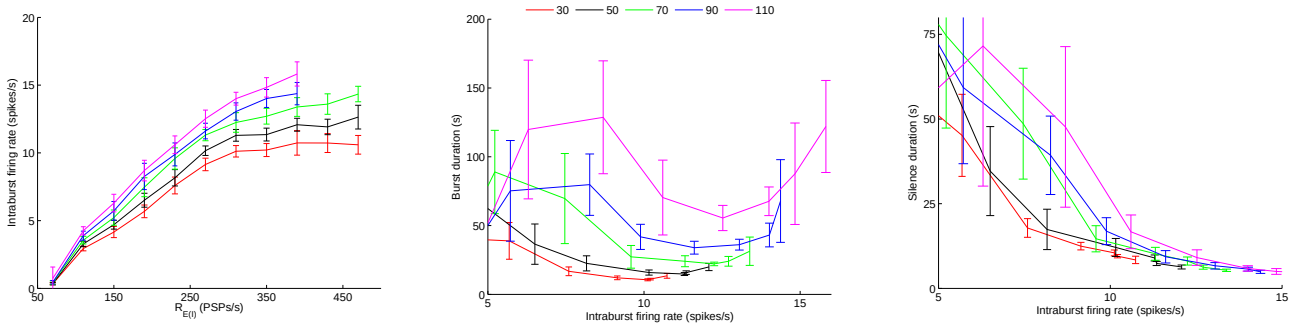

(a) (b) (c)

Figure 4.29: Could a longer lasting DAP ever produce longer bursts? DAP time constants τ_D and burst duration.This experiment was carried out to find if there was a DAP time constant at which the DAP would have a greater effect on burst duration than increases in the input rate. Different τ_D (from 30-110ms) were tried with input rates (10 repetitions of 60 mins, V_p and V_r varied as in Table 4.1), a) Increasing the DAP time constant increased intraburst firing rate, although increases were still linear. No increase in burst duration was observed *in vivo* during dehydration until an intraburst firing rate of around 12 spikes/s was reached after 24 hours.[112]. DAPs with small time constant saturate below this level. b) Burst duration does not increase until a shift to continuous firing is seen. Caution must be taken with interpreting burst duration around the 13Hz mark: up to this burst durations are falling. Afterwards, they do begin to rise, but firing is moving into the continuous range. c) Silence durations was largely unaffected by DAP duration, but continued to reduce over the input range until reaching a base of around 5-10s.

This is hardly surprising: stereotyping the DAP in such an inflexible form without accounting for changes due to calcium dynamics was optimistic, although plateaux were seen with the longer timings seen *in vitro*.

A model of Hodgkin-Huxley type would be difficult to implement, as so many currents attributes are undetermined *in vivo*. It might be possible to sufficiently approximate the necessary calcium dynamics, but this would increase the complexity of the model. The safest option was instead to abstract away from the problem and assume the plateau is successfully formed under some conditions.

Inspiration was taken from the Leng & Brown model [64] for the bistability, but several changes were made. Firstly, both the rest potential and the plateau potential are not active simultaneously: this allows for inclusions of the tipping point concept which allows the autosecretory inhibition and the DAP to be included cleanly. It was important that autosecretory inhibition did not slow firing rate during bursts. Several experiments with adding the DAP to the plateau potential and other methods were tried. Only a small, non-summating DAP was required to match the intraburst firing statistics, but the full voltage the DAP could create was added to the tipping point in the hopes of counterbalancing input rate and increasing burst length under some circumstances.

The distribution of short interspike intervals is a close match. Phasic patterning has been generated to match a subset of the measured range. To then discover which variables could best account for the heterogeneity seen a parameter search has been performed, with resting potential, plateau potential and so on systematically altered.

The parameter testing revealed the model is robust - at no point did it introduce sudden discontinuities in output. It does not necessarily reflect reality exactly, but it does mimic the key features needed for simulating osmotic pressure (a linear increase in firing rate). It also showed the strongest influence in the model tended to be the input rate, which easily outweighed the effects of autosecretory inhibition or DAP summation. Raising the plateau potential increased the intraburst firing rate and therefore DAP voltage without increasing the amount of input required; thus raising the plateau was one of the few ways of increasing burst length. Thus, if under osmotic pressure differences in plateau level could account for different observations, as the plateau level is a sort of gain control.

In general, the hypothesis that cells are driven by a Poisson process (the input), modified by short term processes (the DAP and autosecretory inhibition) has produced a range of convincingly phasic behaviour. The exception to this was at very low input

rates, where the cycle time was unconvincingly long: as a fix the drift was introduced. This has only curtailed the longest burst/silence durations.

Current dynamics are better understood *in vitro*: they are more diffuse and deterministic, thus providing a test of the model's more deterministic mechanics. There were indication a very good match could be produced: the model showed a largely correct shape of intraburst distribution. (with parameters such as the HAP magnitude altered to reflect the dual components of the HAP revealed *in vitro*, this could be centred to the correct mode).

There is also the correlation between mean burst and silence length introduced by a symmetrical tipping point. This almost certainly reflects inadequate dispersion of parameters. For now, it was demonstrated that altering R_E:R_I could destroy the correlation between burst and silence length. Addition of dendritic vasopressin would add an inhibitory influence which could vary between neurons, altering the silence length and also breaking the correlation.

The equations for the model are also more complicated than desirable. In a redesign, it would be worthwhile changing the facilitation voltage to simply be the summated DAP voltage and adapting the autosecretory inhibition and plateau to cope. However, the worst discontinuities are introduced by the tipping point, which changes state immediately and infallibly. Were it to change more slowly, there would be less phasic behaviour in the presence of low input rates, and the drift could then be dispensed with. It's also possible that R_I falls below R_E at low input rates, as there may be less nitric oxide feedback: without the downward pressure provided by R_I, continuous firing at low rates would result.

The system's response to dehydration is congruent with the observed response, although it depends on the parameter framework used to simulate osmotic pressure increases. Regardless of whether the plateau was depolarised, a linear increase in intraburst firing rate and reciprocal of the median interval was seen. Burst and silence durations could be stabilised with the correct range, although no increase in burst duration was observed. This was only observed after a considerably length of time by Wakerley *et al.* [112], and so could reflect rundown of inhibitory mechanisms, or changes in the DAP or other calcium dependent processes.

Chapter 5

Secretion Model

5.1 Introduction

Are vasopressin cells independent of each others functioning? It seems unlikely, given dendritic secretion of vasopressin which may affect a cell's neighbours. So, although functioning on a cell level has been verified by comparison with individual cell recording, a better grasp of the behaviour as a network is required. This is especially true when integrating network features still controversial at experimental level: for example, endogenous vasopressin may be inhibitory, excitatory or regulatory.

There are no simultaneous recording from multiple vasopressin cells with which to compare model network behaviour. There are statistical measures, such as the Q quotient values of activity, that can be used to determine if cells are becoming exhausted or if the network is load balancing effectively. Ultimately, the success of the network is determined by the efficiency of secretion, and this is difficult to quantify simply by looking at individual patterns.

A model of pituitary arginine vasopressin (AVP) secretion is required to help evaluate the network: making the model before the vasopressin network model is completed ensures the result is unbiased.

It is important to note that the model here only has to replicate the existing results and interpolate between them in a sensible fashion, not provide a hypothesis for axonal functioning. The main purpose of this model is to provide a evaluation function for firing; as such it is very important it is as simple as possible. Many of the functions are therefore not tied to biological processes.

5.2 Experimental Evidence and Justification

Why do vasopressin cells fire phasically and not continually? Once the unusual bursting pattern of vasopressin cells was noted, experimentalists turned their attention to the secretion of AVP, to see if the behaviour of axon ending in the pituitary explained the pattern.

A summary of results from the early experiments is provided by Dyball [36]. Secretion is enhanced by a phasic rather than continuous pattern. Key to this is a fatigue mechanism: secretion tails off after a minute of stimulation, and an interval of around about 20s is required for recovery. If burst size increased beyond 45s, a longer interval of 90s would enhance secretion. In the longer term, patterns used for more than an hour are noted as eventually exhausting response, unless of large cycle time.

There is also an early facilitation of vasopressin secretion: as burst duration increases from 5s to 20, the secretion per spike increases linearly. This is a strange result to explain: calcium influx appears to stabilise too early to explain this effect [79], even with a lag, although possibly intracellular calcium stores could play a role.

Although secretion was known to be Ca2+-dependent early on, recent advances in fluorescent indicator dyes to measure Ca2+ levels have provided a good characterisation of calcium dynamics at the axon terminal [79]. Calcium influx is dependent on the frequency of the pattern used: there then occurs a decay on several different timescales. This can cause a plateau of residual calcium: Muschol & Salzberg [79] suggest the pattern of secretion is optimised by maximising this quickly.

Measuring AVP secretion directly has often proved problematic: most sampling techniques have poor time and space resolution, especially compared to calcium dynamics. One alternative is to measure membrane capacitance (during voltage clamp): this changes as the surface membrane distorts to secrete or absorb vesicles (eg [104]).

Secretion does not behave precisely as calcium does. For example, secretion fatigue is seen even in the presence of further calcium influx, and often lags calcium influx by a variable amount [104]. The availability of vesicles at the membrane, and exhaustion of a ready releasable pool may account for some of the nonlinearity. Jackson et al [55] noted calcium concentrations and vasopressin secretion were both maximal around 10Hz, but vasopressin secretion fell off more quickly around this value than calcium concentration, implying a somewhat nonlinear relationship.

A full schematic of available data is in Figure 5.1. In short, as in common with other secretory systems, there appear to be at least two pools of vesicles: a ready

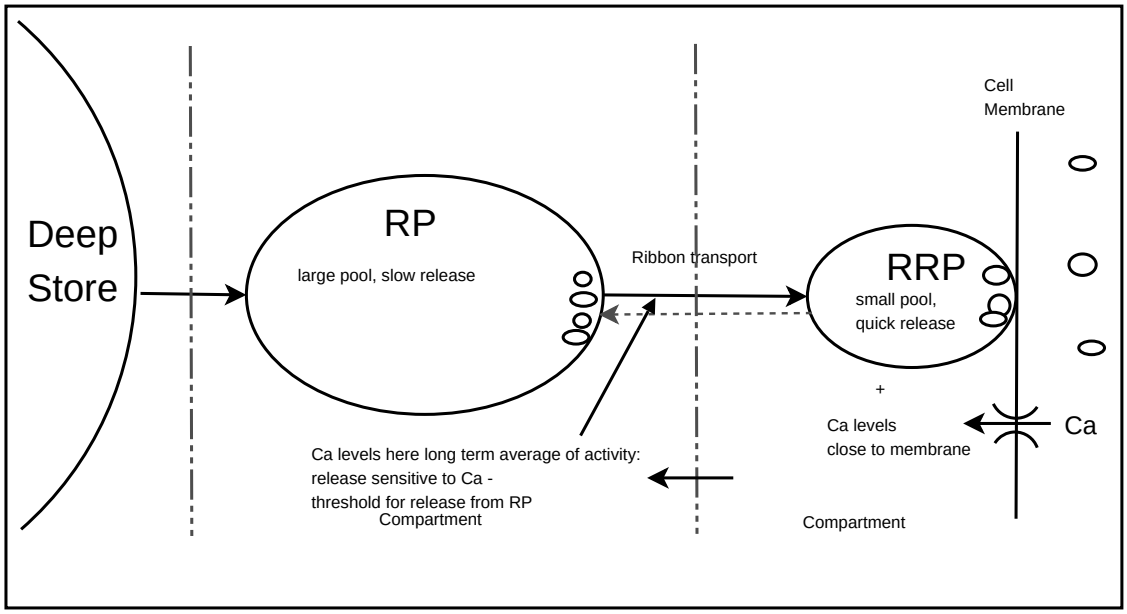

Figure 5.1: Full Schematic for known AVP secretion process. This diagram illustrates the working hypothesis for secretion at the axon ending with known experimental evidence. Although many point remain to be clarified - for example whether the RRP is a separate pool or a subset of the RP - this gives a general outline. Calcium levels build during release, with the RRP dependent on calcium levels close to the membrane, which fluctuate more rapidly than the compartments the RP responds to.

releasable pool (RRP) and a slower yet larger store termed the reserve pool (RP) [45]. The small RRP secretes AVP proportional to calcium change [104], suggesting the pool is located close to the calcium channels in the cell membrane. Ca levels near to the pool will then rise as the calcium current is integrated. The RRP appears to be sensitive to the intracellular Ca concentration, requires a threshold value to activate and thereafter rises with influx until a threshold value is reached [45]. It is responsive to Ca levels belonging to a compartment away from the cell membrane, where Ca may accumulate and disperse in a manner different to submembrane compartments, and in a way that involves more than a single Ca binding step [100].

Further complications from divining the exact relationship between calcium concentration and secretion arise from the methods for measuring calcium, which had to measure an average of the concentration. The resolution in experiments examining secretion is usually not sufficient to separate compartments. In addition, calcium buffers complicate in nonlinear ways the relationship between calcium influx and ca concentration.

The RRP and RP account for secretion in response to a train in the order of seconds. Response variations over a longer time frame, in the order of minutes [12], would have to be accounted for by a third pool. It is also unclear whether the RP secretions directly itself, supplies the RRP, or indeed whether the RRP could be a part of the RP pool as has been suggested for chromaffin cells [110].

No model exists for secretion from vasopressin neurons. However, models do exist for chromaffin cells [52, 31] and has been suggested for melanotrophs [108] along similar lines. There is not enough evidence of the mechanisms at the axon ending in vasopressin cells to be certain their functioning is the same, but this style of secretory mechanism is clearly common and in lack of any contradictory information forms a reasonable working basis for a model. There are also many models of calcium dynamics (eg [90]).

When determining success of this model, unless calcium is modelled explicitly, the best evidence comes from the early papers, which specify secretion amounts for certain patterns. The model built should display both fatigue and facilitation, with a maximal pattern having bursts of between 20-40s and a silence of around 20s. Secretion of AVP should match that seen with different frequencies [79]. This model is not aiming to model all the above complexities at the axon ending: instead it is trying to provide an interpolation from the known data while remaining consistent with the likely underlying mechanism. Later refinements could aim to increase the biological

plausibility.

5.3 Design

The scheme outlined above is too complex, given the computational constraints - and, more importantly - lack of quantification of the many biological functions. This model is intended to provide a system of evaluation for the vasopressin cells networks. As such it should match secretion data on the timescales of importance. It does not have to match the known biology, and indeed, not enough is known of the biologically mechanisms to do so. However, biologically plausibility is helpful for constraining the model.

The secretion data covers time periods from variations in spike patterning (ms, [30]) to hours [12], with less experimental data toward the extremes. Here, the main aim is to match data in the timescale related to bursting, seconds: it will be assumed that small variations in spike timing are largely irrelevant.

The following simplifications are used when converting Figure 5.1:

- The back rate reactions will be modelled implicitly. This is the most likely mechanism for a pool to sense how quickly the one it is feeding is emptying, but it will be assumed it can simply do this.
- Modelling calcium reactions are computationally expensive, and to be avoided. Their main functions in the timescales of interest will be abstracted into a slow reacting variable.

5.3.1 Equations

Secretion is dependent both on the history of the cell - here represented by how depleted the pools are, and a slow variable used to provide an average of recent activity - and on the immediate state. It is difficult to be sure how long secretion continues after a depolarising pulse ceases - the most time resolved measure uses membrane capacitance in which late exocytosis may be screened by endocytosis [45] - but most likely it only ceases within a second.

At least a model that describes the relationship between activity and secretion is needed, and the model developed was inspired by current understanding of secretion from chromaffin cells [52, 31] and melanotrophs ([108]).

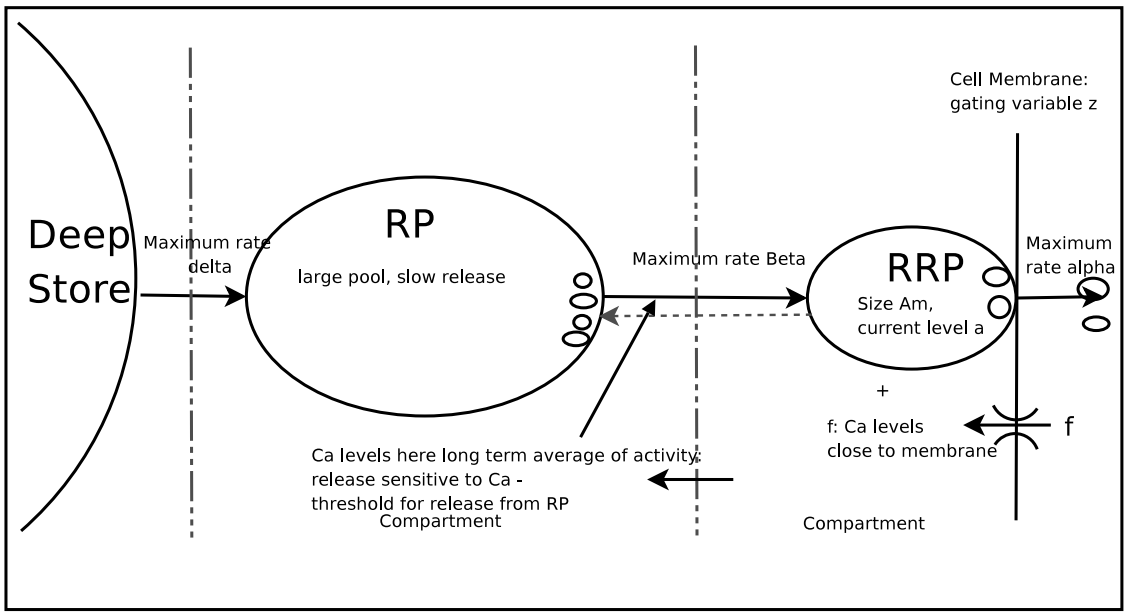

Figure 5.2: Model approximation of full process. Here **z** is the gating variable which cuts off secretion if no recent spike has occurred, **f** is a variable used to calculate facilitation of secretion and **g** is a quick clearance mechanism. The pool refill rate constants are alpha, beta and gamma for the RRP, RP and deep store respectively: the actual output from the pool is also dependent on how full it is.

The model includes:

- **z**, a variable that increases by a constant amount per spike (Z_d) and decays with decay constant Z_d. z is a gating variable used to ensure secretion continues only for a short period after firing.
- **f**, a second activity dependent variable controlling the facilitation, but this time the increase per spike f_i is variable, and decays with time constant F_d. A second decay mechanism for f operates only when z is below a threshold (ie, f will decay more quickly if there has been no activity recently). This is necessary, as f must disperse more quickly during a silence than it accumulates during a burst.
- **g** The second decay mechanism for f, designed to clear it quickly between bursts.
- **Ready Releasable Pool (RRP)**, maximum size A_M, current level a and secretes at a rate constant α modified by f and a.
- **Releasable Pool (RP)**, maximum size B_M, current level b and secretes at a rate constant β modified by levels in the RRP and RP.

- **Deep Store** Assumed infinite, associated rate constant δ

It is assumed here that secretion, x, continues only as long as the cell is depolarised in the wake of a recent pulse, and depends on facilitation the level of the RRP. These factors will be discussed in order and then the equation for secretion produced.

A simplistic measure is used to track whether there has been sufficient recent activity to justify secretion. It is assumed that vasopressin is secreted from the RRP only if activity dependent variable z is sufficiently large. z is incremented (by a constant Z_i) with every spike, and which decays with decay constant Z_d.

$$\Delta z(t) = \begin{cases} Z_i - Z_d z(t-\Delta t)\Delta t & \text{After a spike} \\ -Z_d z(t-\Delta t)\Delta t & \text{Otherwise} \end{cases} \tag{5.1}$$

The question of recent activity is important for facilitation. At a given frequency, secretion per spike increases with the number of spikes fired, up to a limit, so secretion was made proportional to a variable f, incremented by every spike, which decays with decay constant F_d. Facilitation takes up to 15s to develop fully, but only 5s to reverse [101], so f is reset rapidly after firing has stopped, via another variable g.

$$\Delta f(t) = \begin{cases} -F_d f(t-\Delta t)\Delta t + f_i(t) - g(t) f(t-\Delta t) & \text{After a spike} \\ -F_d f(t-\Delta t)\Delta t - g(t) f(t-\Delta t) & \text{Otherwise} \end{cases} \tag{5.2}$$

where f_i is the increase of f with each spike, and g is dependent on z:

$$\begin{aligned} z(t) < Gt \quad & g(t) = G_1(G_1 - z(t))\Delta t \\ z(t) > Gt \quad & g(t) = 0 \end{aligned} \tag{5.3}$$

where G_1, G_2 and G_t are constants. G_t is a threshold above which g reduces f. f_i, the increase in f per spike, is also variable:

$$f_i(t) = (F_2 + (1 - f(t-\Delta t)) f(t-\Delta t)) F_1 \tag{5.4}$$

where F_1 and F_2 are constants. f_i is sigmoidal: initially the increase in f_i will be slow, then accelerate until approaching the maximum at which point it slows again. Figure 5.3 illustrates the behaviour of f, g and z during bursts.

A number of differing forms for f were tried, but this one produced the most appropriate secretion curve. Although f is not equivalent to calcium, the form used above is intended to roughly replicate some of the dynamics. If one thinks of the underlying

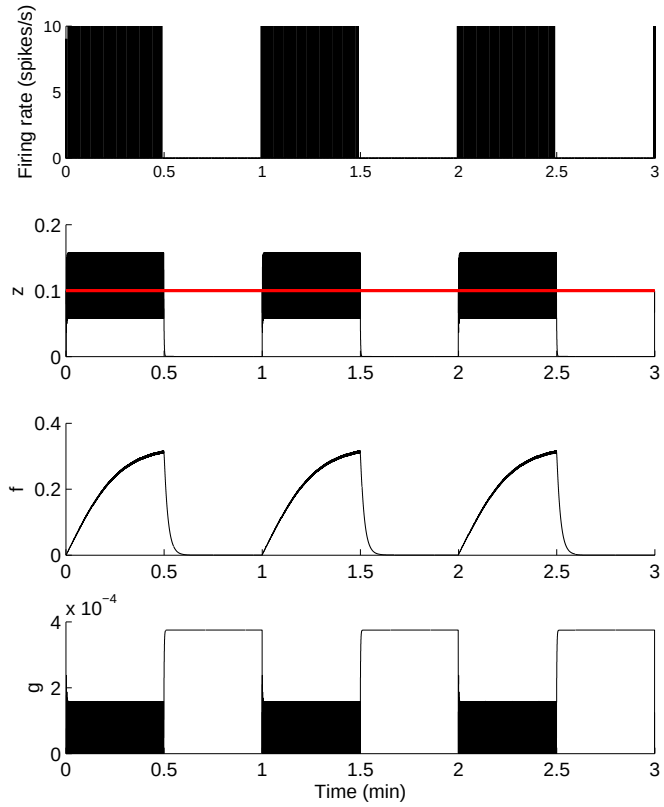

Figure 5.3: Secretion model: z (the gating variable), f (facilitation) and g (activity dependent clearance of f). The top graph here shows the input to the secretion model: bursts of length 30s delivered at 10Hz. Each firing instance increases z, which must increase above A_t (0.01) for secretion to occur. Marked in red is G_t, the threshold below which the fast clearance pump g is activated (bottom trace). The third graph shows f controlling facilitation for secretion: this accumulates during the burst, but is cleared very quickly after a burst by g. In the bottom trace, g is illustrated: while active briefly during firing (z is oscillating around the threshold for g to activate), it is mainly active during the silence where it clears f rapidly. The decay g enforces on f is proportional to f: thus it acts to slow growth of f during a burst and clear f rapidly during silence to prevent bursts evoked close together from benefiting from the last burst's facilitation.

calcium dynamics - although these are complicated by compartmentalisation - calcium will eventually inhibit more calcium entry, but in the mid-range it is boosted by Ca2+ calcium stores. This implies calcium concentration increases most greatly when a medium concentration of calcium exists. This form also produces a steep increase in secretion as stimulation increases, useful for fitting the data.

Secretion, $x(t)$, occurs if z exceeds a threshold, A_t:

$$x(t) = \begin{cases} a(t)\,f(t)^2 \alpha \Delta t & z(t) > At \\ 0 & z < At \end{cases} \tag{5.5}$$

where α is a scaling constant and $a(t)$ is the current level of the RRP. The use of f^2 could reflect multiple binding steps. This results in a counterbalance to pool depletion - although the pool empties, f grows, allowing a sharper, later peak for secretion.

The RRP (maximum size A_M) is replenished by a reserve pool (RP, current level $b(t)$, maximum size B_M). The RRP is depleted by secretion and refills at a rate proportional to its spare capacity:

$$\Delta a = (\beta \frac{b(t-\Delta t)}{B_M}(1 - \frac{a(t-\Delta t)}{A_m}))\Delta t - x(t) \tag{5.6}$$

where β is a constant. In order, the change in RRP level depends on how full the RP is ($\beta \frac{b(t-\Delta t)}{B_M}$), how full the RRP is ($1 - \frac{a(t-\Delta t)}{A_m}$)) and amount secreted ($x(t)$).

One pertinent question is why the amount received by the RRP is scaled by its current level. It is assumed the level of RRP is communicated to the RP. This could be to do with the transport mechanism, a function of calcium levels (the RP may refill the RRP only when Ca is high enough) or via a back rate equalising reaction. This equation is intended only to approximate the underlying process.

The RP is refilled in similar fashion by a deep store (of assumed infinite capacity) at rate δ, the form of which was derived from the results:

$$\Delta b = (\delta(t)(1 - \frac{b(t-\Delta t)}{B_M}) - \beta \frac{b(t-\Delta t)}{B_M}(1 - \frac{a(t-\Delta t)}{A_m}))\Delta t \tag{5.7}$$

The second half of this equation represents the amount lost to the RRP: the first half is the refill from the deep store, again dependent on the level of the RP and a scaling constant δ.

The form of δ was derived from the results (Figure 5.4). Experiments with frequency response indicate high frequency stimulation can be maintained surprisingly well: pool refill must increase to allow the higher secretion (see Results for further

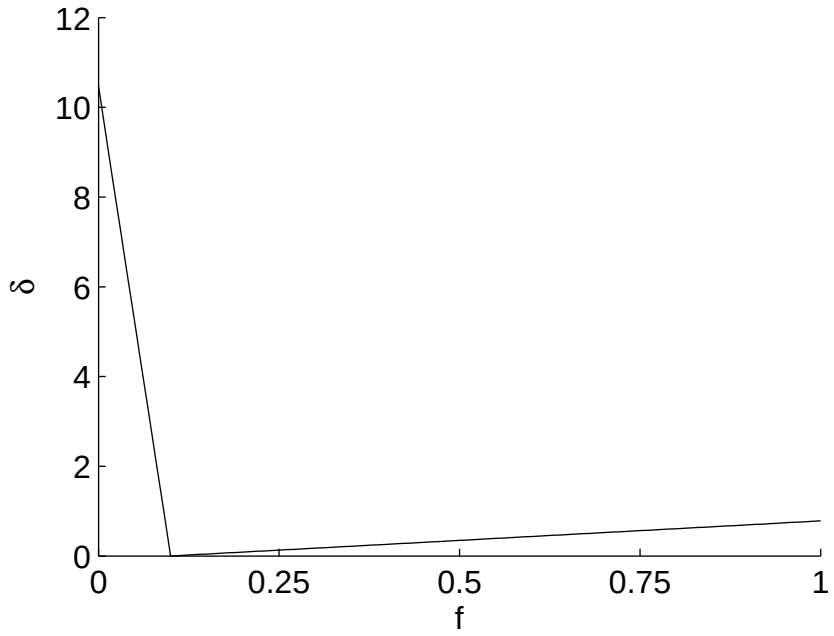

Figure 5.4: δ: RP refill constant for different values of f. Secretion must be maintained during higher frequency stimulation, so the RRP must refill more quickly under high frequency stimulation (during which f is high): yet it must refill even more quickly during silences (at least in the model).

discussion of the response). However, continuous firing is always worse than phasic (Figure 5.9 for details), so a silence must result in a greater gain in than even high frequency firing. This could be due to faster endocytosis, refill of the pool or some other mechanism, but here it is implemented through faster pool recovery.

There are some reports that calcium may inhibit pool recovery, as it may inhibit endocytosis [53]. Functionally, this could explain why a gap in firing is worthwhile. This suggests δ is small if f is high, although f probably clears more rapidly than the equivalent calcium concentration. A second variable could be used to lag pool recovery if further accuracy was required.

There would be other ways to increase refill to help maintain a sustained response - for example, the equation for RP refill could be made second order, and refill according to the rate of replenishment. Without further biologically evidence, there is little to choose between the different possible mechanisms, and computationally it is simply necessary that something increases the refill rate with frequency of stimulation. This method matches the results while keeping nonlinearities to a minimum, so will be used.

The refill exponent is therefore piecewise linear (Figure 5.4):

$$\begin{aligned} f < D_T \quad & d(t) = D_1(D_T - f(t)) \\ f >= D_T \quad & d(t) = D_1(f(t) - D_T) \end{aligned} \tag{5.8}$$

where D_T is a constant.

This is a simple reflection of a combination of two underlying systems, eg different types of pumps with the same cutoff value, or a vesicle pump combined with endocytosis . Without more experimental data, refining this function is impossible. It can be said that the refill function for the RRP must approximate this, in that it must be higher under high frequencies than lower ones and higher yet during silences.

Figure 5.5 illustrates model behaviour.

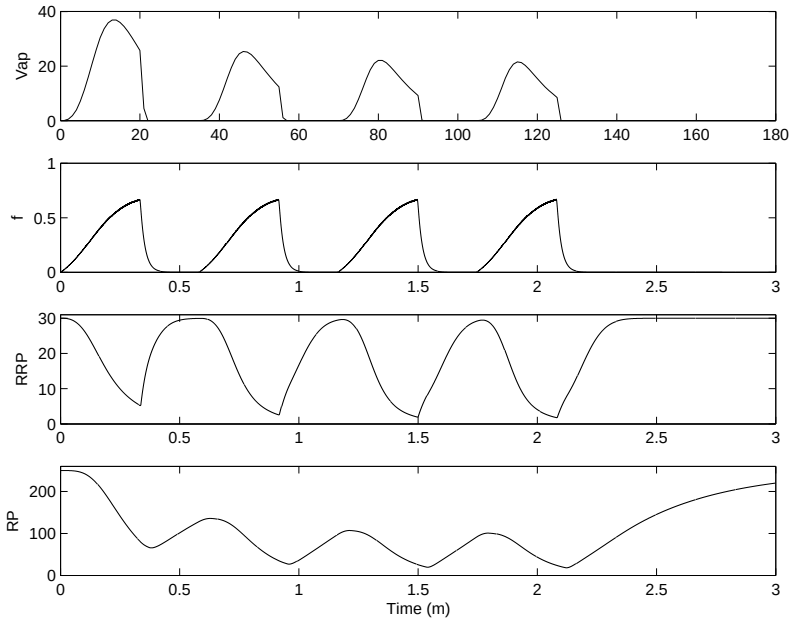

Figure 5.5: Model response to four 20s bursts at 13Hz, 15s silence. From top to bottom: vasopressin secreted (μ U), the variable facilitating secretion $\mathbf{f}$, RRP level and RP level. Notice the fast decay of the facilitation variable after firing has ceased; also rapid recovery of the pools during the silence. The second response is diminished compared to the first, consistent with experimental evidence.

5.4 Methods and Parameters

The design was implemented as a Matlab MEX function using C++. The parameters were fixed for all trials as in Table 5.1.

5.5 Results

5.5.1 Secretion Profile

Investigations into the facilitation effect appear to be exclusive to Shaw et al [101]. They stimulated tissue with 10Hz bursts of varying lengths, with the burst time account for 25%, 50% or 75% of the total cycle time. So, for example, with a burst length of 10s the silence length was 30s, 10s and 3.33s respectively.

They then measured total secretion over 15 minutes. Using this data to calculate secretion per spike, they found that secretion increases linear to the number of spikes, as in Figure 5.6 for around 20s (or the first 200 spikes: without repeating this experiment at different stimulation frequencies, one cannot distinguish.

An issue arises from varying both the burst length and the silence length, the facilitation effect may be obscured by depression. Certainly, the effects of depression can be seen at 30s. Ideally, results from the same experiment with a long enough silence to guarantee replenishment of the system would exist. However, the results for the different proportions of cycle time are quite closely grouped, implying depletion is not distorting results overly.

Matching this in the model unmasks a trade-off: too much depletion and the results for different proportions separate, leading to free different levels of facilitation. It is also difficult to maintain the facilitation effect for 75% on at 15s while allowing for major depletion at 30s. There is not really sufficient data to be sure exactly when and with what force depletion strikes, so the facilitation effect has been mimicked as best possible while maintaining some depletion at 30s. There may well be a more non-linear, closer matching solution, but without further data a simple answer is preferable.

Information on the secretion profile, due to the early constrictions on AVP measurement resolution, is crude. Measurement had to be corrected for diffusion and basal secretion. Cells show a high initial rate of secretion which rapidly falls off, as in Figure 5.8. Subsequent bursts elicit a smaller initial response. Correcting the secretion profile for diffusion would show a higher secretion exhausting more rapidly: the model repli-

Symbol	Description	Value
Variables		
z	Activity-dependent variable (fast)	
f	Facilitation variable (activity-dependent, slow)	
f_i	f increase per spike	
g	z-dependent decay constant	
x	vasopressin secretion	
a	quantity of vasopressin in RRP	
b	quantity of vasopressin in RP	
δ	variable for scaling deep store secretion rate	
Constants		
Z_i	z increase	0.1/spike
Z_d	z decay constant	10
A_t	threshold for z for RRP secretion to occur	0.01
F_d	f decay constant	0.1
G_1	scales g	7.5
G_t	threshold for z for g to be non-zero	0.1
F_1	scales fi	0.02
F_2	scales f_i	0.1
α	scales RRP secretion rate	4.61
β	scales RP secretion rate	37.29
A_M	capacity, RRP	30
B_M	capacity, RP	250
D_1	scaling factor for RP refilling during silence	104.6
D_2	scaling factor for RP refilling during activity	0.87
D_T	constant used to calculate refill	0.1
M	scaling factor for model output (μU)	2.3

Table 5.1: Parameter values for secretion model

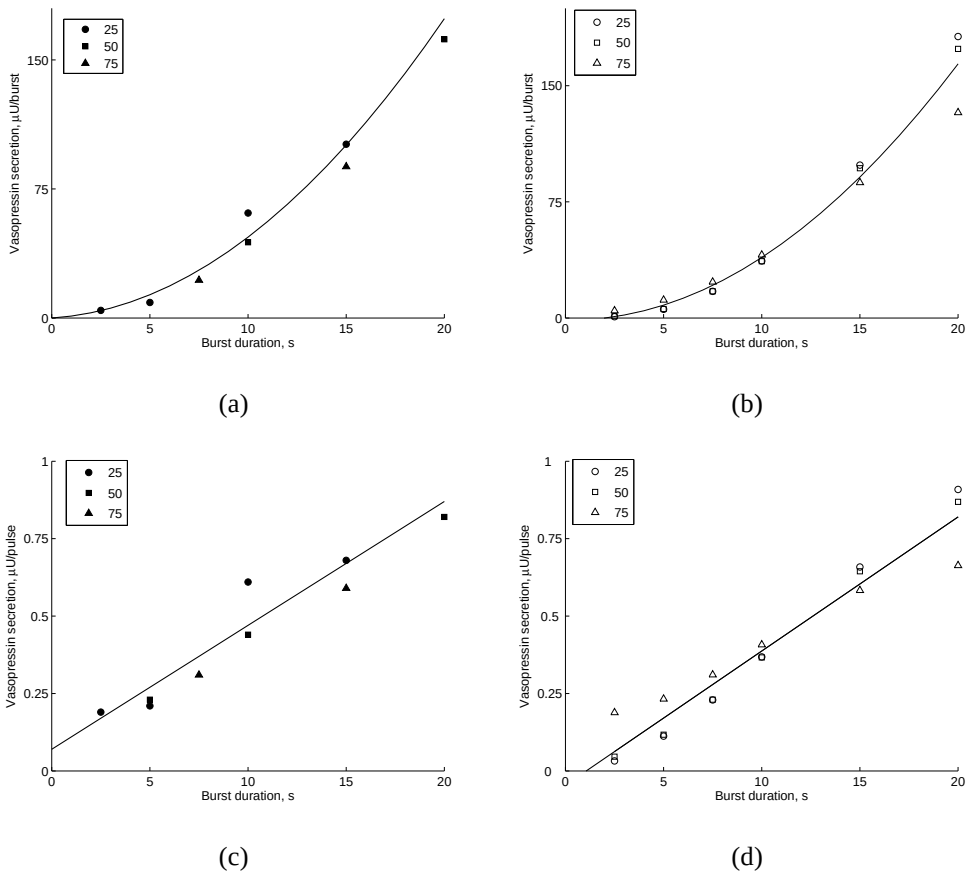

Figure 5.6: Facilitation of stimulus-secretion coupling, model parameters as in Table 5.1. Shaw et al [101] measured vasopressin secretion from isolated neurointermediate lobes in response to electrical stimulation at 10Hz; trains were generated for different proportions of cycle duration (25% for 2.5Hz ○, 50% for 5Hz □, 75% for 7.5Hz △) for 15 minutes. a) *in vitro* data. Secretion per burst. Curve fitted is $y = 0.7x + 0.4x^2$ b): Modelled results. Curve is fitted to 20s, and is $y = 0.42x^2 - 0.1916x - 1.33$. c) *in vitro* data. Secretion per spike increases linearly. Results with all three stimulation frequencies can be fitted by the same line ($0.07 + 0.04x$, $R^2 = 0.91$), suggesting that depletion did not have a large effect. d): model match to data. Line fitted is $0.043x - 0.046$, $R^2 = 0.94$.

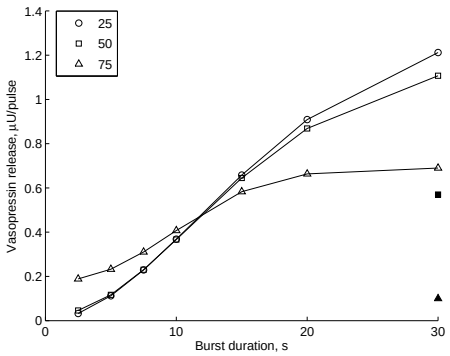

Figure 5.7: Depletion during different intensities of stimulation: Shaw et al [101] measured vasopressin secretion from isolated neurointermediate lobes in response to electrical stimulation at 10Hz; trains were generated for different proportions of cycle duration (25% for 2.5Hz ○, 50% for 5Hz □, 75% for 7.5Hz △) for 15 minutes. Filled points are original *in vitro* data, shown at 30s for comparison of depletion: unfilled symbols are model data. The model shows depletion at 30s, although less than originally observed. There is also much more depletion at 30s with the 7.5-Hz pattern than with 5 or 2.5Hz, reflecting less time to recover between bursts of stimulation. The 7.5Hz pattern also releases more than the other patterns at the very low burst size tried (2.5s): at this stimulation, silences are only 0.8s long. Although very little is actually secreted (see a), the facilitation variable f has insufficient time between bursts to clear and so the efficiency per spike is relatively high.

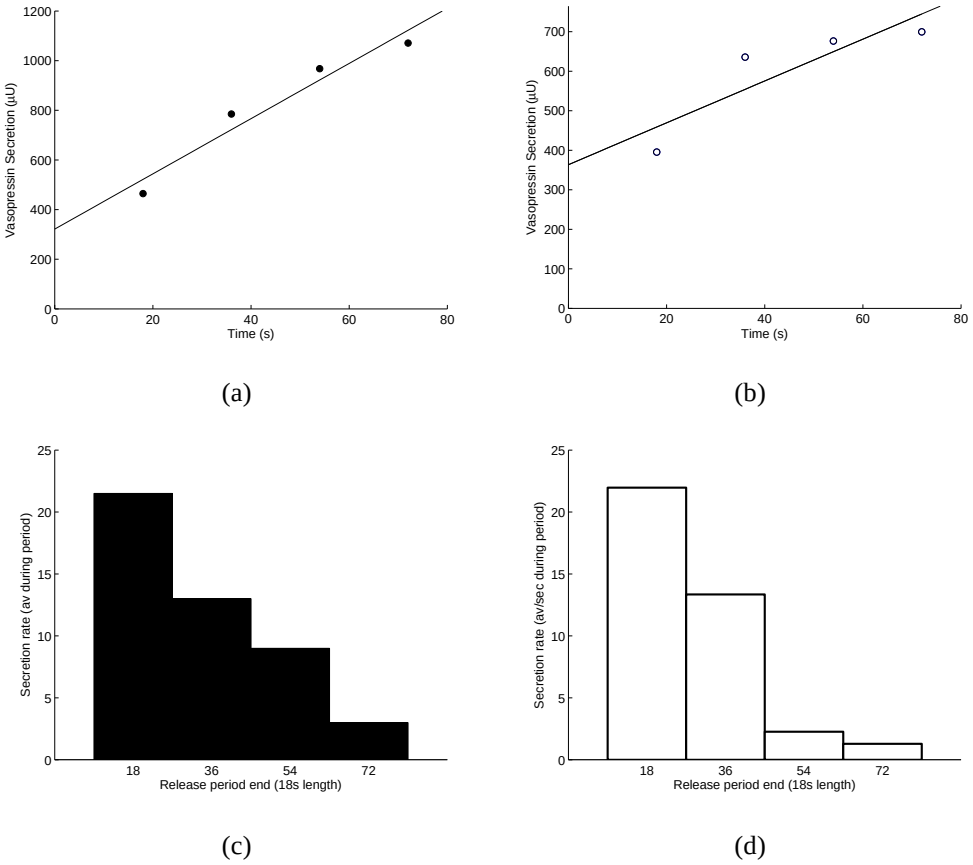

Figure 5.8: Depletion over longer timescales. Left: Experimental results in rat neurointermediate lobes from Bicknell et al [12] showing (top) mean total secretion over different stimulation periods and (bottom) secretion rate during consecutive 18s periods. Right: Model equivalent data. In both cases, secretion rate drops after 18s.

cates this. It all shows only partial recovery after the first burst, as seen experimentally, although to continue showing this for successive spikes would require a further, longer term limited resource of vesicles.

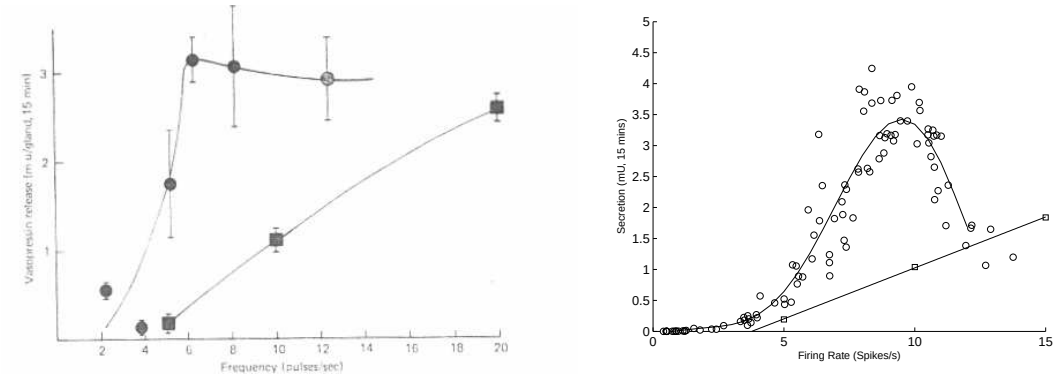

(a) (b)

Figure 5.9: Secretion in phasic and continuous firing. Phasic firing (○) is more successful at eliciting secretion than the same number of spikes arranged continuously (□). a) *in vitro* data from [35]. Five patterns prerecorded from vasopressin cells *in vivo* were used to stimulate secretion from multiple glands, so the variability in this graph is due to variation in secretion at the axon ending. Phasic firing is consistently more successful at stimulating secretion than continuous firing. To mimic these experiments, the firing pattern model was used to generate a range of firing patterns by increasing V_r in steps of 0.15mV from -68.25m to -65.25mV, with 5 cells generated at each step. The cells had $R_{E(I)}$s between 60PSP/s and 460PSP/s uniformly distributed. The model results match the experimental data very closely.

One important feature of vasopressin cells is that spikes organised phasically, into bursts, should secrete more than the same number of spikes arranged regularly, or even with a similar clustering to phasic burst spikes but without any long silences [13, 30, 35].

These experiments are difficult to repeat, as many use recordings from vasopressin cells as stimulation, and these cannot be exactly replicated. For example, Dutton & Dyball [35] repeated their experiments with many different axon endings, but only their original five recordings to cover the entire phasic range (Figure 5.9). Although they supply burst and silence averages for these recordings, there is such variation between recording it is difficult to generate trains that may be considered equivalent. Using the earlier developed vasopressin model to generate spike trains, a wide range of

response can be seen. It can be concluded that phasic firing certainly secretes more than continuous firing, and there does seem to be a point around 9Hz where secretion levels off, but nothing more. the optimum secretion rate is higher than that found by Dutton & Dyball [35], but allowing for variability illustrated by the model and probably present in the biology when confronted with spike trains of the same average this is acceptable, especially when considered with the evidence on frequency response.

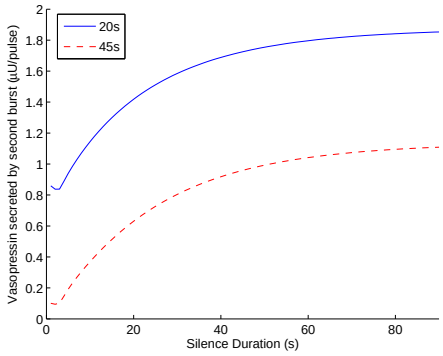

Figure 5.10: Recovery in the model: effect of silence duration. The model was stimulated with a burst of 20s and of 45s at 13Hz, and the secretion from a second burst of the same duration as the initial burst measured. After a small gap, necessary for the slow variable to decay before recovery can start, recovery is exponential. Consistent with Dyball, Barnes and Shaw ([37], as quoted in [36]), a longer period is needed for recovery after a longer burst.

For phasic firing to be effective, a break in firing should be beneficial. Critical to this is the recovery function. In the model, recovery is exponential but slowed by the fast variable (see Figure 5.10), which produces no recovery in the first few seconds after a burst, consistent with Dyball, Barnes and Shaw ([37], as reported in [36]). With a train of 20s, they reported more recovery at 5s, but no significant further recovery after 20s. This is roughly reconcilable with the results here. After a longer burst of 45s, they found a gap of 22.5 to 40s produced around the same result, but a longer interval of 90-135s further increased secretion and avoided the run-down usually seen over long stimulation (1 hour+).

The model does not concur with this - to do so, either the slow variable would have to clear less quickly, inhibiting recovery for longer, or a third release pool would be required, or the recovery of the pool would have to further depend on how empty it was, or some similar mechanism.

Whether this is worth the overhead is an interesting question. Again, data is some-

what sparser than desirable. This could make long bursts more profitable than they should be, something that may be reflected in the higher peak for phasic activity in Figure 5.9. Plotting the recovery normalised to the number of spikes, however, shows the shorter burst to be more efficient (Figure 5.10). Longer term depletion may or may occur *in vivo* where the system can clearly maintain a response over several days of dehydration.

5.5.2 Frequency Response

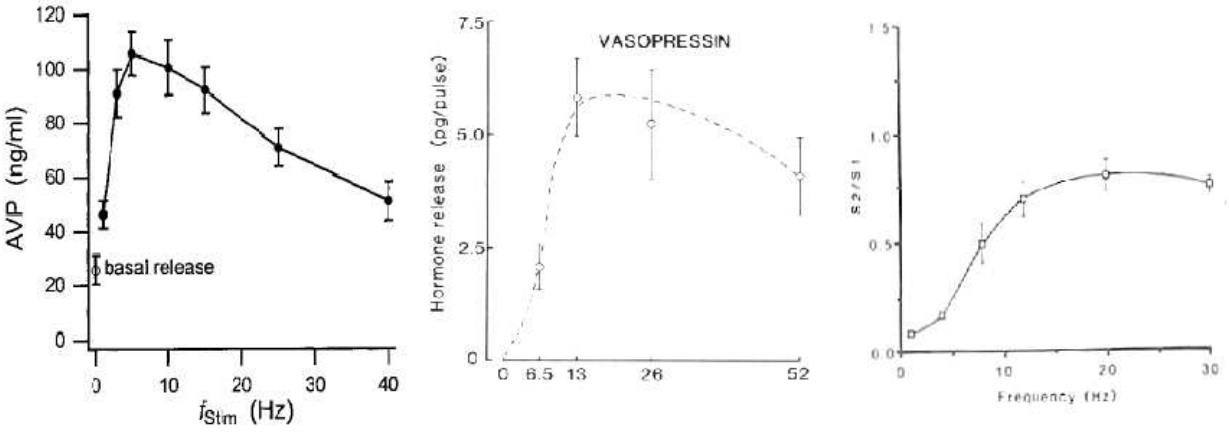

Figure 5.11: Experimental Data on Frequency Response. *in vitro* preparations were stimulated with spike trains at the noted frequencies. From L to R, using 40 spikes [79], 156 spikes [61] and 600 [14]. The shape of the frequency response is consistent across experiments.

The previous section covered the model's response to burst and silence duration. How should it respond to changes in input frequency?

Conventionally, maximal vasopressin secretion is held to be between 10-13Hz (Fig 5.11). For modelling this at low frequencies, the stimulation should be insufficient to prevent the larger decay on the slow variable becoming significant. However, clearly this is not solely responsible for the lack of secretion during long stimulation periods (even at low levels, both the pools will eventually be emptied, with the low level of plateau secretion insignificant in overall secretion - see Figure 5.12.)

Low frequency stimulation must therefore also fail to refill the pool: the δ or refill function exponent modifies according to time since last spike (see Design). Figure 5.5.2 shows the model's frequency response: this predicts a peak around 13-14Hz,

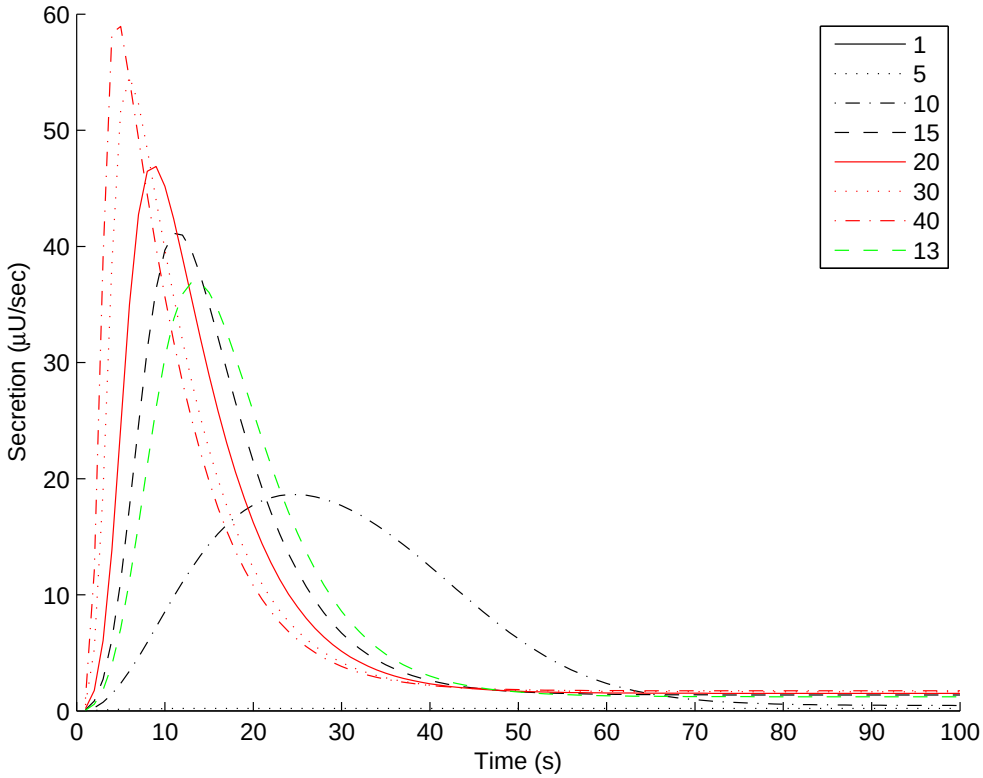

Figure 5.12: Model secretion in response to continuous trains of spikes at different frequencies. Secretion over a continuous spike train at frequencies indicated was measured. The bulk of the secretion occurs sooner as the frequency increases: secretion then settles into a plateau level proportional to stimulation frequency. At frequencies below 5z, the response is almost non-existent, as this is insufficient stimulation to begin secretion.

consistent with experimental results. The experimental data is not sufficiently resolved to be certain where exactly the peak should lie. The cumulative total predicts what results should be found for a spike train of a particular number of spikes: were this experiment repeated with a spike train sufficient long to be sure of reaching the plateau level, the δ function could be adjusted for a more precise match. Bursts are rarely more than a minute at high frequencies though, so the current data suffices for physiological conditions.

5.6 Conclusion

This model produces a realistic secretion profile over short to medium term timescales. Longer term depletion is absent from the model, although it exists *in vitro* and may *in vivo*.

The model replicates facilitation and depression. It extrapolates from the available data: thus it can predict the results were Shaw *et al.*'s [101] experiments on facilitation to be repeated at different frequencies for stimulation, or with a constant large silence length (Figure 5.6). One can also derive frequency response from spike trains with arbitrary length from Figure 5.5.2.

One curiosity has come out of the model design: the realisation that facilitation must reset more quickly than it accumulates. If it didn't, bursts with very small silences between them would gain from accumulation of f, and this happened in early versions of the model forcing the introduction of the quick clearance mechanism g. The facilitation effect was then non-linear, as small burst lengths then secreted more per spike than they should have been able to do so. This can still be seen on the Figure 5.6, with the 75% burst proportion: with a burst length of 2.5s, the silence is only 0.8s long. This is almost continuous firing, although not of a type seen naturally, and it is efficient at stimulating secretion as it manages to accumulate f without overally depleting the pools as the total amount secreted is small. This would be worth exploring experimentally, although it is currently probably outwith experimental resolution to find where the transition between the facilitations form the last spike wears off and the refill of the pool begins.

The model may also be incorrect at very short timescales: Cazalis et al [30] tried stimulating secretion with the same phasic patterning, but the spikes within the bursts ordered either regularly or from the distribution seen in vasopressin cells. The phasic patterning was more efficient than the regular bursts at evoking secretion. This does

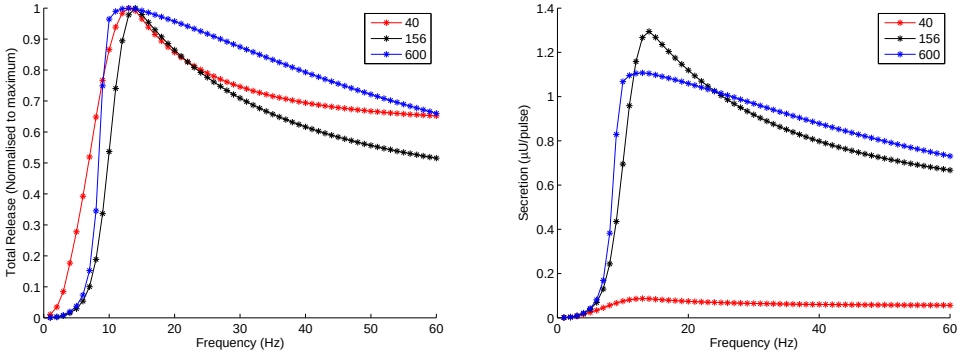

(a) (b)

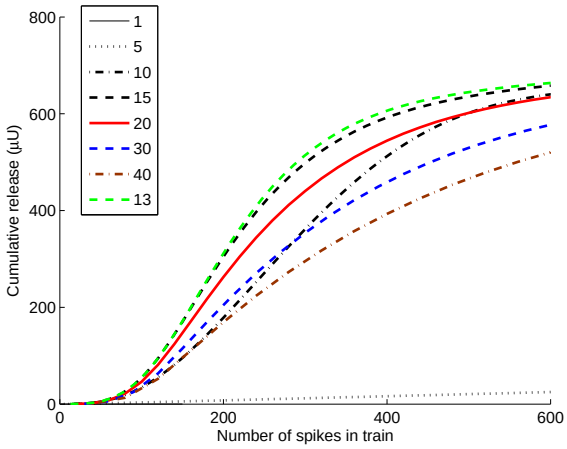

(c)

Figure 5.13: Frequency response: Model response to spike trains with frequencies indicated with 40, 156 and 600 spikes to match those in Figure 5.11. a) Total secretion. Maxima, regardless of the number of spikes in the train, are between 11-14Hz. The maximum secreted falls off at different rates; as the frequency increases, the axon ending saturates in terms of response and it is then mainly the duration of stimulation that matters. b) Secretion per spike. Maximal secretion is 14Hz for 156 spikes, and around that for 600 spikes. The relative invariance to number of spikes in the train indicates this is genuinely a response to frequency of spikes, rather than the burst length resulting from different burst lengths, until high frequency stimulation. c) The cumulative secretion graphs indicates how length of spike train affects results. 600 spikes is a burst of 45s at 13Hz; 156 is 12s; although the longer burst will trigger depletion, the facilitated secretion at the beginning of the burst compensates for this.

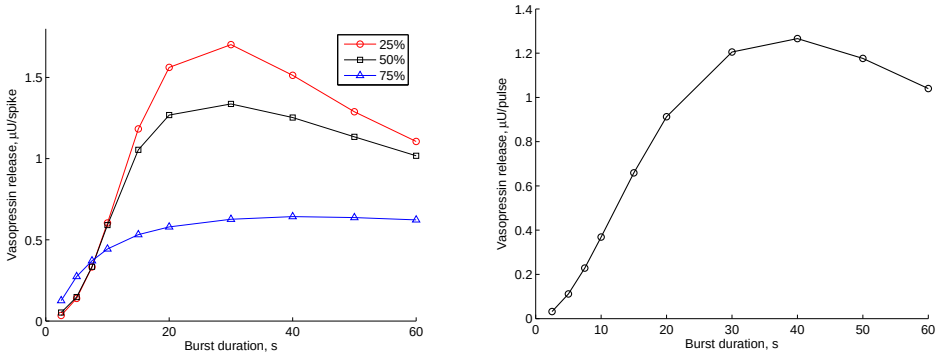

(a) (b)

Figure 5.14: Predictions from the model: these are more in the nature of extrapolating from the experimental evidence than new theories on working of the axon ending. a) Repeating the facilitation experiment done by Shaw *et al.* (see Figure 5.6) with trains of 13Hz rather than 10Hz will increase depletion and cause the different percentages of cycle time active to further separate. It is also useful to calculate more data points for this, as there was previously only one showing depletion (at 30s). b) Repeating Shaw *et al.*'s experiment, but with a gap of 80s between bursts to allow for recovery at the axon ending. This graph is similar to Figure 5.6, suggesting depletion has had little effect upon the results.

not occur in the model (data not shown): this may reflect difficulties in constructing the spike train suitably or the lack of frequency adaptation.

The intention here was not to provide a model to explain the working of the axon: this model is intended to be purely descriptive of the relationship between stimulus and secretion. As such, with the exception of the pools, no explanation has been given for the forms of G, f or δ except for how they contribute to the final result. They are deliberately not tied to biophysical processes, and do the minimum necessary to replicate the results without increasing the chance of unpredictable behaviour. The form of δ, for example, would be undesirable in a biophysical model as one would have to provide an explanation for its form, especially as it is somewhat awkwardly piecewise linear.

However, this model could be extended to try and provide a model of functioning at the axon ending. To do so would also certainly require modelling of calcium processing: different speed of influx and buffering could then help refine the form of G and δ (almost certainly a compound of two different functions).

Chapter 6

Population Model

6.1 Introduction

A model to generate firing patterns and a second model of secretion have been developed: when linked, they form a complete formulation from action potential generation to secretion.

The next step is to form a network of cells, and explore the influences of diversity in the population and the differing methods of stimulating it. The simplest possible network is one with no lateral connections and no network influences: it is then only the heterogeneity of the network than distinguishes it from the performance of an individual cell.

As the simplest network has no connection, shared inputs or other shared factors, it will be referred to as a population. Later expansions can then use this as a benchmark to gauge the effectiveness of network level influences.

6.2 Parameter Search

The population is simply a collection of cells, with distributed parameters. The behaviour of the population can be understood by firstly examining a single cell, and then extrapolating to how a collection of variable cells will behave.

To understand how a heterogeneous population of cells may respond to changes in V_r and $R_{E(I)}$, first secretion from one cell was analysed, with 60min of data produced for each combination of parameters. Vasopressin cells are depolarised when osmotic pressure rises [80]: but it is not clear whether this affects V_p or just V_r. Three values of V_p were therefore included in a parameter search, as well as varying V_r and

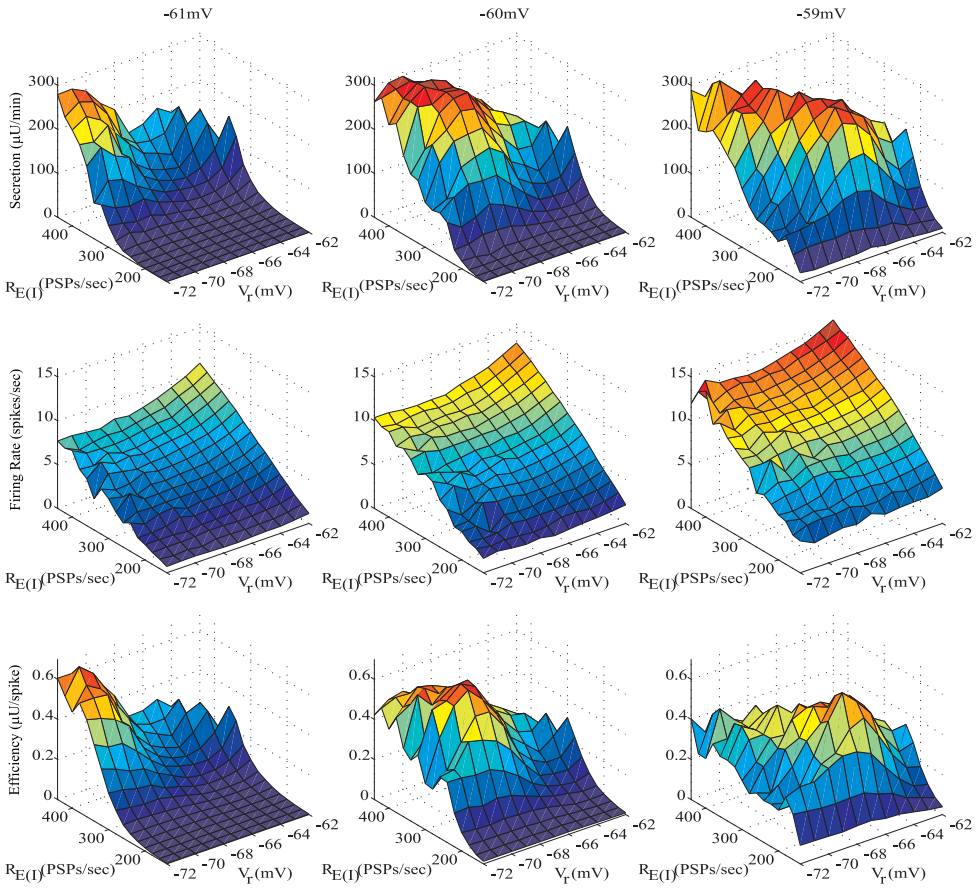

Figure 6.1: $R_E(I)$, V_r and V_p effects on secretion. Results from one cell run for 60min for each value of V_r and $R_E(I)$ shown, with three different values of V_p (61, 60 and 59mV). Other parameters are as in Table4.1. Top: Secretion/min. Maxima (V_r, $R_E(I)$) are at (-71mV, 440PSPs/sec) when V_p= -61mV, at (-70mV, 380PSPs/sec) when V_p= -60mV and at (-71mV, 400 PSPs/sec) when V_p= -59mV. Middle: mean firing rate over the 60 min. Bottom: secretion (μU) per spike. As the plateau rises, the V_r for maximal secretion also rises and $R_E(I)$ falls. Optimal secretion efficiency does not significantly differ for different values of V_p: for -61mV, it is 0.66μU/spike at (-71mV, 420 PSPs/sec), for -60mV, it is 0.63μU/spike at (-69mV, 320PSPs/sec), and for -59mV, it is 0.65μU/spike at (-67mV, 220PSPs/sec). The higher the plateau, the lower $R_E(I)$ and higher V_r is for optimally efficient secretion.

$R_E(I)$ (Fig.6.1). For more depolarised values of V_p, the most efficient secretion needs a more depolarised V_r and a lower $R_E(I)$. Thus, when V_p= -61mV the maximum efficiency (0.66μU/spike) is at V_r= -71mV, 420PSPs/sec. When V_p= -60mV, the maximum (0.63μU/spike) is at V_r= -69mV, 320PSPs/sec, and when V_p= -59mV the maximum (0.65μU/spike) is at V_r= -67mV, 220PSPs/sec. These values of V_p and V_r may be slightly lower than the average recorded *in vivo* (typically more -67mV to -65mV), but this may reflect compensation for the lack of vasopressin inhibition in the model, or one of the other simplifications (eg lack of PSP scaling). The values are not outwith those seen biologically.

The efficiency of secretion depends on both the intraburst firing rate and on burst and silence durations. The most efficient firing rate is around 13spikes/sec. At more depolarised V_p, there is a smaller difference between V_t and V_p, so smaller fluctuations in v_m trigger spikes, and so the $R_E(I)$ required for an intraburst rate of 13spikes/sec is lower. The most efficient pattern has bursts of between 20s and 60s and silences of $>$20sec. Transitions between bursts and silences occur when v_m crosses the tipping point, and this happens more often if V_r is closer to V_t.

At a more depolarised V_p, a lower $R_E(I)$ is needed for the optimal intraburst firing rate, so there is less fluctuation in v_m, and hence fewer state changes. For ideal burst and silence durations, V_r must therefore also be depolarised. Thus, for a higher V_p, a smaller change in $R_E(I)$ is needed for efficient secretion, and most efficient secretion is at a higher V_r than with a lower V_p. If the currents supporting the plateau are unaffected by osmotic pressure, the response will depend on V_r and $R_E(I)$.

The maximum secretion rate for all cells is at a more hyperpolarised V_r than the level for maximum total secretion (280 μU/min, V_r=-71mV, $R_{E(I)}$ = 440PSP/s for V_p = -61mV; 303 *mu*/min, V_r=-70mV, $R_{E(I)}$ = 380 PSPs/s for V_p=-60mV; 318 PSP/s V_r=-71, $R_{E(I)}$ = 440 PSP/s for V_p = -59mV) . The most efficient strategy is to fire only until depletion outweighs facilitation, but to maximise total secretion, longer bursts are needed, although they are less efficient. Silences must be long enough to allow replenishment of the RRP. Figure 6.2 shows secretion efficiency, intraburst firing rate, burst durations and silence durations for different values of V_r and $R_E(I)$ with a V_p of -60mV; the optimal firing pattern has a mean burst duration of $\sim$22sec, silences of $\sim$15sec, and an intraburst rate of 11.7spikes/sec, close to the values observed by [112] for rat vasopressin cells during early dehydration. Maximum secretion needs longer bursts ($\sim$25sec), silences of $\sim$15sec and an intraburst rate of $\sim$13spikes/sec.

The most effective strategy would be first secrete efficiently, and then to sacrifice

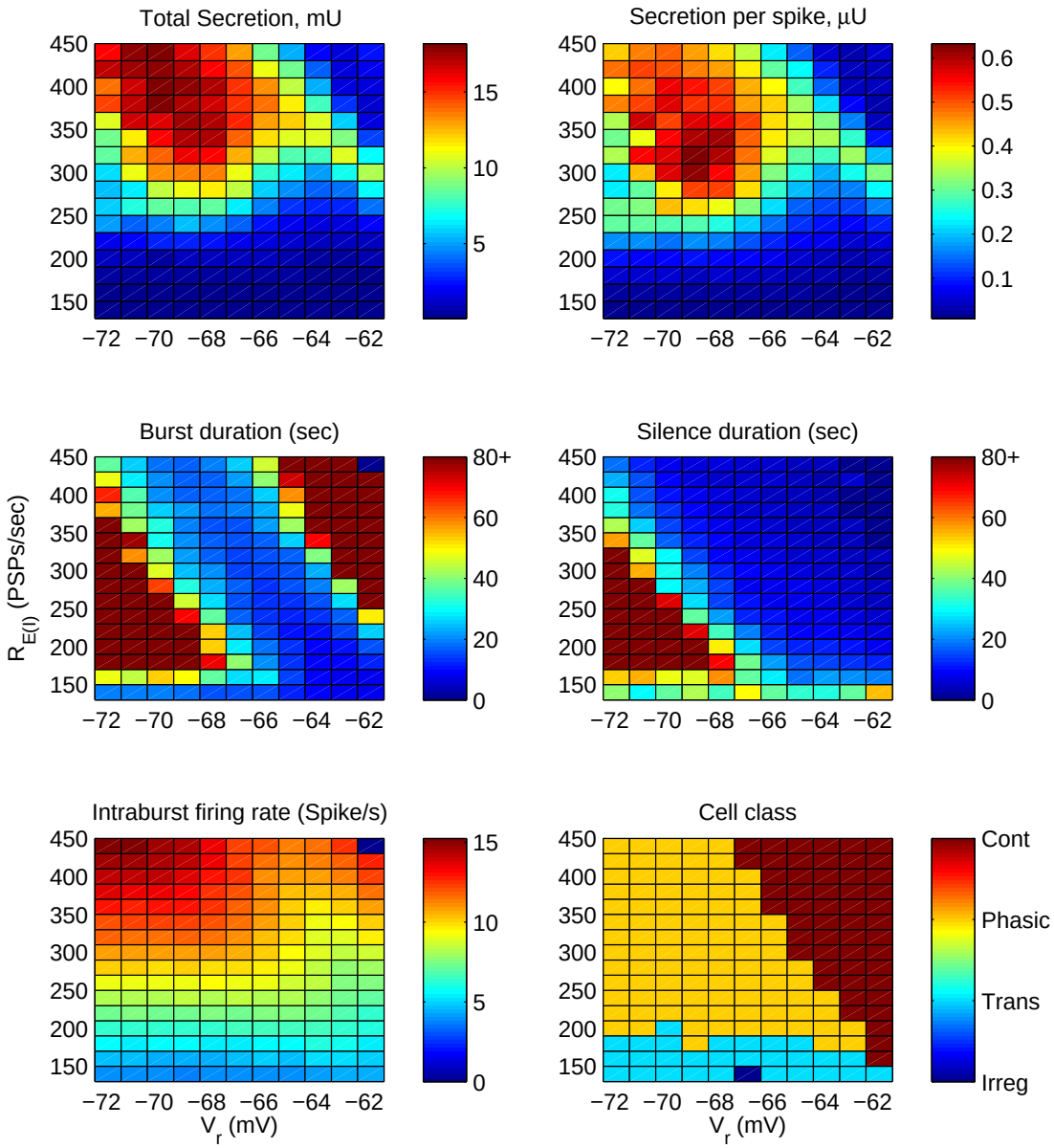

Figure 6.2: Burst and silence durations; the effect of patterning on secretion. V_p= -60mV, and data as in Figure 6.1 . a) Total secretion in 60mins. B: efficiency. C: Burst and D: silence durations. V_r and $R_E(I)$ at greatest efficiency has burst and silence durations $\sim$15-20sec, consistent with Wakerley et al [112]. The maximum secretion rate is with bursts of $\sim$30sec and silences of $\sim$20sec, again consistent with Wakerley et al. E: an intraburst rate of 13spikes/sec is close to optimal. F: class of cell, based on mean firing rate and activity quotient (Q). As their firing rate increases, cells with more depolarised V_r begin to fire continuously, producing less secretion.

efficiency in favour of total secretion in response to sustained challenges. This suggests that after the most efficient point, hyperpolarisation or equivalent autosecretory inhibition will be required to maximise release.

It is notable that the suggested values for maximum efficiency are towards the hyperpolarised end of the range of membrane potentials measured in vasopressin cells (8-16mV below resting potential [20], which in this case would suggest -69.25mV to -61.25mV). Resting potential is difficult to accurately determine, as the measures used may have damaged the cell membrane: it's also possible that currents underpinning the plateau potential may have further confused matters. It's also possible that some of the model parameters may not quite be correct (for example, if the PSP magnitude were reduced, the distance between the resting potential and firing threshold would then contract for the same results: the tipping point dynamics could also be altered).

A number of parameter regimes are essentially aliases in the search space, and thus the importance on the actual values used should not be overemphasised. This applies to the plateau potential as well. The statistics for maximal efficiency were quoted for a plateau of -60mV; but the intraburst firing frequency, burst and silence durations and the efficiency and roughly the same for plateaus of -59mV and -61mV (Figure 6.2).

This suggests that depolarising the plateau has little effect upon efficiency or total secretion. The patterns for maximum secretion rate do differ more significantly (Figure 6.4), but secretion rate is more of a ridge than a peak when examined on the graphs, suggesting that many patterns have similar secretory rates.

The behaviour of a single cell can be understood by tracing a path though the parameter search: increasing firing rate and depolarisation of V_r will correspond to heading uphill, towards the peaks when starting from the bottom most corner. The network will smear this trace depending on the variance of its parameters. Thus although the parameter search indicates there is little sensitivity to the plateau value in a a single cell provided the other parameters are altered to compensate, it may be a network amplifies this difference depending on how narrow the peaks are in the parameter space.

To analyse this, construction of a model population is necessary.

6.2.1 Entropy

Bhumbra and Dyball [10] have developed methods for measuring entropy in vasopressin cells, as an extra measure simple enough to be useful but beyond the simple first or second order statistics usually used. The entropy here is the entropy of the log

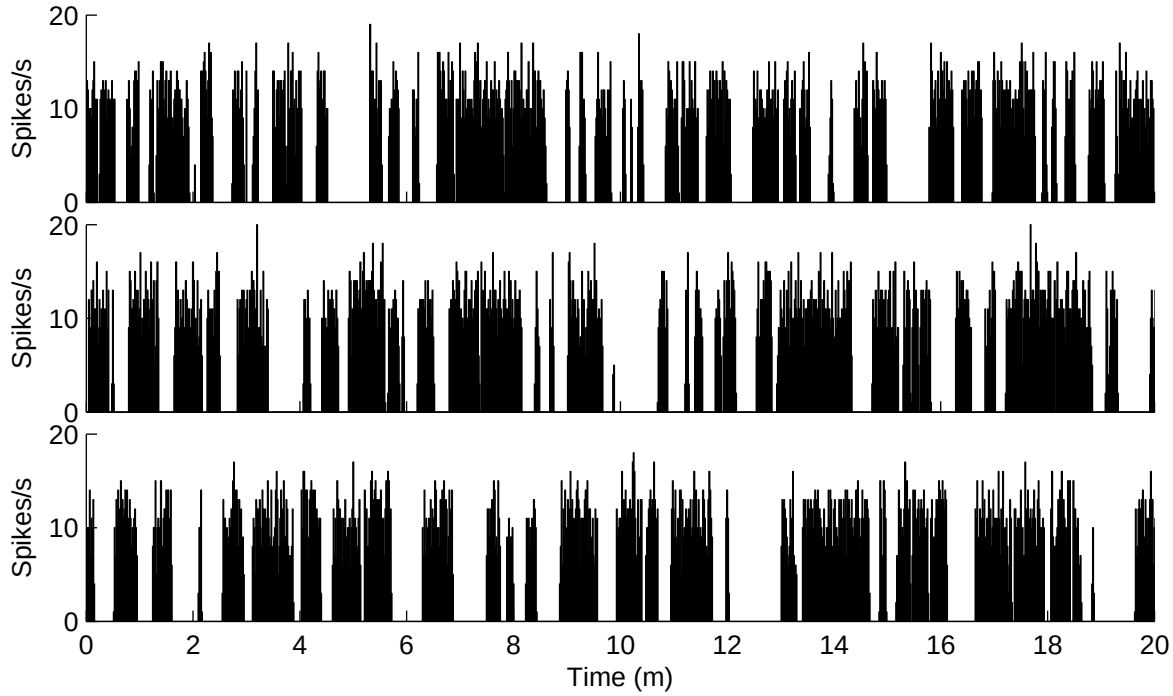

Figure 6.3: Firing patterns at the point of maximal efficiency for each plateau level tried during the parameter search. The patterns are all very similar, indicating that for each choice of plateau a set of parameters can be found to produce the same results. First 20 mins of 60 min runs illustrated. Top: V_p -61mV, resulting efficiency 0.66μU. Mean burst duration 20s, silence 15s, Intraburst Firing Rate (IFR) 11.5 spikes/s, Firing Rate 6.6 spikes/s. Middle: V_p -60mV, resulting efficiency 0.63 μU. Mean burst duration 22s, silence 15s, IFR 11.7 spikes/s, MFR 7.0 spikes/s. Bottom: V_p -59mV, resulting efficiency 0.65 μU. Mean burst duration 29s, silence 18s, IFR 11.1 spikes/s, MFR 6.8 spikes/s. Classification rates over 99% in all cases.

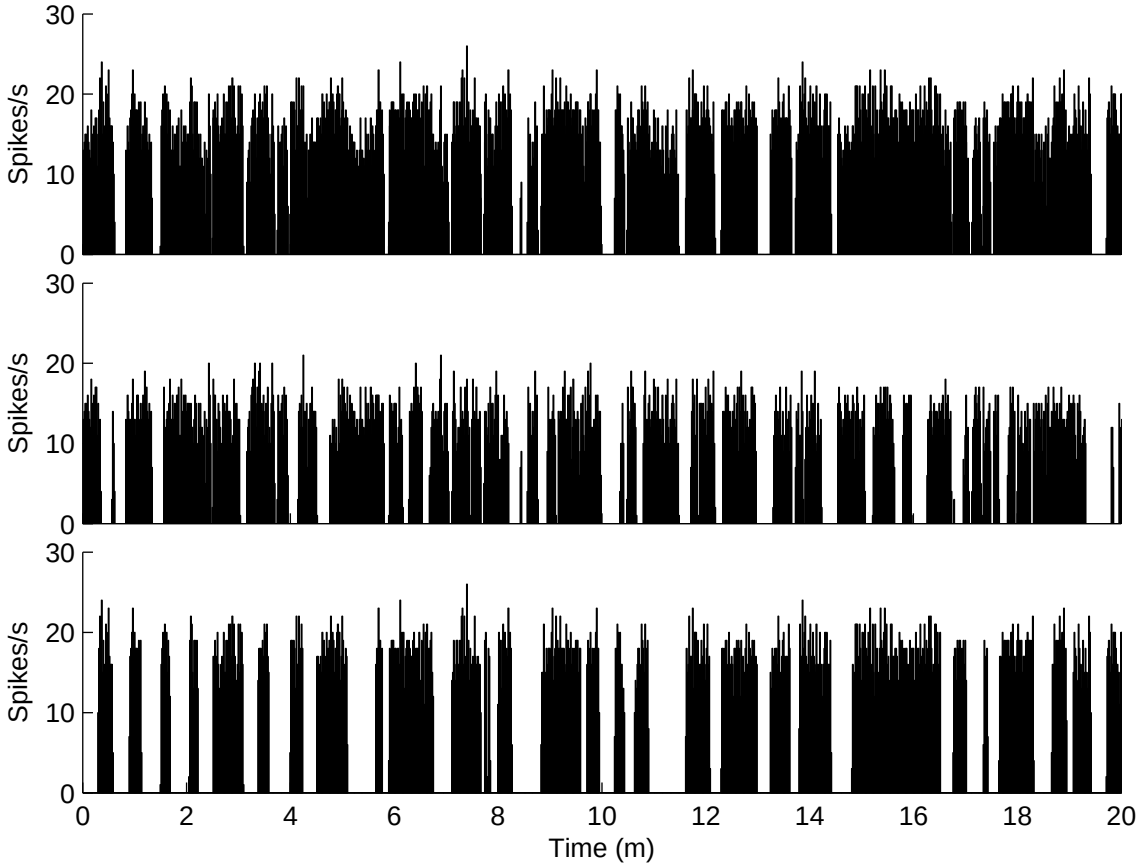

Figure 6.4: Firing patterns at the point of maximal secretion rate for each plateau level tried during the parameter search.The patterns are all very similar, indicating that for each choice of plateau a set of parameters can be found to produce the same results. First 20 mins of 60 min runs illustrated. Top: plateau -61mV, resulting rate 318 μU/min. Mean burst duration 33s, silence 17s, Intraburst Firing Rate (IFR) 17.4 spikes/s, Firing Rate 11.4 spikes/s. Middle: V_p=-60mV, resulting secretion 303 μU/min. Mean burst duration 25s, silence 13s, IFR 13.4 spikes/s, MFR 8.9 spikes/s. Bottom: plateau -59mV, resulting rate 280 μU/min. Mean burst duration 33s, silence 17s, IFR 17.4 spikes/s, MFR 11.4 spikes/s. Classification rates over 99% in all cases.

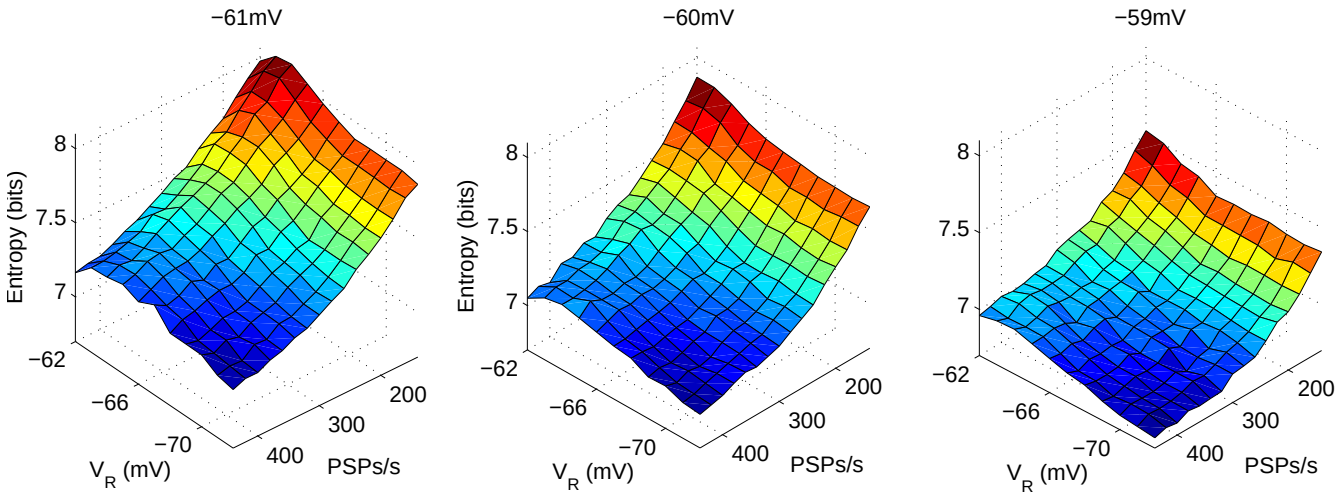

Figure 6.5: Entropy calculated for each point of the parameter search for plateaux of -61mV, -60mV and -59mV. Entropy falls as $R_{E(I)}$ increases. Once into the phasic firing range, depolarisation has relatively little effect although more depolarised cells tended to have a higher entropy.

interval distribution; log is used as it prevents the influence of the long intervals cloaking the shorter intervals, although this will make it more sensitive to intraburst firing changes than phasic patterning changes in vasopressin cells. The entropy provides a measure of the uncertainty regarding when the spikes in a train will occur: a perfectly regular spike train has an entropy of 0 and so can only provide basic rate information, whereas a Poisson process has a entropy of 7.95 bits/s. Theoretically, this reflects the coding capacity of the cell, but here is better viewed as a guide to how structured or complex the cell firing is. It is useful experimentally: cells may differ significantly in firing in ways not easily found by examination of firing rate, standard deviation of firing rate and Q value along. for example, cells with more pronounced afterhyperpolarisations may have their firing dominated by it, producing a more deterministic output as others will have to rely more on EPSP arrival. The experiments here are repeated partly to see if the model does produce a reasonable match to the statistics provided but also to see if Bhumbra and Dyball's hypothesis that it should be possible to determine the relative influences of deterministic versus nondeterministic responses to rises in osmotic pressure (depolarisation versus EPSP and IPSP rate increases).

Using their software, entropy was analysed for each of the first 5000 intervals of the firing patterns generated by the parameter search to see if patterns generated by the model produce entropies close to the ones they measured.

The mutual information was calculated for adjacent log intervals: this is used as an alternative to correlation coefficients as it does not assume a Gaussian distribution [10]. Mutual information (MI) in the model was usually zero: only 13 of the 176 cells (7%) were non zero, and the maximum seen was 0.0062. To check if the mutual information is significant, the intervals are shuffled 100 times and their mutual information measured: only if none are found to have greater mutual information than the initial measurement is it deemed significant.

This suggests there were not firing motifs: firing in the model is largely driven by the input, and the facilitation voltage is clearly not significant enough to impose patterning. Cells registering non-zero MI were all at firing rates greater than 300 PSPs/s. The mutual information seen by Bhumbra et al. *in vivo* (about 0.16 bits) may be caused by the frequency adaptation or interplay between medium term influences such as the DAP and autosecretory inhibition. To know how significant the lack of MI is in the model would require some knowledge of its effect upon secretion. It is possible the MI is only significant due to the frequency adaptation at the beginning of the burst when many short intervals are grouped together, something that may only exist to establish the plateau which the model includes anyway.

Increasing the plateau increased MI (at -59mV, 26 cells had non-zero MI: average 0.0049(0.0011), range 0.0034-0.0081, at -61mV, 2 cells had non-zero MI of 0.0043 and 0.0046). Again, cells displaying non-zero MI tended to have high input rates and depolarised V_r.

Entropy over the grid is displayed in Figure 6.5. The range seen in generally in concordance with Bhumbra & Dyball [11] (they measured mean entropy at $\sim$ 7.4 per bit before NaCl infusion, less afterwards). Entropy increases as the resting potential depolarises but drops as input rate increases. The highest entropy measured was above the 7.95 bits/spike for a Poisson process of constant rate, suggesting that longer term influences were predominating. Increasing the input rate triggers more DAPs and autosecretory inhibition, reducing the irregularity of the train and therefore the entropy.

Bhumbra & Dyball found depolarising the cell, at least *in vitro*, had little effect on entropy although a mild tendency towards a decrease in entropy. Here, depolarising V_r increased the entropy modestly unless V_p was also depolarised: perhaps more indication that the plateau may also alter during osmotic pressure.

Increasing the plateau decreased entropy, from a maximum of 8.0994 at V_p=-61mV, V_r=-64mV $R_{E(I)}$= 140 PSPs/s to a minimum of -6.7664 at V_p=-59mV, V_r=-72mV $R_{E(I)}$= 440 PSPs/s.

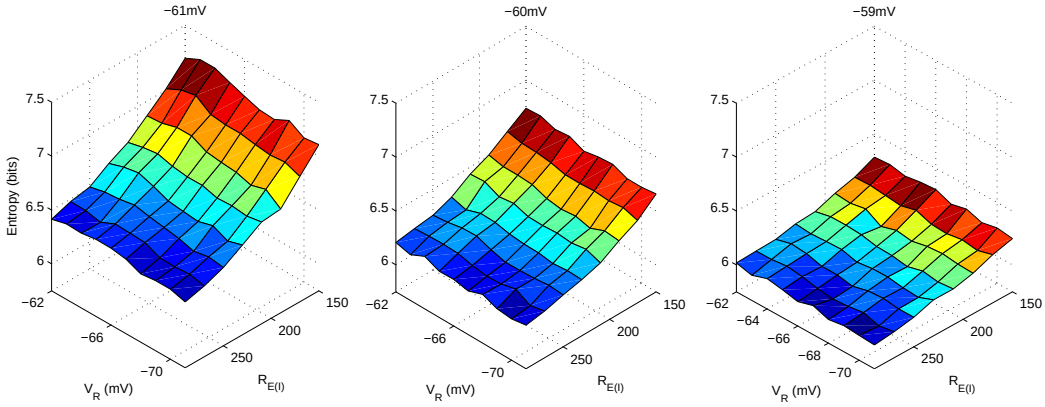

Figure 6.6: Entropy calculated using the *in vitro* time constants of 60ms and 294ms for the HAP and DAP respectively. The input range covered is slightly smaller than for the *in vivo* parameters (to 300 PSP/s instead of 390 PSP/s; otherwise parameters are identical. The entropy is lower than *in vivo*, regardless of parameters: the range covers also falls much more dramatically as the plateau increases. Depolarisation of V_R only have relatively little effect: depolarisation of V_p undoubtedly reduces entropy.

The model cells use a far greater change in input rate than depolarisation to simulate osmotic pressure, and it is this that would predominate causing an overall decrease entropy consistent with the *in vivo* recordings. However, *in vitro*, input rates may change far less due to the destruction of afferents in the preparation. Bhumbra *et al.* found an increase in firing rate and insignificant decrease in entropy in response to depolarisation *in vitro*; when osmotic pressure was applied they saw an increase in entropy, although their sample included both oxytocin and vasopressin cells.

The results of running the model with the *in vitro* time constants is in Figure 6.6. Depolarisation of V_R has relatively little effect, whereas depolarisation of the plateau results in a fall in entropy. Entropy ranged between 5.97 - 7.26 bits. Mutual information was again tiny or insignificant: only 28 of the 240 points had non-zero MI, and the maximum was 0.0076. Firing rates ranged between 0.77 - 5.54 spikes/s.

The lack of response with the plateau fixed at a depolarised level (as it would be *in vitro*) would reflect the lack of change in entropy observed *in vitro*. However, more investigation is required into how the model could account for significant mutual information. It would also be useful to try stimulation of axon ending with patterns generated by the model and some prerecorded *in vivo* with significant MI, so the impact of possible spike motifs in the firing could be assessed (this could also be used to

evaluate whether frequency adaptation is useful for secretion or simply a side effect of establishing the plateau).

6.3 Creating the Population

There is little data on how variable parameters should be *in vivo*. Ideally, the population generated should be heterogeneous enough to be generally applicable, but no more to minimise the representative sample size required.

A successfully heterogeneous population should have:

- A range of modes
- Mean firing rates consistent with those observed
- A variety of different cell types. Differing proportions of phasic firing have been observed, but phasic cells do not constitute the majority of firing pattern until osmotic stress is applied.
- Different burst and silence durations, preferably uncorrelated.

6.3.1 Parameter Choice and the Starting State of the Network

As a starting point, the values used previously were considered (Table 4.1). These were for a population of cells already firing phasically, yet as few as 13% of neurons may fire phasically under osmotically normal conditions [112] and the majority of cells fire under 2 spikes/s (eg see [38]), ie non phasically. The secretion model parameters were not varied: while there is probably significant variation *in vivo*, this is largely unresearched especially with respect to corresponding possible optimisation of firing. Brimble and Dyball [21] measured the mean firing rate of 22 neurons as 2.7 ± 2.8 (std dev) spikes/sec; median 2.3; range 0 - 9.6. This corresponds well with the mean seen by Wakerley et al [112] (2.1 spikes/s, range 0.5-2.5 spike/s, 65 neurons), although their range was far narrower despite monitoring a greater number of neurons. Both identified vasopressin neurons by failure to response to milk ejection. The likeliest cause of discrepancy is that Brimble & Dyball picked up one fast continuous cell, while Wakerley et al didn't. The parameters for the network should probably allow occasional generation of rare very excited cell, but will mostly cover the smaller range.

Parameter	Value (std)
Plateau potential, V_p	60 (0.2)mV
Rest potential, V_r	70.0 (0.5)mV
Increase in autosecretory inhibition, I_w	0.015 (0.0015) mV/spike
Autosecretory Inhibition time constant, $1/\lambda_w$	5 (0) s
EPSP rate, R_E	170(10) Hz
EPSP:IPSP ratio (percent), $R_E : R_I$	100 (10)
Drift time constant, D	60 (3) s
DAP time constant,τ_D	69(0) ms
HAP time constant, τ_H	12.5(0) ms

Table 6.1: Population model parameters

The mean input rate was therefore dropped to 170 PSPs/s to produce a quieter population, with other parameters varied until the distribution was with the correct range (main parameters as in Table 6.1). 100 cells were then generated, and output calculated for 30 minutes. The mean firing rate of this population was 2.4 (0.6), with firing rates from 1.0 - 4.0 spikes/s and a median of 2.4 spikes/s. 15 cells were firing phasically, with 4 firing in a slow irregular fashion and the remainder firing classed as transitory.

This population had a satisfactory range of modes (37.5s - 62.5s), and covariance was 93(1.8)%.

6.3.2 Simulating Osmotic Pressure

As stated in the literature review, input rates should rise in response to rises in osmotic pressure, and the cell will depolarise. However, it is difficult to ascertain specifics from the literature on the magnitude and rate on the changes especially under *in vivo* conditions. There are also differences in response to acute and chronic challenges, possibly due to to differing influence from slower inhibitory feedbacks (especially vasopressin, which lags 30mins behind the challenge [70]).

The cationic conductance modulated by osmotic pressure activates above 275 mosmol/kg, and is still responsive up to the largest stimulus tested (325 mosmol/kg) in rats (set point $\sim$295 mosmol/kg) [81]. However, depolarisation *in vivo* is probably not more than a few mV (G Leng, personal observation). The parameter search also indicates depolarisation of more than a few mV is unlikely to increase secretion, as the risk of

collapse of bistability and continuous firing increases, so depolarisation in the simulations will be tuned to provide maximal efficiency, ie it will be assumed each strategy would use the depolarisation best for efficiency, although this might be a different depolarisation to the other strategies, for fair comparison.

A further issue is how depolarisation should affect the plateau. It is not even proven the plateau exists, so no experimental data exists on sensitivity. Our experience with the instability of DAP summation suggest that other currents support the plateau, and this is consistent with experimental evidence ([40, 64]). The plateau depolarises *in vitro* [25] but this could be because the slower DAP dynamics allow more summation than would be seen *in vivo*: bursts may be regenerative *in vitro* but not *in vivo* [3, 42, 22]) for this reason.

It then seems more likely that V_p is fixed: however, a fixed and moving plateau can be tested. [5] notes the plateau tends to be maximised with moderate firing: after this, the AHP predominates. However, dynamics are slower *in vitro* than *in vivo*.

6.4 Results

6.4.1 Osmotic pressure, with plateau fixed during rises

The parameter search suggests how the population will respond to certain types of challenge. In the search space, depolarising moves along one axis, and increasing the input rate another. The space for possible start points for the network is also quite large given the criteria.

An illustration of the maximal efficiency will be made. The parameter search has indicated this point lies around -69mV (assuming for now that the plateau is fixed around -60mV), which would suggest a starting state of V_r around -70mV. $R_{E(I)}$ can then be altered until the distribution is plausible.

Likewise, an optimal strategy for a plateau which depolarises to the same extent as the resting potential can be devised.

Leng et al. [62] showed that vasopressin cells *in vivo* increase their firing rate linearly as osmotic pressure increases. The model population similarly responds linearly to an increase in $R_{E(I)}$ (Fig.6.7). Importantly, this results in a linear increase in secretion, as observed *in vivo* [34]. The linear increase in secretion cannot be sustained beyond $\sim$8spikes/sec, above which both efficiency and total secretion drop. The cells fire shorter, more frequent and intense bursts, and then move into continuous fir-

ing (Fig.6.9), and either continuous firing or high-frequency stimulation with short silent periods is inefficient, and cannot maintain the secretion rate. There was not much continuous firing observed in this model population: if V_r was more distributed, there would be more cells with high V_r which would switch to continuous firing more quickly. This can be predicted from the parameter search, which shows that, as $R_{E(I)}$ or depolarisation increases, continuous firing is more probable.

The maximum efficiency of the population is 0.66 μU/spike, at step 9. At this point the population has a mean rest voltage of -69mV and mean $R_{E(I)}$ of 350 PSP/s. The parameter search predicted a maximum secretion of 0.63μU/spike at V_r=69mV, 320PSP-s/sec: very close to the population behaviour. The population can be considered as an integral over an area of the parameter search: the higher $R_{E(I)}$ can be accounted for by the population covering as much of the peak as possible.

Of interest is that the population efficiency is higher than the maximum predicted by the parameter search: this suggests either all neurons are close to the optimal value, or (more likely), there is a distribution of efficiencies in the population, some of which are higher than the maximum found by the parameter search. the parameter search did not cover all values, and while some deviation is to be expected due to the stochastic nature of the input, it may be higher efficiencies can be gained by varying other parameters.

The population at the most efficient point does show a range of efficiencies (0.53 - 0.76, median 0.67 μU/spike). There is not any obvious correlation between higher efficiency and any one parameter (R^2 values < 0.1).

Looking at the phasic patterning more closely (Figure 6.10), the burst and silence durations stabilise at values which are approximately in line with those observed by Wakerley et al.: however, the associated intraburst firing rates are higher than observed by about 5 spikes/s. Although their burst analysis was more imprecise than the one used here (they will have measured a burst at the end of the next second), this cannot account for a discrepancy this large.

It may be possible to reflect this by altering parameters: it is already known at least one inhibitory feedback, vasopressin, is missing. However, the goal here is to check how well the parameter search reflects the population performance. The data is also not unequivocal: it does not include standard deviations, nor does it include the cycle length under initial conditions, which [9] reference as around 50s: they then saw a fall, although that experiment was in monkeys.

An experimental bias towards short period cells exist, as these are more reliably

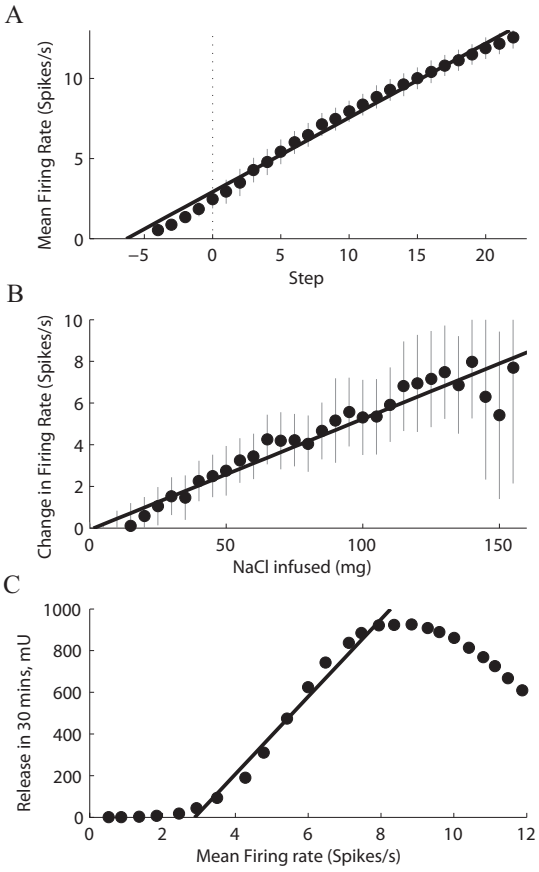

Figure 6.7: Plateau fixed: model response to simulated osmotic pressure with only V_r depolarised, not V_p. A: Effect of simulated osmotic pressure rises on the mean firing rate of a population of 100 model cells, run for 30min (parameters in Table 6.1). Each step corresponds to a rise of 0.25mV in V_r and 20PSPs/sec in $R_{E(I)}$. The maximum depolarisation from step 0 is 1.0mV, so after step 4, $R_{E(I)}$ only is changed. Line fitted from step 0 on, 0.46x+2.92, R2=0.99. B: Data from Leng et al. [62]: Response of vasopressin cells to i.v. infusion of hypertonic NaCl. The variation in firing rate here is clearly greater than in the model, particularly in the later stages, but the linear trend is clearly visible. C: In the model, secretion rate increases approximately linearly as the mean firing rate increases above $\sim$3spikes/sec, until a mean firing rate of about 9 spikes/sec is reached. The regression line is fitted between steps 1 and 11 (for maximal secretion: line fitted is 186x-536, R2=0.98).

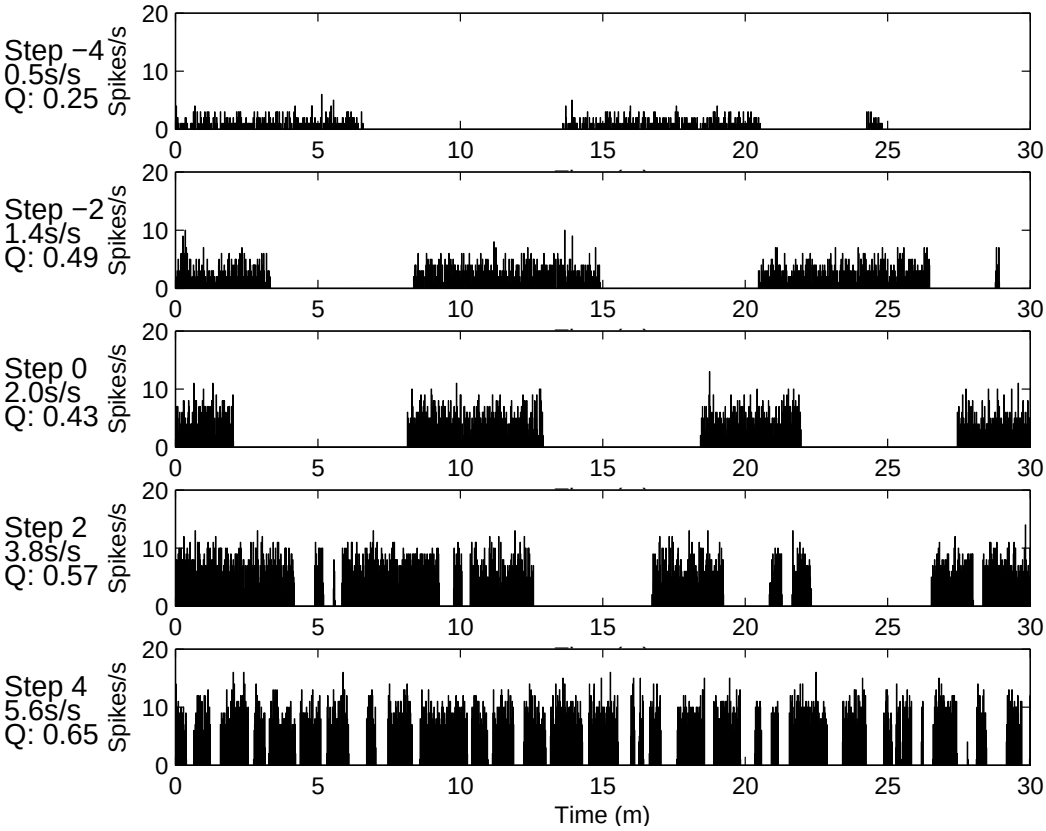

Figure 6.8: Sample firing patterns with raised osmotic pressure. This illustrates one cell's response to increasing osmotic pressure: intraburst firing rate rises steadily, and cycle length drops.

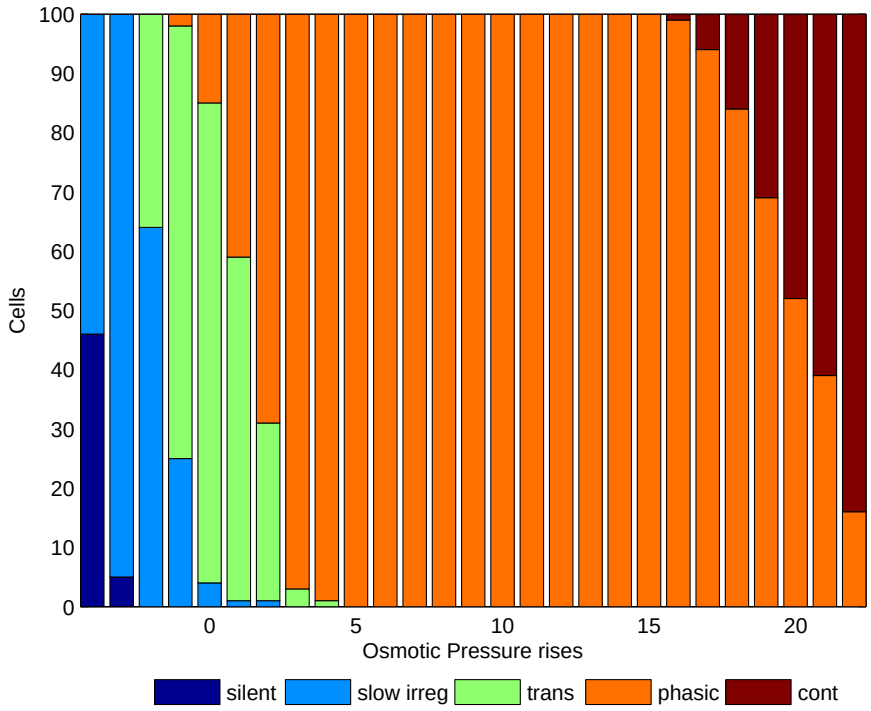

Figure 6.9: Cell classification as osmotic pressure is raised. As osmotic pressure rises, cells switch to phasic firing, and then some become continuous. Colour lightens as activity increases: black, silent; dark grey, slow irregular; grey, transitional; light grey, phasic; white, continuous.

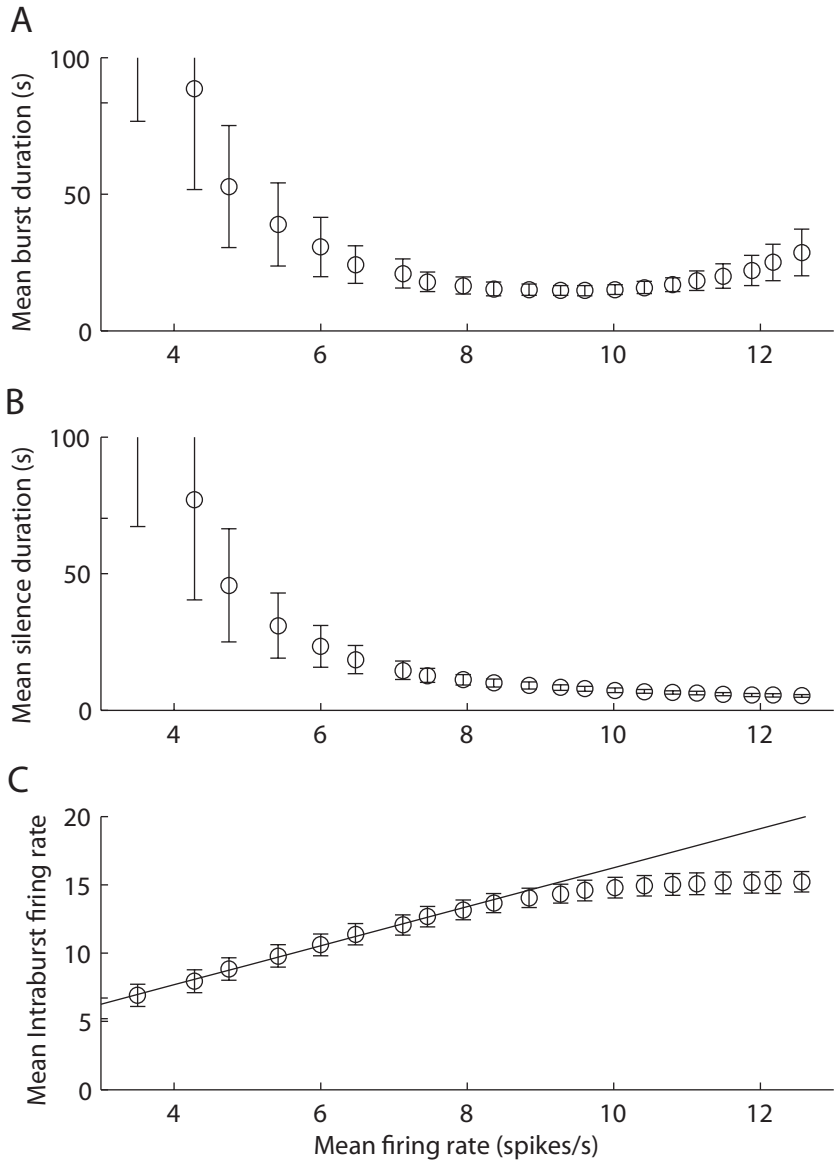

Figure 6.10: Burst/Silence durations in phasic cells. Steps with phasic cells were analysed. The burst (A) and silence (B) durations fall to a value around $\sim$20s for bursts 10s for silence, close to the values seen during dehydration by Wakerley et al [112]. This occurs at higher intraburst firing rates (C) than observed by Wakerley et al, suggesting parameter adjustment may be required. Cell classification $>$ 90% plotted, over 90 cells passed per step.

.

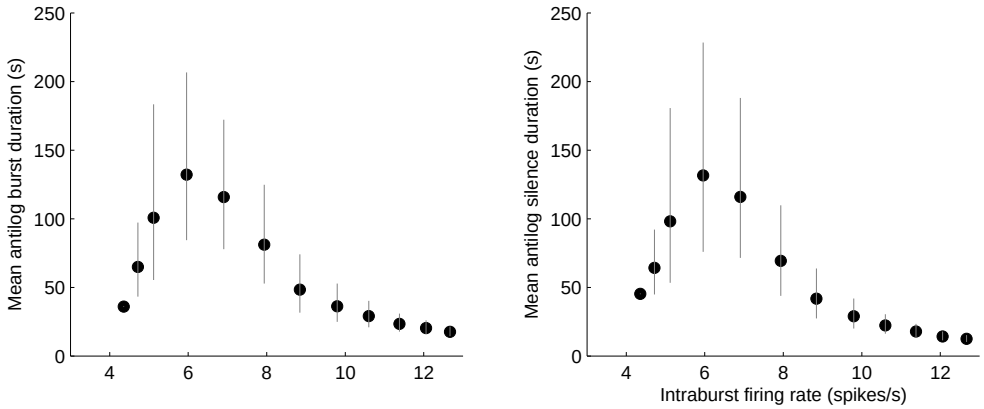

Figure 6.11: Antilog Burst/Silence durations in phasic cells. Using antilog transformed values to minimise the impact of outlying long period cells that may not be recognised as phasic under normal conditions. The burst and silence duration here are still falling, but within a far more biologically plausible range. This graph is limited to the relevant intraburst firing range [112]: burst and silence durations are falling throughout the critical range (6-12 spikes/s).

processes. To check the means were not being inflated by outlying long cycle cells, the antilog statistics were also calculated (Figure 6.11). These also indicate a fall in cycle length, but of smaller magnitude.

Increases in burst duration have been reported after 24 hours of dehydration [112] or hypertonic NaCl injection [21]; here although a rise in burst duration is seen after extreme stimulation, this is accompanied by a fall in silence duration reflective of the lack of critical inhibitory feedbacks (eg dendritic vasopressin and possibly other dendritically secreted inhibitory substances) at this level.

6.4.2 Different activation strategies with the plateau fixed

The model population responds much like vasopressin cells *in vivo* to changes in osmotic pressure, but do these changes increase secretion efficiently? In response to an increase in osmotic pressure, vasopressin cells receive more EPSPs and IPSPs and are depolarised directly; we do not know the relative costs of these strategies, but we can assess their relative efficiency. Simulations were run of 100 model cells with parameters randomised for each run (Table6.1) for 10min for each of the following challenges:

1. EPSP rate only changes, increasing by 20EPSPs/sec/step (’unbalanced input’).

2. EPSP and IPSP rates increase by 20PSPs/sec/step (’balanced input’).

3. Depolarisation of 0.25mV/step ('depolarisation alone').

4. Depolarisation of 0.25mV/step and 20EPSPs/sec/step ('joint unbalanced').

5. Depolarisation of 0.25mV/step and 20EPSPs and 20IPSPs/sec/step, up to a maximum of 1mV depolarisation ('joint balanced').

Depolarisation in these simulations was limited to 1mV (along with a 1mV hyperpolarisation under 'hyposmotic' conditions).

In each case, a population of 100 cells was generated, using the same parameters. Populations should not differ at step 0: this was confirmed using two-way ANOVA (p=0.65) .

The mean firing rate, efficiency of secretion (total secretion divided by the number of spikes) and secretion rate for each of these strategies was calculated (Fig.6.12). All strategies produced an increase in secretion that was approximately linear with firing rate up to $>$11spikes/sec, except the depolarisation strategy. Depolarising V_r increases the chances of a burst beginning, but also the chances of it ending, so this strategy does not increase the mean firing rate until bistability in the model collapses and firing becomes constant (around step 9, or -67.75 with a plateau of -60 in this case). Both of the unbalanced strategies produce a steep increase in firing rate, but many cells fire continuously (the mean Q rises to $>$0.8). As a result, their maximum efficiency is low (around 0.3μU/spike, half the most efficient strategy), and maximum secretion is also low. In the model, an approximate balance of inhibitory and excitatory input is necessary to maintain phasic firing.

The most efficient secretion is by raising $R_{E(I)}$, either alone (maximum mean efficiency 0.65μU/spike,) or with depolarisation (0.66 μU/spike). The rise in $R_{E(I)}$ produces a similar firing rate, but the depolarisation in the 'joint balanced' strategy results in a different patterning of spikes from the 'input rate only'. The difference is insignificant (ttest, p=0.2). In both cases the maximum occurred at step 9, so they had identical input rates. The joint secretion achieves a slightly lower secretion rate (31mU/min for 'joint balanced', 32mU/min for 'balanced input', difference significant: ttest, p=1e-6), but at a slightly lower input rate (Step 11 instead of step 12). That such a small difference is significant probably reflects lack of variation in the population.

These results are dependent on the starting point of the network: they do however broadly confirm that extrapolation from the parameter search is possible. The parameter search predicted a peak in efficiency at a resting voltage of -69mV and $R_{E(I)}$ of

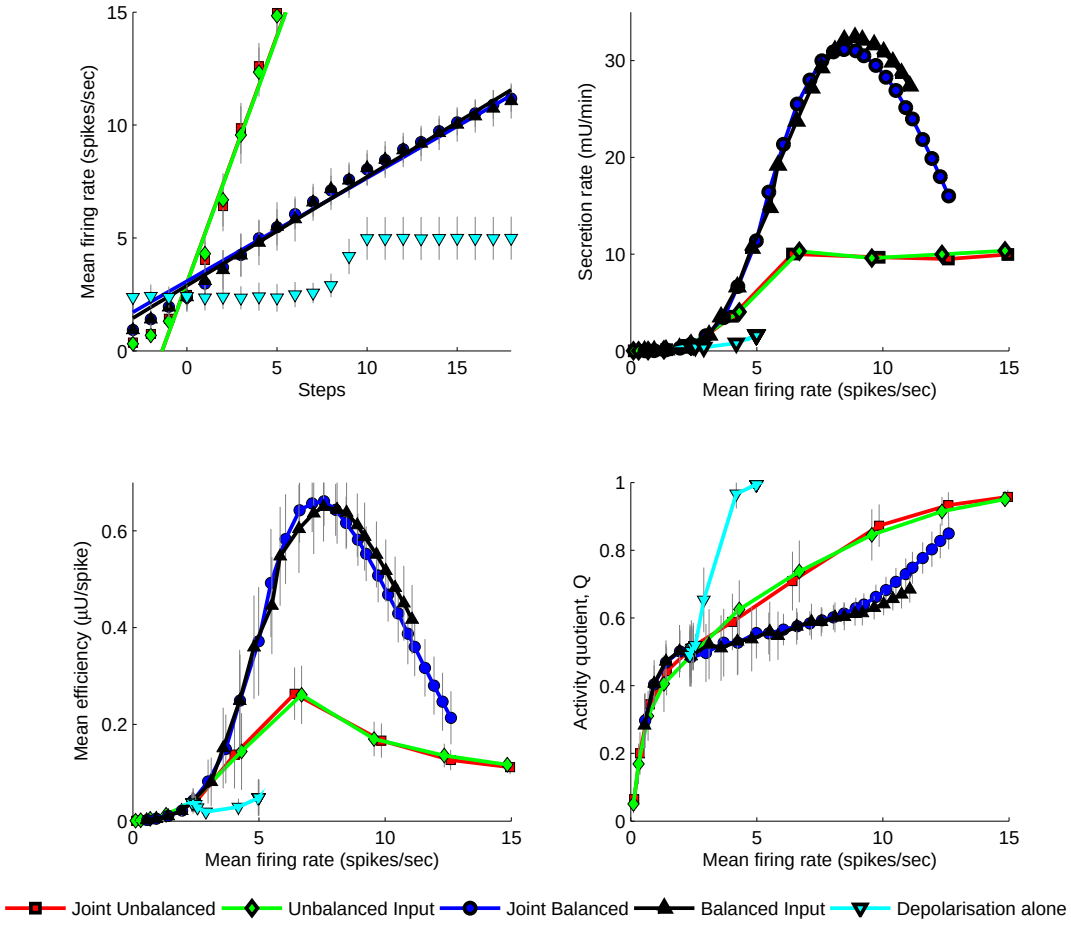

Figure 6.12: Population response to different types of activation. Populations of 100 model cells were generated (Table 6.1). Top Left: Mean firing rate vs activation level, where activation is by a) Joint Unbalanced: depolarisation by 0.25mV/step and an increase in RE of 20EPSPs/sec/step, □; b) Unbalanced Input: a progressive input in RE, (20EPSPs/sec/step), symbol ◇; c) Joint Balanced: depolarisation by 0.25mV, and an increase in $R_{E(I)}$ of 20PSPs/sec/step, o; d) Balanced Input: a balanced increase in $R_{E(I)}$, (20PSPs/sec/step), △ and e) Depolarisation of V_r by 0.25mV/step, ∇ .Unbalanced strategies produce steep rises of firing rate, whereas depolarisation of V_r barely changes the firing rate. Lines fit have R^2 of 0.99 Top right: secretion rate vs mean firing rate. Most secretion is with the balanced joint strategy. Bottom Left: Efficiency (mean secretion/spike). The balanced joint strategy is the most efficient. Bottom Right: Q values: Unbalanced strategies cause continuous firing ($Q > 0.8$), resulting in inefficient secretion.

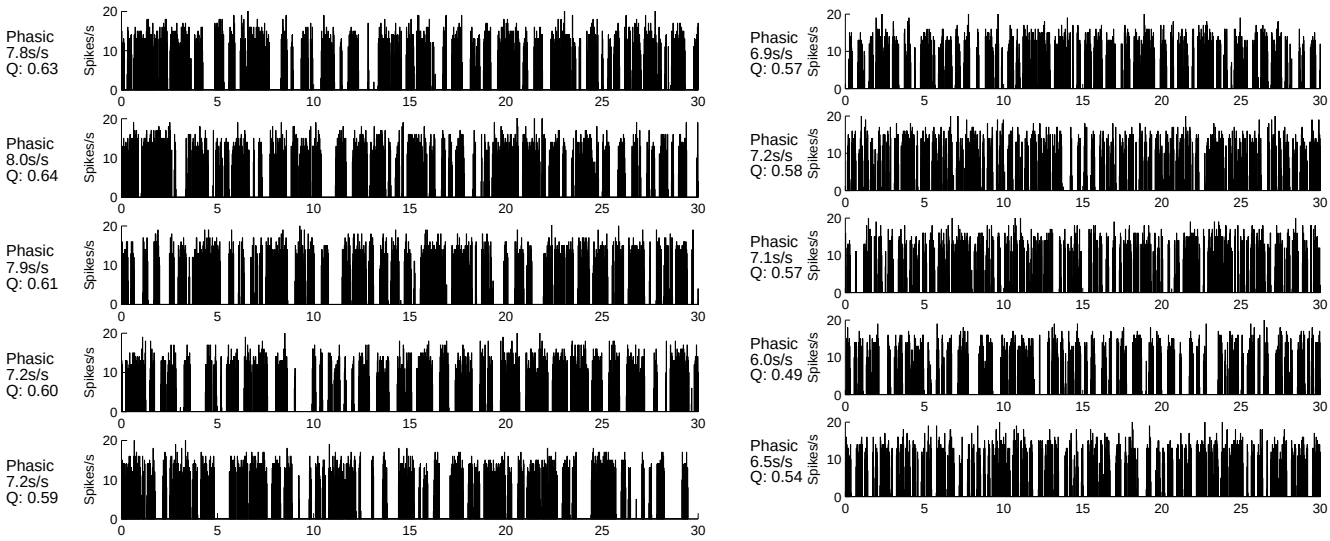

(a) Balanced Input

(b) Balanced Joint

Figure 6.13: Sample population responses: Balanced Input (left) vs Balanced Joint (right). Some sample patterns from the most efficient point (Step 9) for Balanced Input and Balanced Joint. the intraburst firing rate is 12.8 spikes/s for both. Balanced Inputs has slightly longer bursts and silences (27 $\pm$ 8s and 19 $\pm$ 6) versus Balanced Joint 18 $\pm$ 4s for bursts, 13s $\pm$ 3s for silences

Parameter	Value (std)
Plateau potential, V_p	60.5 (0.2)mV
Rest potential, V_r	68.0 (0.5)mV
EPSP rate, R_E	190(10) Hz
Depolarisation per step	0.15mV
$R_{E(I)}$ increase per step	5 PSP/s
Maximum Hyperpolarisation	1mV
Maximum Depolarisation	1.5mV

Table 6.2: Plateau depolarises: parameter values. Most parameters are the same as in the previous experiments (Table 6.1), but the starting point of the populations has been altered slightly to create a reasonable starting population. Key differing parameters are stated here: the plateau is lower, the rest potential is depolarised and the increase in $R_{E(I)}$ and depolarisation per step is lower.

320 PSP/s (see Table 6.4). However, only a millivolt separates the joint balanced and balanced input strategies: this is clearly not enough to distinguish them in terms of efficiency, although the parameter search predicted a lower value at -70mV, 320PSP/s (0.57μU/spike instead of 0.66μU/spike).

Maximal secretion rate was predicted at -70mv, 380PSP/s. This point was passed during the balanced input strategy, which actually maximised at 410 PSP/s (the parameter search predicted around 99% of the maximum at 400PSP/s). There is therefore some noise in the parameter search, but the general maximum values occurs close to what one would predict from the parameter search.

So, far the population results have confirmed that extrapolation from the parameter search is reliable. In general, regardless of whether the plateau is fixed, a strategy that maintains a linear output can be found. However this has involved populations with fairly low variance.

6.4.3 Plateau depolarised during raised osmotic pressure

The maximum efficiency did not vary much with different plateau levels during the parameter search, the secretion rate possible did, although generally at relatively hyperpolarised resting potentials. More generally, the parameter search suggests that a depolarised plateau will require a lower $R_{E(I)}$ and depolarised V_r.

With a plateau of -59mV, the maximum efficiency was at V_r=67mV, 220PSPs/sec.

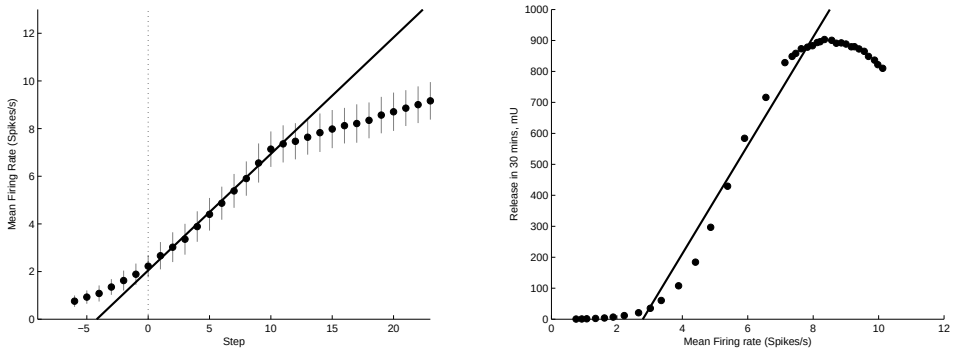

(a) (b)

Figure 6.14: Plateau depolarises during raised osmotic pressure: response to simulated osmotic pressure. Left: Effect of simulated osmotic pressure rises on the mean firing rate of a population of 100 model cells, run for 30min (parameters in Table6.2). Each step corresponds to a rise of 0.15mV in V_r and 5PSPs/sec in $R_{E(I)}$, far less than when the plateau was fixed. The maximum depolarisation from step 0 is 1.5mV, so after step 10, $R_{E(I)}$ only is changed. This breaks the linearity of the response, but at a point where the the response cannot be maintained anyway. Line fitted from step 0 to step 10, 0.49x+2.05, R2=0.99. Right: The secretion rate increases approximately linearly as the mean firing rate increases above $\sim$3spikes/sec, until a mean firing rate of about 9 spikes/sec is reached. The regression line is fitted between steps 0 and 17 (for maximal secretion: line fitted is 175x-488, R2=0.98).

Starting with a plateau of -60.5mV and assuming that V_r depolarises in line with the plateau suggests a starting point around -68mV. $R_{E(I)}$ was then adjusted to produce a population with a mean firing rate of 2.2 spikes/s (median 2.2, range 1.3-3.6 spikes/s) .

The plateau is more depolarised than when fixed, so a far smaller increase in $R_{E(I)}$ is required to cover the available range (Figure 6.14). Secretion peaks at 903mU, with mean parameters V_r = -67.5mV, V_p = -59mV and $R_{E(I)}$ = 280 PSPs/sec. The secretion efficiency peaks at 0.64μU /spike with mean parameters V_r = -67.5mV, V_p = -59mV and $R_{E(I)}$ = 240 PSPs/sec, around the values predicted by the parameter search. Maximum efficiencies are similar to those observed with a fixed plateau.

As the plateau is depolarising to -59mV, V_r can also start at a more depolarised level, and the resulting phasic patterning is well within the observed physiological range (Figure 6.15, Table 6.3). The falling standard deviations indicate the pattern becomes more regular, something also observed (Figure 6.16).

Observed by Wakerley et al. [112]			Model Population Results			
IFR (spikes/sec)	Burst Duration (s)	Silence Duration (s)	Number of cells	IFR (spikes/sec)	Burst Duration (s)	Silence Duration (s)
			93	4.72 (0.52)	35.70 (15.22)	43.25 (16.35)
			96	5.26 (0.62)	42.69 (15.70)	42.76 (13.92)
			97	5.86 (0.69)	45.96 (20.79)	43.72 (18.28)
6.31	20.42	17.38	99	6.58 (0.79)	40.12 (16.59)	39.80 (18.25)
			100	7.35 (0.81)	34.33 (12.97)	30.95 (12.97)
			100	8.13 (0.84)	31.34 (12.88)	26.11 (9.47)
8.91	23.99	12.88	100	8.94 (0.84)	26.45 (9.82)	22.08 (8.21)
			100	9.72 (0.87)	23.29 (8.26)	18.92 (7.08)
10.47	20.89	13.49	100	10.56 (0.88)	20.42 (5.89)	16.46 (5.44)
			100	11.32 (0.85)	19.45 (5.22)	14.41 (4.24)
12.02	45.71	14.45	100	12.08 (0.86)	17.61 (4.06)	12.51 (2.97)
			100	12.30 (0.80)	17.52 (3.89)	12.11 (3.09)
			100	12.49 (0.81)	16.82 (3.46)	11.66 (2.72)

Table 6.3: Comparison of burst and silence durations during dehydration: observations from rats dehydrated for up to 24 hours from Wakerley et al [112] are compared with those from a population of 100 model cells with the parameters described in Table 6.2. Although the model population shows a fall in burst and silence duration, values are not dissimilar to those observed. Same data as Figure 6.15

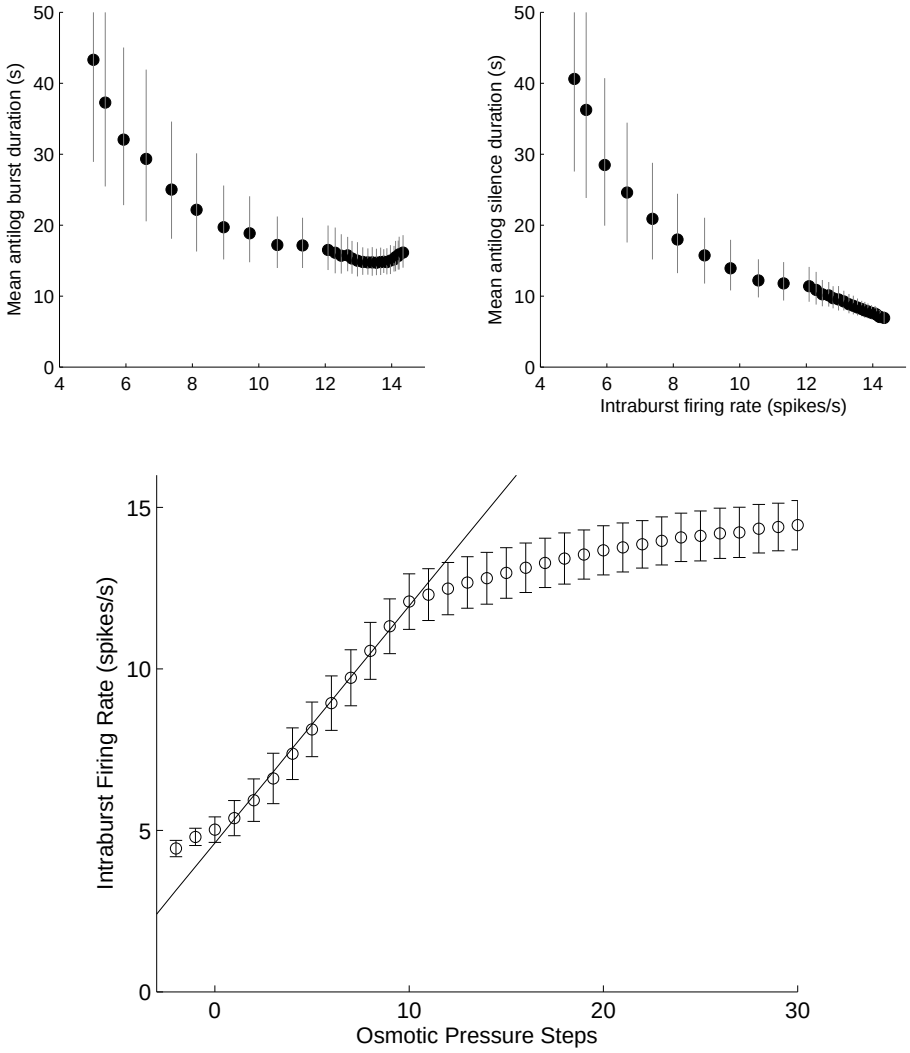

Figure 6.15: Plateau depolarised during raised osmotic pressure: phasic patterning. Top: Antilog Burst/Silence durations in phasic cells. The burst/silence durations are much shorter than with the fixed plateau, because V_r can start at a more depolarised level and still be efficient. steps plotted have more than 90 cells processed at the 90% catogorised level. While burst and silence duartions are still falling between 6-12 spikes/s, the range measured by Wakerley et al, they are plausible values. Bottom: firing rate increases linearly as osmotic pressure increases in the phasic range. The intraburst firing rate increases less quickly after step 10, as the cells no longer depolarise after this point: line fitted from step 0 to step 10, R^2 = 0.99.

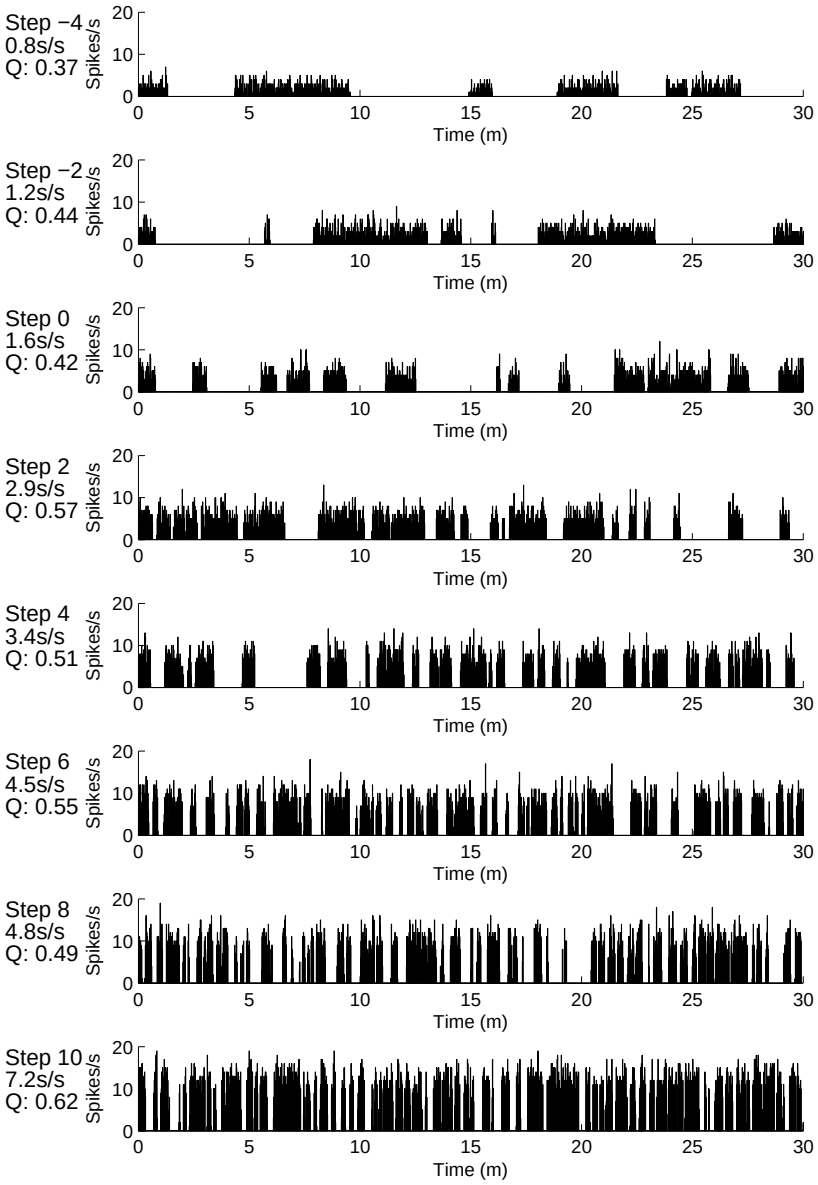

Figure 6.16: Sample firing from cell with plateau depolarisation during raised osmotic pressure. These cells do not start with long burst times: as osmotic pressure increases, the cells fire shorter but more frequent and intense bursts.

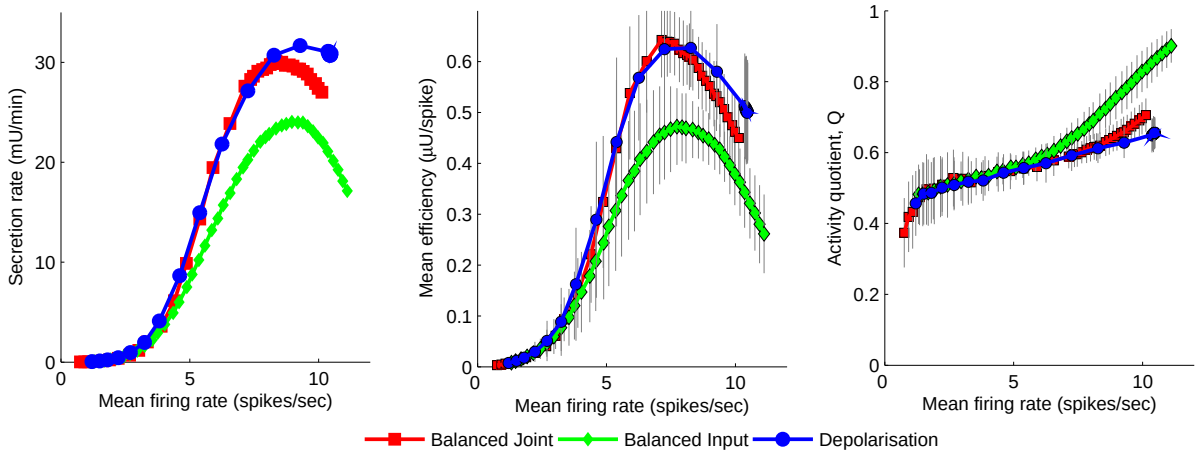

Figure 6.17: Plateau depolarised during raised osmotic pressure:different strategies. This time, the relatively high starting input rate and rest potential benefits the sole depolarisation strategy: it covers only -0.9 to +3mV, but covers most of the necessary firing range very efficiently. Raising the input rate without depolarisation is relatively ineffective:V_p and V_r are too close together for this strategy to succeed and it lapses into continuous firing. The joint strategy is as efficient as depolarisation until rises in PSP rate cause it to overbalance: the activity quotient increases and it ceases to be as effective.

Depolarising the plateau means a different, and more realistic starting state can be used and efficient results can still be achieved. However, the model is very sensitive to changes in plateau level: increasing it results in a rapid increase in firing rate, requiring only very modest changes in $R_{E(I)}$ to further increase firing rate. This would require precise control. The more the plateau can depolarise, the more important afferent control is.

This was confirmed by trying different strategies: increasing the depolarisation only and the input rate only. Both produced a linear increase in firing, as before, but the secretion efficiency varied (Figure 6.17).

The balanced input strategy was now far less efficient than either depolarisation or joint depolarisation and balanced joint (maximum efficiencies respectively 0.47 μU/spike, 0.63 μU/spike and 0.64 μU/spike). The maximums occurred at +220PSP/s for balanced input, +2.4mV for depolarisation and +1.5mV and + 50PSP/s for the joint strategy.

Although they produce similar efficiencies, the patterning at the most efficient point is quite different: depolarisation has longer burst and silence durations and a lower

Results	V_p (mV)	V_r (mV)	$R_E(I)$ PSPs/sec	Value μU/spike
Parameter				
Search	-61	-71	420	0.66
	-60	-69	320	0.63
	-59	-67	220	0.65
Plateau Fixed				
Balanced Joint	-60.0	-69.0	350	0.66
Balanced Input	-60.0	-70.0	350	0.65
Depolarisation	-60.0	-70.25	170	0.05
Plateau Depolarises				
Balanced Input	-60.5	-68	410	0.47
Balanced Joint	-59.0	-66.5	240	0.64
Depolarisation	-58.1	-65.6	190	0.63

Table 6.4: Maximum efficiencies predicted by parameter search versus those found. For populations following the depolarisation only strategy, the original input rate is clearly fixed, whereas for joint input, V_r and V_p are fixed. In both cases with Balanced Joint strategies the maximum depolarisation allowed has been reached before the maximum efficiency. Generally, maximums have been found around those predicted by the parameter search: if V_r is more hyperpolarised the input rate is increased to compensate, and if V_r is depolarised the input rate reduces. This indicates the parameter space is behaving in a predictable fashion with respect to V_r, V_p and $R_{E(I)}$.

intraburst firing rate than the joint balanced strategy (31s, 25s and 9.7 spike/s versus 18s, 13s and 12 spikes/sec respectively). That they have roughly the same efficiencies suggests a number of patterns will produce roughly the same secretory output.

After all strategies have peaked in terms of efficiency, the depolarisation only strategy proceeds to increase the secretion rate to 32mU/min (at +2.7mV) whereas the joint strategy cannot sustain even its highest value (30 mU/min, at +1.5mV and +90 PSP/s). The difference is significant (Ttest, p=9.4e-6) Raising the input rate alone results in a maximum of 24mU/min at +280PSPs/s.

The intraburst firing rates are around the same in both cases (11.0 spike/s for depolarisation, 13.4 spikes/sec for joint balanced), but the depolarisation only strategy has a higher burst and silence duration (27s bursts, 21s silence versus 15s burst, 9s silence).

So far, the parameter search has accurately predicted the values found by the populations. Here, the population is moving between values explored in the parameter search, but generally the maximum values can be predicted by interpolating form the parameter space.

6.4.4 Summary of population results

The model population has been able to replicate the secretory response well under a variety of strategies, although the response collapses eventually. While it can be concluded that a balanced of inhibition and excitation is necessary to maintain the phasic response and therefore release, it is harder to say anything conclusive about the relative merits of depolarisation and input rate rises, both of which are know to occur.

Either could potentially replicate the secretory response, although in the case of depolarisation this relies upon the plateau being able to depolarise as well. It is clear that firing rate is very sensitive to changes in the plateau level, and given that variance in biological systems is inevitable, perhaps depolarisation must be very slow to avoid system collapse. It is also possible that the depolarisation serves a different purpose, such as triggering conditions allowing plateau creation.

It can be concluded that the more the plateau can depolarise, the less change in input rate is required for secretion: however, experimental data indicates that the input rate could increase several fold.

The best strategy depends upon the level of the plateau: depolarised plateaux will produce high intraburst firing rates, and so will tend to benefit more from adjustment to V_r which alters the patterning without increasing the intraburst firing rate to inefficient extents.

Hyperpolarised plateaux, however, will require higher input rates to reach the optimum firing frequency. A higher input rate forces more state changes, however, and therefore to maintain the ideal burst and silence durations the rest voltage will have to be hyperpolarised. Depolarisation pf $V_R$is therefore not a good strategy unless the plateau also depolarise.

If the network begins with a wide distribution of starting plateaux (here, it was quite conservative) then a mixed strategy may represent the best course. This will be especially true if plateaux can also depolarise to different degrees: here, all vasopressin cells have been able to depolarise in identical fashion.

However, all of this has been derived using a population of cells, not a network.

While vasopressin cells probably do not have many lateral connections, but they can influence each other by dendritic vasopressin.

6.5 Dendritic Vasopressin: possible effects

The model lacks a crucial component: dendritic vasopressin. Building in a method for cells to influence each other by dendritic bundles should not be particularly hard. Unfortunately, it is much harder to determine what vasopressin should actually do and when it should do it.

It is not clear even if vasopressin is entirely inhibitory or not. Assuming that it is, there are number of reported ways it could inhibit cells, including reducing the EPSP magnitude [59], increasing the firing threshold [1], depolarising the cell [1], etc.

To try and determine which of these possibilities may be helpful in extending the dynamic range of the network, parameter searches were performed with:

- Different PSP magnitudes (2.1mV, 2.3mV, 2.7mV)
- Different mixes of EPSP:IPSP (110%, 90%).
- Longer autosecretory inhibition (10s half life), i_w dropped to 0.005 to keep overall levels of autosecretory inhibition roughly constant.
- Longer drift time constant, to check this was not a significant factor in hyperpolarised potential doing well to 2 minutes).

Each parameter search consisted of 30 mins worth of data per point, with V_r varying from -72 to -63mV in steps of 1mV, and V_p of -59,-60 and -61mV. The results are most clearly visualised with the plateau of -59mV.

In these grids, depolarisation is equivalent to moving right and increases in input rate are downwards. The base grid indicates the response to this in the cells: once they have reached the maximum rate on this grid, further increases will result in lower secretion. A peak at a high input rate and depolarisation would offer a theory as to why the population carries out these actions, as the cells experience increases in input rate and depolarise during osmotic pressure.

In particular, finding a parameter that can be changed after the point of maximal efficiency to increase secretion rate would be useful.

The first noticeable thing is that more autosecretory inhibition increases the total secretion, indicating a slower acting feedback is very effective. One would expect

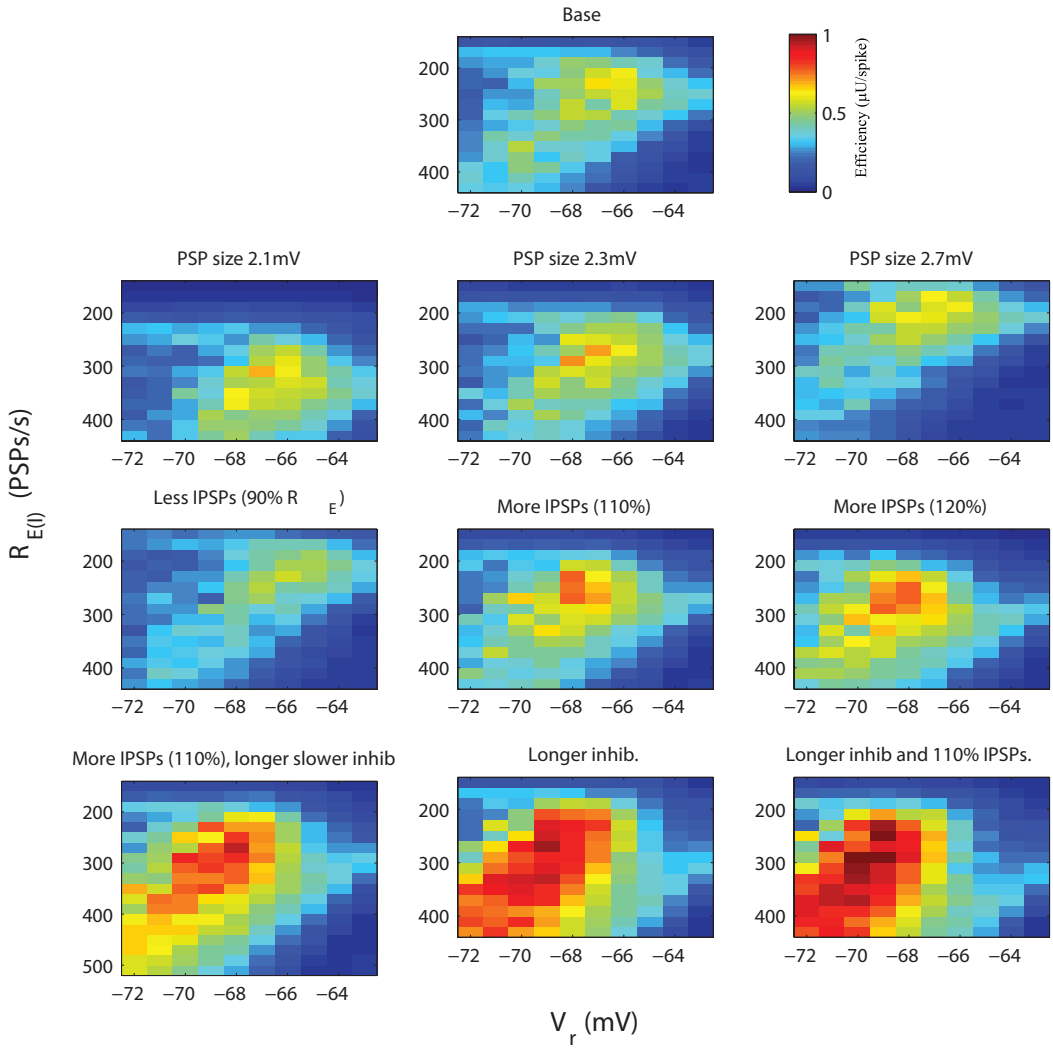

Figure 6.18: Efficiency in (μ U/spike) with modified parameters. An exploration of the parameter space, looking for the equivalent of hyperpolarisation (ie, the highest point moving right). Here the plateau is -59mV through all runs, as this allows the parameter space to be explored with smaller input rates. A number of parameters were altered, all others were kept as in Table 4.1: the PSP size was 2.45mV, autosecretory inhibition per spike I_w 0.015 and the inhibitory half life 3657ms.. Reducing the PSP size (second row) means the same efficiency can be achieved with a more depolarised V_r, so this is a potential candidate of vasopressin. The drift has relatively little effect on results (Longer drift time: 2 mins). Spreading the autosecretory inhibition over a longer period by increasing the half life to 10s and lowering I_w to 0.005 also have relatively little effect. Reducing the IPSP:EPSP ratio ('Less IPSPs' reduced efficiency, even if autosecretory inhibition was increased to try and compensate. Increasing the IPSP:EPSP ratio to 110% however improved results, as did then increasing the autosecretory inhibition.

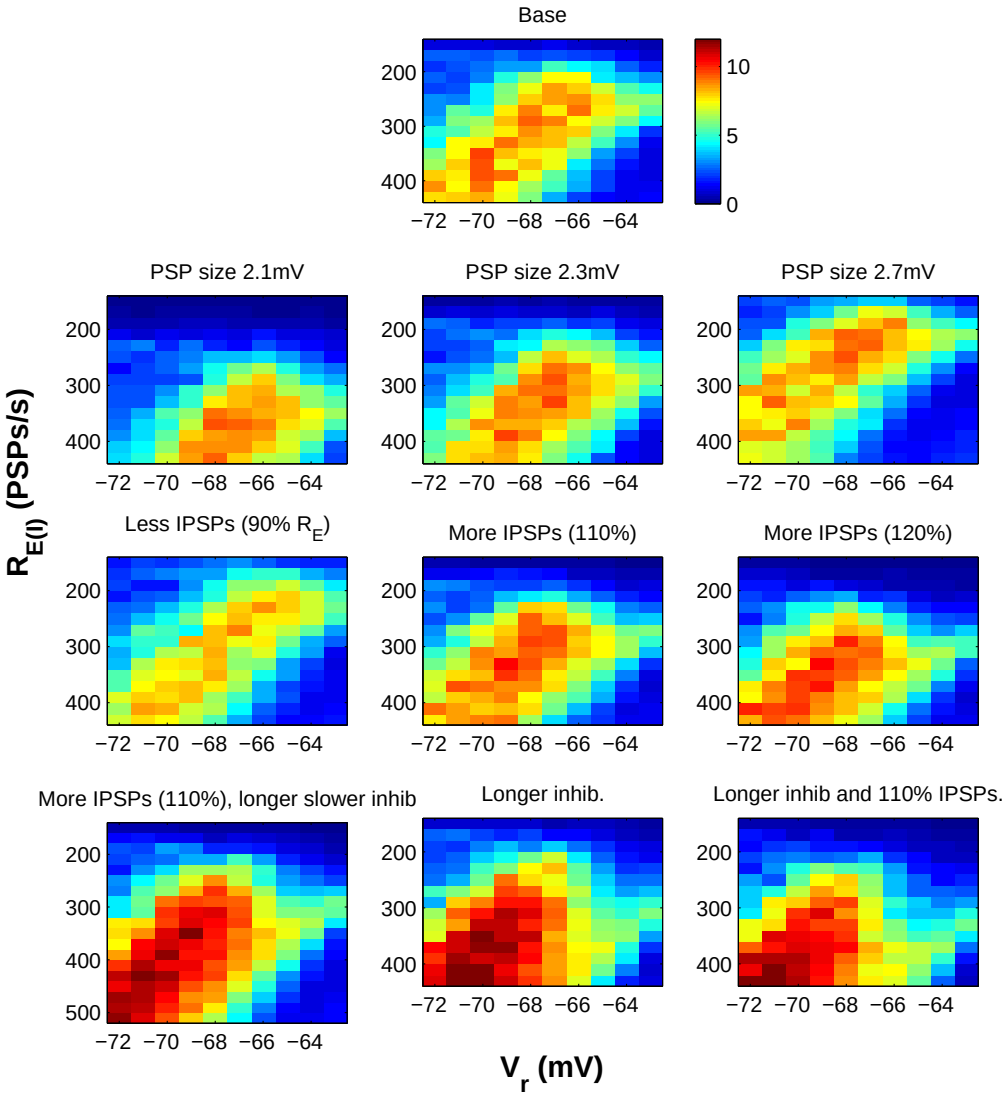

Figure 6.19: Total secretion (mU) with modified parameters. An exploration of the parameter space, looking for the equivalent of hyperpolarisation (ie, the highest point moving right). Here the plateau is -59mV through all runs, as this allows the parameter space to be explored with smaller input rates. A number of parameters were altered. The base parameters are as in Table 4.1: the PSP size was 2.45mV, autosecretory inhibition per spike I_w 0.015 and the inhibitory half life 3657ms.. Reducing the PSP size (second row) means the same efficiency can be achieved with a more depolarised V_r, so this is a potential candidate of vasopressin. The drift has relatively little effect on results (Longer drift time: 2 mins). Spreading the autosecretory inhibition over a longer period by increasing the half life to 10s and lowering I_w to 0.005 also have relatively little effect. Reducing the IPSP:EPSP ratio ('Less IPSPs' reduced efficiency, even if autosecretory inhibition was increased to try and compensate. Increasing the IPSP:EPSP ratio to 110% however improved results, as did then increasing the autosecretory inhibition.

the secretion efficiency to increase with longer lasting autosecretory inhibition: if the only criteria was efficiency per spike there would be the luxury of waiting as long as possible for axonal recovery.

However, the strategies with longer autosecretory inhibition succeeded in secreting more than those without. Maximum secretion was still seen at hyperpolarised levels, although with much lower efficiency.

In the model, only the distance between the firing threshold and the rest potential and plateau potential is important: the absolute values are irrelevant. Raising the firing threshold could therefore act as equivalent to hyperpolarisation.

As for other strategies, increasing the PSP magnitude is equivalent to decreasing the PSP rate: this seems somewhat pointless as a strategy. Although increasing the IPSP:EPSP ratio can increase efficiency of secretion, longer autosecretory inhibition is more effective.

It seems from this that dendritic vasopressin could increase secretion rate simply by acting in the same way as the current autosecretory inhibition but over a longer time period. There is no need to deplete inhibitory stores until the cell has begun firing at a reasonable rate, and the autosecretory inhibition would act to dampen the system when the input rate fell after osmotic challenge finished. It could even allow for depolarisation of the firing threshold, allowing maximisation of secretion.

There is another strategy it could pursue. Not all cells are firing efficiently at the same time: what is really required is a way of tuning cells so all are as efficient as possible within their limitations.

This analysis has assumed that the system is trying to maximise efficiency and/or total secretion. It's possible that the cost of firing is not high and thus the output per spike is not important. It has been assumed here that the system would seek to minimise energy consumption by minimising firing, but it could be that precision in the system is more important (in which case studies of the coding capacity as represented by entropy become particularly important). To clarify this requires more data on the tolerances of vasopressin cells - neurotoxicity of firing (if any), energy consumption and some idea how precise the response must be to regulate the system possible. Modelling of blood volume and osmotic pressure could possibly help clarify the last point.

In summary, it would appear there is no one parameter that increases secretion and justifies depolarisation: maximal secretion still tends to happen at hyperpolarised levels. More autosecretory inhibition would be beneficial, but the likest approach is a combination of factors. Further research is required.

Chapter 7

Conclusions

7.1 Overview

The aim of this PhD was to construct a framework for evaluating the relative performance and implications of models. By providing a benchmarked system, it becomes possible to evaluate the relative significance of assumptions.

Computational modelling has grown in popularity as a tool for neuroscience; a proliferation of models that shows no sign of ending has sprung up making predictions on all areas of neuroscience. However, to date it is unclear what constitutes a 'good' model. Usually the minimum criteria is that it matches the available results. It is also understood that good models include the fewest possible components to match the data, in order to exclude extraneous results. For this purpose predictions are usually made, although here the more formal process of a parameter search has been carried out.

Without any formal criteria for evaluating models, it becomes difficult to train modellers: how are they supposed to know what is effective? It is also difficult to refine techniques. This is a recognised problem in the field, and one that some effort is being made to address although this is still in its infancy.

The brain also has a distressing tendency not to use the simplest seeming possible solution, which inevitably leads to conflicts for modellers as to which features to include. Neurons are complicated devices, and to date researchers have simply had to make their best guess as to what may be significant, what may be duplication or accident of evolution.

To formalise any of this requires a benchmark; but to construct a benchmark requires function to be related to a measurable purpose. The vasopressin system pro-

vided an ideal opportunity for this, as the secretion of the neurons allows modelling to go beyond the firing patterns.

This PhD has begun the construction of the framework and provides exciting opportunities for further work. A model of firing in vasopressin cells was developed, and then linked to a model of what the firing should do to. The modelling then moved from cell to network level, as a population was constructed, and then to system level as the output was evaluated by considering whether it would succeed in regulating blood volume and osmolarity.

The construction of the models then took place in this context; all models had to be computationally lightweight and replicate the key features necessary for network secretion.

7.2 The firing pattern model

7.2.1 Design

The firing pattern model had to generate patterns that replicated the key features of vasopressin neurons in a simple way. At the time the model was developed, the main information was the statistical features recorded by Sabatier et al. [97] on the ISI, hazard functions and first/second order statistics on firing rate and burst patterning. Additional information was provided by Wakerley et al. [86], and the key features of the cells challenged by osmotic pressure from [112].

It was decided to exclude frequency adaptation from the model if this simplified it, as the steady state is more important in network firing. Modelling then began by testing Andrew and Dudek's theory

> DAPs sum to form a plateau potential, thus increasing the likelihood of further spikes and their DAPs, which in turn add to the plateau potential and prolong the burst

[3].

This kind of theory, simple and elegant is ideal for testing using computational modelling, and when an integrate and fire model was adapted to include it it explained the *in vitro* results admirably. Plateaux formed. Unfortunately, the same did not hold true with the faster dynamics of *in vivo* firing: the DAP was simply too transient to support plateau formation.

This does not mean Andrew and Dudek's theory is wrong, merely that the model could not confirm it. This could be due to the simplified nature of the DAP or omission of other currents. Without more information, the safest thing to do was abstract away from the difficulty and assume the plateau (or a functional equivalent) would be formed under some circumstances.

Although the design was inspired by the bistable model, there were a number of decisions to be made. It was important firing rate did not slow throughout a burst which affected the form of the autosecretory inhibition. Isolated firing during otherwise quintessence period should be minimised. Burst and silence durations should be variable.

The previous model failed because it could not form a plateau, although the idea of using a Poisson input and threshold modified by the HAP and the DAP was clearly correct for generating firing. Key to this model was the decision to force creation of a plateau by providing a second resting potential and to introduce a tipping point to control the mechanics of phasic firing. This allowed the autosecretory inhibition to be included without interfering with firing. Phasic patterning could not be controlled in a way separate from firing: the two and linked by the input rate.

The model went through a number of design iterations while the behaviour (especially of the tipping point) was finalised. Once the idea of introducing a tipping point to make explicit the probabilities of a state change occurred, factors like the autosecretory inhibition - which had to terminate bursts without slowing firing rate - became relatively straightforward. For example, clearly firing must occur to trigger a burst, making the firing threshold the logical upper value for the tipping point: but what should the lower tipping point be? In the end, the lower tipping point was placed symmetrically, although the logical place would have been the resting potential. This would have made silences shorter than bursts.

The choice of a symmetrical tipping point has had implications, mostly that mean burst and silence duration correlated and to an extent with the intraburst firing rate.

The model is still fundamentally an integrate and fire model driven by a Poisson input, but influenced by more deterministic factors. It has provided a coherent picture of firing generation, but also exposed anomalies.

The intraburst firing properties can be tightly controlled by modifying the HAP time constant (for the mode), DAP time constant (intraburst firing rate), $R_{E(I)}$ and the plateau level (intraburst firing rate).

Phasic patterning is more complex: the burst duration depends on the distance be-

tween V_t and V_r, R_E and R_I, the autosecretory inhibition I_w and the DAP. The DAP's influence appears fairly limited: although burst duration increases when V_p is depolarised (Figure 4.26) suggesting the extra DAPs exert some effect the input rate has far more effect (Figure 4.29). At no point does the extra DAPs created by firing outweigh the increase in firing rate necessary to create the extra firing. Again, this indicates the structural problems with the DAP.

The autosecretory inhibition should affect silence duration, but apart from preventing bursts restarting within around 5s it has more effect on burst duration: clearly once autosecretory inhibition accumulates past a certain point it tends to end bursts, and the inhibition therefore never grows large enough to significantly prolong silences.

The silence duration depends on the displacement of the lower tipping point (currently symmetrical to that used for bursts), R_E and R_I. It is relatively invariant to autosecretory inhibition. As the factors in determining burst length and largely the same as determining silence length, mean burst length correlated with mean silence length if none of the parameters were varied. Both are also heavily influenced by $R_E(I)$, as is the intraburst firing rate leading to further undesirable correlations. It is likely that there is variability in R_E:R_I, the HAP time constant (for varying intraburst firing rate) and even the lower tipping point (which would translate to some cells having a faster plateau refractory period than others), so this can be dispensed with.

The dependence of the phasic patterning upon the input rate has had one further effect: when the input rate is increased, as it is during osmotic pressure, transitions become more frequent and burst and silence durations tend to decrease. Originally it was anticipated that the medium term, more stable influences such as the DAP and autosecretory inhibition would predominate at high input rates and stabilise the burst and silence duration: this doesn't seem to happen. While the results are mostly consistent with the observations under dehydration, it does not explain the extended burst durations sometimes observed. This is one of the areas where design changes to the model could improve.

This model has clarified theory, and replicated most of the extensive experimental results. It provides a valuable basis for further exploration of the cells, particularly with regards to the autosecretory feedbacks. Although the model has not been used to make many predictions - mainly because of the missing autosecretory feedbacks (especially dendritic vasopressin) - it has been used to thoroughly explore the functioning of vasopressin cells and help elucidate the results of osmotic pressure (particular with regards to the plateau potential).

7.2.2 Possible Improvements

The model can currently produce a 'typical' cell without frequency adaptation with reasonable intraburst firing mechanics (the ISI histogram is a very close match). However, there are two key areas for improvement:

- Burst/silence hazard functions
- Increasing variability in the model to produce less typical cells, including those firing non phasically.

The burst/silence hazard functions in the model are only partially correct: while after $\sim$20s bursts and silences do terminate randomly, previous to that medium term influences should prevent early termination. This does not happen in the model. Unfortunately this data was not available until well after the model had been designed and implemented.

The model was designed with the simplest possible form of autosecretory inhibition, assuming it would accumulate per spike. However as pointed out by Roper [94] autosecretory inhibition is almost certainly also subject to secretory mechanisms. Successful experimentation with this would solve at least one problem in the model: that if the autosecretory inhibition is raised it tends to end bursts early rather than prolong silences (although this is consistent with the evidence that dynorphin influences burst termination [25] but not burst initiation.) Autosecretory Inhibition more realistic would be lagged and limited. Longer bursts could then be explained as rundown of the autosecretory inhibition mechanism.

Lagged autosecretory inhibition would mean bursts would be less likely to terminate in the first $\sim$20s: the eventual autosecretory inhibition would also be larger, and the silence hazard function may also be corrected at this point.

The second point is more an extension of a model than a correction: the model was designed to replicate phasic firing. At the moment irregular firing occurs during low input regimes (realistically), but tend still to be cyclic. Currently, the drift curtails what would otherwise be a very long period firing pattern. There is no evidence either exists in vivo.

One possibility is to make phasic firing less reliable. The tipping point transition is currently instantaneous and infallible. Neither is likely. It would be interesting to explore the consequences of the tipping point moving more slowly: this would create

a region where the model was unstable, and may only fire an isolated spike begin a burst.

Ideally, the tipping point would begin to move but be dragged back to the resting state in absence of further firing. Under low input regimes, this would cause the plateau to constantly collapse: this would probably be a more convincing form of slow irregular firing. This would also increase variation in the model: it is currently less variable than *in vivo* (eg Figure 6.7), although his would also require larger sample sizes both *in vivo* and *in silico*.

At the moment, because autosecretory inhibition is unlagged it must be kept relatively weak: phasic patterning is imposed by the tipping point. Currently the lower tipping point is based on the separation of V_t and V_r. It is assumed after a period of no or weak firing the plateau collapses: here this happens when the membrane voltage falls low enough to make sufficient firing unlikely. But perhaps separation should be enforced more by the autosecretory inhibition: if it grew sufficiently large to push the tipping point a significant distance, the lower tipping point could be further away. With low input rates, autosecretory inhibition would fail to accumulate sufficiently to push the tipping point within the range of v_m (which would also be less variable, leading to constant irregular firing.

This would enable elimination of the drift, something that should exist mainly though autosecretory inhibition wearing off if it exists at all.

Once autosecretory inhibition in the model has been improved - which would probably involve modelling dendritic vasopressin as well - it could then be used to generate changes in burst and silence hazards during osmotic stimulation. This would provide a useful experimental prediction, given that under osmotic pressure autosecretory feedbacks increase and this should be reflected in the hazards.

7.3 Stimulus-Secretion model

7.3.1 Design of the secretion model

The stimulus-secretion model was designed simply to provide a match to available physiological data. It would have been unnecessary to include realistic descriptions of the underlying biology, as the purpose of the model was only to prove a secretion profile for any firing pattern. A look-up table would have sufficed had sufficient data existed; instead extrapolation from the available data was necessary.

To extrapolate in a safe a fashion as possible required staying close to the known functioning of the axon ending. Although there is some understanding on the processes involved in vasopressin systems no model existed. Fortunately other secretory systems likely to be similar had been modelled, and so a pool structure inspired by these was used.

The idea of a ready releasable pool, reserve pool and deep store has been explored before and was adapted here. It allows the model to display the key features of facilitation and depletion. When activity begins, the RRP releases its vesicles quickly: as it becomes empty the RP refills it. The nature of facilitation means that the RP must be larger than the RRP: the RRP can therefore be kept full and continue secreting at full rate. Without the RRP, secretion would slow more rapidly as the emptiness of the secreting pool increased. As it is, by using the RRP facilitation can occur as secretion can be maintained until the RP begins to run short.

The RRP and RP control the short term dynamics of secretion, but it is the deep store which dictates what the system is ultimately capable of, through the refill function δ. δ controls the rate at which the deep store refills the RP. High frequency stimulation can have a sustained response, so the deep store must refill the RRP proportional to frequency. However, release from the deep store must be even more during silences as secretion is greater when pauses exist during firing - phasic firing is more efficient than continuous. This leads to the strange non-linear form of δ.

The other oddity in the model is that the secretion rate of a pool depends on how empty the pool it is refilling is, something it would have to sense somehow - probably through back rate reactions.

The model has provided a realistic secretion profile under different conditions, and confirmed that a secretory pool set-up is a likely contender for providing this.

7.3.2 Possible improvements

This model currently operates with fixed parameters, but axon endings clearly vary biologically. It would be useful to have some idea of the range of variation *in vivo* and even whether this is in any way connected to firing patterns. For example, do endings with slow refill functions tend to have phasic patterns with longer silences?

7.4 The population model

The population model duplicated and varied the firing pattern model to produce a range of firing patterns. The stimulus-secretion model parameters were left unvaried, so all model neurons had identical axon endings. Secretion from the population was then evaluated under osmotic pressure.

The model neurons were unconnected and independent: thus the nomenclature as population rather than network. Nevertheless, the population could replicate the linear secretion under osmotic pressure. Individual cells tended to respond with increases of secretion, but the population response was sharper.

This provided the framework for benchmarking. As an initial test, the input was unbalanced by unhitching R_E and R_I: only R_E was altered. This unbalanced the model, leading to continuous firing with a disastrous effect on secretion. It is the first time the link between a balanced input rate and secretion has been shown.

The effects of depolarisation have also been quantified. Generally, depolarisation of the resting potential makes little difference to secretion efficiency. It is possible the depolarisation *in vivo* serves some other purpose such as strengthening the plateau somehow. More likely though is that this reflects the lack of inhibition in the model: hyperpolarised resting potentials tend to do well under high input rates as the bistability is maintained. Improving the autosecretory inhibition as mentioned previously would probably improve this.

If the plateau depolarises, this decreases the increase in the input rate necessary for release. The linear secretion can be replicated regardless of the plateau value.

Phasic patterning was realistic for most stages of the simulated dehydration, although no increase in burst sizes was ever seen. As mentioned earlier, this may reflect a flaw in the autosecretory inhibition (it cannot deplete).

7.4.1 Possible Improvements

Now the framework has been constructed, new features can be built into the model and the effect on secretion evaluated. Refinements to the model can be tested to see if they are improvements.

7.4.2 Connected Network

Evidence from the SON indicates most cells are probably not connected [60] however input sharing could go on and some lateral connectivity could be tested, if only to see if this actually results in a degradation of performance.

The population acts as a low pass filter [98]: as delivering excitement to the system causes the cells to flip state (quiet cells become excited, excited cells overexert themselves, causing an extra spurt of autosecretory inhibition and terminating the burst). An interconnected network may not manage this as successfully.

7.4.2.1 Modelling dendritic release of vasopressin

Undoubtedly this would be useful, both from an experimental point of view (there is still controversy over whether dendritic vasopressin is inhibitory or regularising) and computation (load balancing, for example, being a common problem).

The main problem is not coding dendritic release - adding it to the model would in fact be straightforward - but designing its action. There is little information on the time course of dendritic release (especially as regards its ties to activity), and on what exactly dendritic vasopressin should do. Assuming the easiest action - it is inhibitory - it is still unclear if it should alter the membrane potential, PSP sizes or rates, plateau potential, resting potential or firing threshold.

It is also unclear how to fairly compare the new network to the non-dendritic one. Simply picking a suboptimal parameter value in the non-dendritic release network and then deliberately tuning the other to optimise that value is clearly not an unbiased comparison.

For dendritic vasopressin to be computational advantageous something must happen under osmotic pressure to make dendritic secretion worthwhile. Either a parameter such as PSP magnitude may have to evolve to compensate for the increase in input rate, or - perhaps more likely - it becomes more important that individual cells are tuned for maximal output (although this would require a local feedback, whereas vasopressin seems more of a population signal). An obvious way the dendritic network could score over the non-dendritic network is to homogenise the network to the most efficient set of parameters.

The parameter searches carried out for different parameters dendritic vasopressin could alter showed that hyperpolarised, high input rate neurons still tended to release the most. The hyperpolarisation in this case enforced the phasic patterning: it is there-

fore likely that lagged inhibition may do the same, although some experiments suggest the k-opioid receptors are the most likely source for this.

An avenue for future exploration would then be to have dendritic vasopressin provide a lagged, large inhibitory impetus to the tipping point. There are reports of cells becoming excited under osmotic pressure [11] and vasopressin [47], a cell inhibited by others may become active if its oppressors are themselves inhibited.

7.4.2.2 Modelling the renal system

Here, it has been assumed that the linear response of the neurons was optimal: while it often true that systems with a heavy lag require a controlled response this hasn't been proved. A further avenue would be to build a more complete, although still abstract simulator in an attempt to test the effectiveness of the linear release.

7.4.2.3 Further heterogeneity

The population here generated a significant number of differing phasic cells, but particularly at low input rates where behaviour is largely dependent on deterministic processes (the drift), variation is low. There could also be more variation in firing rate: exploring the consequences of a less uniform HAP and DAP and differing levels of dendritic vasopressin could increase the variability considerably.

So far, variation in population has been confined to the firing pattern generator: all our model cells effectively have the same axon. There is significant variation at the axonal level (see [35]), where the same patterns produced different levels of secretion), and it would be interesting to know if the cell adapts its firing to this. Experimental evidence is currently too sparse on this subject.

7.4.2.4 Other theories of vasopressin cell functioning

The model built here for firing was heavily based on Leng & Brown's [64] theory of bistability. However, it is possible other theories may be developed, and there may be subtleties in how whatever underpins phasic firing is implemented.

This would provide an extremely useful test for the framework. Suppose an alternative theory was implemented in a model. The tests for whether a model replicates in vivo firing are mainly based on grouped statistics: thus it is possible a different model would match the experimental statistics for phasic firing while producing fundamentally different firing patterns to the ones presented here.

Secretion could then be used to find the features responsible for significant differences. Searching for the differences experimentally could be then time consuming, especially as most models can be altered to match new data, but pinpointing the differences likely to be significant would help provide guidance on where to look. Arguably, more efficient techniques are more likely to be adopted, but if this is not the case this is also interesting.

7.4.3 Other tests for the network

- **Other challenges, for example hemorrhage** Dehydration was picked as the main challenge as there was sufficient data on the resulting firing patterns, and it is also a realistic challenge to the system. In this case, loss of blood volume will force the network to choose between defending blood volume (by secreting ADH, thus forcing osmotic pressure up) or defending osmolarity. The system can clearly only cope with both up to a certain point: it should eventually reflect biology and defend blood volume by secreting ADH.

- **Network degradation** In the actual network, this would occur due to injury, ageing and disease. Biologically, the network should continue to function extremely well until a critical proportion of neurons are lost: at the point, the network collapses. This would require feedback mechanisms to balance the network.

- **Different forms of inhibition** Vasopressin cells have multiple inhibitory feedbacks, of which only two (IPSPs and a simple form of autosecretory inhibition possibly closest to dynorphin) have been included in the model. It would be interesting to include others to see if these make any difference to performance.

- **Penalty for firing** Firing is expensive in terms of resources and possibly toxic: by adding a penalty for firing which 'kills' any cells exceeding a threshold, it would be possible to experiment with pressure in the system and see if it can be made to adapt - for example by load balancing through dendritic vasopressin.

- **Testing 'refinements' to the model** Are refinements improvements? Which differences in firing are crucial? The framework can be used to test this. It would also be interesting to try recorded patterns from *in vivo* vasopressin cells, to see what their performance would be, although this may require more study of variation at the axon ending.

7.5 Summary

Vasopressin cells are highly non-linear processing units; they generate complex patterns of activity that are coupled to secretion by complex non-linear mechanisms. The non-linearities of secretion have been studied extensively in vitro, leading to the hypothesis that vasopressin cells discharge phasically to optimise the efficiency of stimulus secretion coupling (see [63]). Nevertheless, vasopressin secretion increases linearly in response to linear increases in plasma osmotic pressure, which produces both a linear depolarisation and an increase in inhibitory and excitatory synaptic input; this linearity applies over a wide dynamic range above a set point at about the normal plasma osmotic pressure.

Here, the logical coherence of this account was tested. A population of model cells was produced, with realistic firing patterns and secretion. This involved designing novel, quantitatively accurate models. Computer models are used mainly to clarify theory and predict behaviour. As it is known what the response of the vasopressin system is, which aspects of the model are important for "physiological performance", and which might simply be variations still considered "good enough" for the system to tolerate [73] it can be evaluated. For computational modellers, this offers the possibility of comparing different mechanisms and constraints with the functional consequences.

It has confirmed that the cells are bistable oscillators: the essence of the theory by Leng and Brown [64]. This theory has proven itself able to replicate the phasic patterning and intraburst firing statistics of the cells.

And yet, it hasn't proven to be quite that simple. If the cells were simply driven by short term, stochastic influences the phasic firing pattern should have a shorter cycle length as the input rate increases. The model shows this quite clearly. But the cells themselves show a range of behaviour, including increased burst duration.

Originally, it was supposed that the increased transitions imposed as the input rate rose would be counterbalanced by the DAP: however, the stabilising influence of the DAP proved to be too transient to outweigh the input fluctuations, although the intraburst firing rate is within the observed range.

This suggests that either the form of the DAP is incorrect, that too many fluctuations in the input are being used to generate the firing or that some other component is missing or incomplete. Both the DAP and the model parameters have been derived as closely as possible from the experimental evidence.

The interplay of the longer term, more deterministic influences in the model is an

ongoing research area, especially with regards to incorporating dendritic vasopressin. The construction of the framework means that the ideal balance between short term stochastic influences and longer term deterministic ones can be explored. It can also be used to evaluate the effects of different models or changes in conditions; here this has been demonstrated by trying different regimes for osmotic pressure. This PhD has created the framework necessary to advance research in a quantifiable fashion.

Appendix A

Abbreviations and terms

For the convenience of the reader, a table of abbreviations and terms is included.

Term	Full name
AVP	Arginine Vasopressin
ADH	Antidiuretic Hormone, synonym for AVP
HAP	Hyperpolarising AfterPotential
DAP	Depolarising AfterPotential
PVN	paraventricular nucleus
SON	supraoptic nucleus
ISI	Interspike Interval
OVLT	Organum Vasculosum Laminae Terminalis
autosecretory inhibitory	The inhibitory term in the model used as a generalisation of the the medium timescale inhibitory secretory influences on firing (particularly though not necessarily exclusively dynorphin). Referred to as I_w in the model equations (eq 4.7). This is the inhibition used to alter the tipping point and thus the probability of burst initiation and termination
COV	coefficient of variance
CCK	Cholecystokinin
IFR	Intraburst firing rate

Table A.1: Abbreviations

Symbol	Description
V_p	Plateau potential
V_r	Rest potential
I_w	Increase in autosecretory inhibition
λ_w	Autosecretory Inhibition decay constant
R_E	EPSP rate
R_I	IPSP rate
A_F	Facilitation voltage
D	Drift time constant
A_D	DAP magnitude
τ_D	DAP time constant
A_H	HAP magnitude
τ_H	HAP time constant
τ_m	Membrane time constant
V_t	Unmodified firing threshold
Δ_t	time step
A_P	PSP magnitude
A_F	Facilitation voltage

Table A.2: firing model symbols

Symbol	Description
z	Activity-dependent variable (fast)
f	Facilitation variable (activity-dependent, slow)
f_i	f increase per spike
g	z-dependent decay constant
x	vasopressin secretion
a	quantity of vasopressin in RRP
b	quantity of vasopressin in RP
δ	variable for scaling deep store secretion rate
Z_i	z increase
Z_d	z decay constant
A_t	threshold for z for RRP secretion to occur
F_d	f decay constant
G_1	scales g
G_t	threshold for z for g to be non-zero
F_1	scales fi
F_2	scales f_i
α	scales RRP secretion rate
β	scales RP secretion rate
A_M	capacity, RRP
B_M	capacity, RP
D_1	scaling factor for RP refilling during silence
D_2	scaling factor for RP refilling during activity
D_T	constant used to calculate refill
M	scaling factor for model output (μ U)

Table A.3: Secretion model symbols

Bibliography

[1] H. Abe, M. Inoue, T. Matsuo, and N. Ogata. The effects of vasopressin on electrical activity in the guinea-pig supraoptic nucleus in vitro. *Journal of Physiology*, 337:665–85, Apr 1983.

[2] R. D. Andrew. Endogenous bursting by rat supraoptic neuroendocrine cells is calcium dependent. *J Physiol*, 384:451–65, Mar 1987.

[3] R. D. Andrew and F. E. Dudek. Burst discharge in mammalian neuroendocrine cells involves an intrinsic regenerative mechanism. *Science*, 221(4615):1050–2, Sep, 9 1983.

[4] R. D. Andrew and F. E. Dudek. Analysis of intracellularly recorded phasic bursting by mammalian neuroendocrine cells. *Journal Of Neurophysiology*, 51(3):552–66, Mar 1984.

[5] R. D. Andrew and F. E. Dudek. Intrinsic inhibition in magnocellular neuroendocrine cells of rat hypothalamus. *J Physiol*, 353:171–85, Aug 1984.

[6] W. E. Armstrong. Morphological and electrophysiological classification of hypothalamic supraoptic neurons. *Progress In Neurobiology*, 47(4-5):291–339, 1995.

[7] W. E. Armstrong, B. N. Smith, and M. Tian. Electrophysiological characteristics of immunochemically identified rat oxytocin and vasopressin neurones in vitro. *J Physiol*, 475(1):115–28, Feb, 15 1994.

[8] E. Arnauld and J. du Pont. Vasopressin release and firing of supraoptic neurosecretory neurones during drinking in the dehydrated monkey. *Pflugers Archiv. European Journal Of Physiology*, 394(3):195–201, Sep 1982.

[9] E. Arnauld, B. Dufy, and J. D. Vincent. Hypothalamic supraoptic neurones: rates and patterns of action potential firing during water deprivation in the unanaesthetized monkey. *Brain Research*, 100(2):315–25, Dec, 19 1975.

[10] G. S. Bhumbra and R. E. J. Dyball. Measuring spike coding in the rat supraoptic nucleus. *J Physiol*, 555(Pt 1):281–96, Feb, 15 2004.

[11] G. S. Bhumbra, A. N. Inyushkin, M. Syrimi, and R. E. J. Dyball. Spike coding during osmotic stimulation of the rat supraoptic nucleus. *J Physiol*, 569(Pt 1):257–74, Nov, 15 2005.

[12] R. J. Bicknell, D. Brown, C. Chapman, P. D. Hancock, and G. Leng. Reversible fatigue of stimulus-secretion coupling in the rat neurohypophysis. *J Physiol*, 348:601–13, Mar 1984.

[13] R. J. Bicknell and G. Leng. Relative efficiency of neural firing patterns for vasopressin release in vitro. *Neuroendocrinology*, 33(5):295–9, Nov 1981.

[14] C. A. Bondy, H. Gainer, and J. T. Russell. Effects of stimulus frequency and potassium channel blockade on the secretion of vasopressin and oxytocin from the neurohypophysis. *Neuroendocrinology*, 46(3):258–67, Sep 1987.

[15] A. Borowski. Web based learning in endocrinology. `http://cal.man.ac.uk/student\_projects/2002/MNBY9APB/THEPITUITARYANATOMY.htm`, 2002.

[16] C. W. Bourque. Calcium-dependent spike after-current induces burst firing in magnocellular neurosecretory cells. *Neuroscience Letters*, 70(2):204–9, Oct, 8 1986.

[17] C. W. Bourque. Transient calcium-dependent potassium current in magnocellular neurosecretory cells of the rat supraoptic nucleus. *J Physiol*, 397:331–47, Mar 1988.

[18] C. W. Bourque. Ionic basis for the intrinsic activation of rat supraoptic neurones by hyperosmotic stimuli. *J Physiol*, 417:263–77, Oct 1989.

[19] C. W. Bourque, J. C. Randle, and L. P. Renaud. Calcium-dependent potassium conductance in rat supraoptic nucleus neurosecretory neurons. *Journal Of Neurophysiology*, 54(6):1375–82, Dec 1985.

[20] C. W. Bourque and L. P. Renaud. Membrane properties of rat magnocellular neuroendocrine cells in vivo. *Brain Research*, 540(1-2):349–52, Feb, 1 1991.

[21] M. J. Brimble and R. E. Dyball. Characterization of the responses of oxytocin- and vasopressin-secreting neurones in the supraoptic nucleus to osmotic stimulation. *J Physiol*, 271(1):253–71, Sep 1977.

[22] C. H. Brown. Rhythmogenesis in vasopressin cells. *Journal of Neuroendocrinology*, 16(9):727–39, Sep 2004.

[23] C. H. Brown and C. W. Bourque. Autocrine feedback inhibition of plateau potentials terminates phasic bursts in magnocellular neurosecretory cells of the rat supraoptic nucleus. *J Physiol*, 557(Pt 3):949–60, Jun, 15 2004.

[24] C. H. Brown, P. M. Bull, and C. W. Bourque. Phasic bursts in rat magnocellular neurosecretory cells are not intrinsically regenerative in vivo. *European Journal of Neuroscience*, 19(11):2977–83, Jun 2004.

[25] C. H. Brown, G. Leng, M. Ludwig, and C. W. Bourque. Endogenous activation of supraoptic nucleus kappa-opioid receptors terminates spontaneous phasic bursts in rat magnocellular neurosecretory cells. *Journal Of Neurophysiology*, Feb, 22 2006.

[26] C. H. Brown, M. Ludwig, and G. Leng. kappa-opioid regulation of neuronal activity in the rat supraoptic nucleus in vivo. *Journal of Neuroscience*, 18(22):9480–8, Nov, 15 1998.

[27] C. H. Brown, M. Ludwig, and G. Leng. Temporal dissociation of the feedback effects of dendritically co-released peptides on rhythmogenesis in vasopressin cells. *Neuroscience*, 124(1):105–11, 2004.

[28] C. H. Brown, J. A. Russell, and G. Leng. Opioid modulation of magnocellular neurosecretory cell activity. *Neuroscience Research*, 36(2):97–120, Feb 2000.

[29] P. M. Bull, C. H. Brown, J. A. Russell, and M. Ludwig. Activity-dependent feedback modulation of spike patterning of supraoptic nucleus neurons by endogenous adenosine. *Am J Physiol Regul Integr Comp Physiol*, pages –, Feb, 23 2006.

[30] M. Cazalis, G. Dayanithi, and J. J. Nordmann. The role of patterned burst and interburst interval on the excitation-coupling mechanism in the isolated rat neural lobe. *J Physiol*, 369:45–60, Dec 1985.

[31] R. H. Chow, J. Klingauf, and E. Neher. Time course of Ca2+ concentration triggering exocytosis in neuroendocrine cells. *Proceedings of the National Academy of Sciences of the United States of America*, 91(26):12765–9, Dec, 20 1994.

[32] A. Davies, A. Blakely, and C. Kidd. *Human Physiology*. Churchill Livingston, 2001.

[33] N. de Mota, A. Reaux-Le Goazigo, S. El Messari, N. Chartrel, D. Roesch, C. Dujardin, C. Kordon, H. Vaudry, F. Moos, and C. Llorens-Cortes. Apelin, a potent diuretic neuropeptide counteracting vasopressin actions through inhibition of vasopressin neuron activity and vasopressin release. *Proceedings of the National Academy of Sciences of the United States of America*, 101(28):10464–9, Jul, 13 2004.

[34] F. L. Dunn, T. J. Brennan, A. E. Nelson, and G. L. Robertson. The role of blood osmolality and volume in regulating vasopressin secretion in the rat. *J Clin Invest*, 52(12):3212–9, Dec 1973.

[35] A. Dutton and R. E. Dyball. Phasic firing enhances vasopressin release from the rat neurohypophysis. *J Physiol*, 290(2):433–40, May 1979.

[36] R. Dyball. The importance of bursting in determining secretory response: how does a phasic firing pattern influence peptide release from neurohypophysial vasopressin terminals. In G. Leng, editor, *Pulsatility in Neuroendocrine systems*, chapter 10. CRC Press, 1988.

[37] R. E. Dyball, P. R. Barnes, and F. D. Shaw. Significance of phasic firing in enhancing vasopressin release from the neurohypophysis. In H. Kobayashi, H. Bern, and A. Urano, editors, *Neurosecretion and the biology of Neuropeptides*. Springer-Verlag, 1985.

[38] R. E. Dyball and P. S. Pountney. Discharge patterns of supraoptic and paraventricular neurones in rats given a 2 per cent NaCl solution instead of drinking water. *Journal of Endocrinology*, 56(1):91–8, Jan 1973.

[39] A. W. Fisher, P. G. Price, G. D. Burford, and K. Lederis. A 3-dimensional reconstruction of the hypothalamo-neurohypophysial system of the rat. The neurons projecting to the neuro/intermediate lobe and those containing vasopressin and somatostatin. *Cell And Tissue Research*, 204(3):343–54, 1979.

[40] T. E. Fisher and C. W. Bourque. Voltage-gated calcium currents in the magnocellular neurosecretory cells of the rat supraoptic nucleus. *J Physiol*, 486 (Pt 3):571–80, Aug, 1 1995.

[41] L. G. Lateral hypothalamic neurones: osmosensitivity and the influence of activating magnocellular neurosecretory neurones. *J Physiol.*, 326:35–48, May 1982.

[42] M. Ghamari-Langroudi and C. W. Bourque. Caesium blocks depolarizing afterpotentials and phasic firing in rat supraoptic neurones. *J Physiol*, 510 (Pt 1):165–75, Jul, 1 1998.

[43] M. Ghamari-Langroudi and C. W. Bourque. Flufenamic acid blocks depolarizing afterpotentials and phasic firing in rat supraoptic neurones. *J Physiol*, 545(Pt 2):537–42, Dec, 1 2002.

[44] M. Ghamari-Langroudi and C. W. Bourque. Muscarinic receptor modulation of slow afterhyperpolarization and phasic firing in rat supraoptic nucleus neurons. *Journal of Neuroscience*, 24(35):7718–26, Sep, 1 2004.

[45] D. R. Giovannucci and E. L. Stuenkel. Regulation of secretory granule recruitment and exocytosis at rat neurohypophysial nerve endings. *J Physiol*, 498 (Pt 3):735–51, Feb, 1 1997.

[46] L. Gouzenes, N. Sabatier, P. Richard, F. Moos, and G. Dayanithi. V1a- and V2-type vasopressin receptors mediate vasopressin-induced Ca2+ responses in isolated rat supraoptic neurones. *Journal of Physiology*, 517:771–9, Jun 1999.

[47] L. Gouznes, M. G. Desarmnien, N. Hussy, P. Richard, and F. C. Moos. Vasopressin regularizes the phasic firing pattern of rat hypothalamic magnocellular vasopressin neurons. *Journal of Neuroscience*, 18(5):1879–85, Mar, 1 1998.

[48] W. Greffrath, W. Magerl, U. Disque-Kaiser, E. Martin, S. Reuss, and G. Boehmer. Contribution of Ca2+-activated K+ channels to hyperpolarizing

after-potentials and discharge pattern in rat supraoptic neurones. *Journal of Neuroendocrinology*, 16(7):577–88, Jul 2004.

[49] W. Greffrath, E. Martin, S. Reuss, and G. Boehmer. Components of after-hyperpolarization in magnocellular neurones of the rat supraoptic nucleus in vitro. *J Physiol*, 513 (Pt 2):493–506, Dec, 1 1998.

[50] G. Hatton. Phasic bursting activity of rat paraventricular neurones in the absence of synaptic transmission. *J Physiol.*, 327:273–84, 1982.

[51] G. I. Hatton and Z. Li. Intrinsic controls of intracellular calcium and intercellular communication in the regulation of neuroendocrine cell activity. *Cellular and Molecular Neurobiology*, 18(1):13–28, Feb 1998.

[52] C. Heinemann, R. H. Chow, E. Neher, and R. S. Zucker. Kinetics of the secretory response in bovine chromaffin cells following flash photolysis of caged Ca2+. *Biophysical Journal*, 67(6):2546–57, Dec 1994.

[53] S. F. Hsu and M. B. Jackson. Rapid exocytosis and endocytosis in nerve terminals of the rat posterior pituitary. *J Physiol*, 494 (Pt 2):539–53, Jul, 15 1996. unread.

[54] K. Inenaga, T. Nagatomo, K. Nakao, N. Yanaihara, and H. Yamashita. Kappa-selective agonists decrease postsynaptic potentials and calcium components of action potentials in the supraoptic nucleus of rat hypothalamus in vitro. *Neuroscience*, 58(2):331–40, Jan 1994. unread: don't have.

[55] M. B. Jackson, A. Konnerth, and G. J. Augustine. Action potential broadening and frequency-dependent facilitation of calcium signals in pituitary nerve terminals. *Proceedings of the National Academy of Sciences of the United States of America*, 88(2):380–4, Jan, 15 1991.

[56] I. K and Y. H. Excitation of neurones in the rat paraventricular nucleus in vitro by vasopressin and oxytocin. *Journal of Physiology*, 370:165–80, Jan 1986.

[57] K. Kadowaki, J. Kishimoto, G. Leng, and P. C. Emson. Up-regulation of nitric oxide synthase (NOS) gene expression together with NOS activity in the rat hypothalamo-hypophysial system after chronic salt loading: evidence of a neuromodulatory role of nitric oxide in arginine vasopressin and oxytocin secretion. *Endocrinology*, 134(3):1011–7, Mar 1994.

[58] K. Kirkpatrick and C. W. Bourque. Activity dependence and functional role of the apamin-sensitive K+ current in rat supraoptic neurones in vitro. *J Physiol*, 494 (Pt 2):389–98, Jul, 15 1996.

[59] S. B. Kombian, D. Mouginot, M. Hirasawa, and Q. J. Pittman. Vasopressin preferentially depresses excitatory over inhibitory synaptic transmission in the rat supraoptic nucleus in vitro. *Journal of Neuroendocrinology*, 12(4):361–7, Apr 2000.

[60] G. Leng. The effects of neural stalk stimulation upon firing patterns in rat supraoptic neurones. *Journal of Physiology*, (326):35–48, 1982.

[61] G. Leng and R. J. Bicknell. Patterns of Electrical activity and Hormone Release from Neurosecretory cells. In F. Labrie and L. Proulx, editors, *Endocrinology*, pages 1020–1023. Elsever, 1984.

[62] G. Leng, C. H. Brown, P. M. Bull, D. Brown, S. Scullion, J. Currie, R. E. Blackburn-Munro, J. Feng, T. Onaka, J. G. Verbalis, J. A. Russell, and M. Ludwig. Responses of magnocellular neurons to osmotic stimulation involves coactivation of excitatory and inhibitory input: an experimental and theoretical analysis. *Journal of Neuroscience*, 21(17):6967–77, Sep, 1 2001.

[63] G. Leng, C. H. Brown, and J. A. Russell. Physiological pathways regulating the activity of magnocellular neurosecretory cells. *Progress In Neurobiology*, 57(6):625–55, Apr 1999.

[64] G. Leng and D. Brown. The origins and significance of pulsatility in hormone secretion from the pituitary. *Journal of Neuroendocrinology*, 9(7):493–513, Jul 1997.

[65] G. Leng and N. Sabatier. Vasopressin and homeostasis: Running hard to stay in the same place. In R. Paton and L. Mcnamara, editors, *Multidisciplinary approaches to theory in medicine*. Elsevier, 2005.

[66] Z. Li and G. I. Hatton. Ca2+ release from internal stores: role in generating depolarizing after-potentials in rat supraoptic neurones. *J Physiol*, 498 (Pt 2):339–50, Jan, 15 1997.

[67] Z. Li and G. I. Hatton. Reduced outward K+ conductances generate depolarizing after-potentials in rat supraoptic nucleus neurones. *J Physiol*, 505 (Pt 1):95–106, Nov, 15 1997.

[68] X. Liu, W. Zhang, and T. E. Fisher. A novel osmosensitive voltage gated cation current in rat supraoptic neurones. *J Physiol*, 568(Pt 1):61–8, Oct, 1 2005.

[69] M. Ludwig. Dendritic release of vasopressin and oxytocin. *Journal of Neuroendocrinology*, 10(12):881–95, Dec 1998.

[70] M. Ludwig, M. F. Callahan, I. Neumann, R. Landgraf, and M. Morris. Systemic osmotic stimulation increases vasopressin and oxytocin release within the supraoptic nucleus. *Journal of Neuroendocrinology*, 6(4):369–73, Aug 1994.

[71] M. Ludwig and G. Leng. Autoinhibition of supraoptic nucleus vasopressin neurons in vivo: a combined retrodialysis/electrophysiological study in rats. *European Journal of Neuroscience*, 9(12):2532–40, Dec 1997.

[72] M. Ludwig, K. Williams, M. F. Callahan, and M. Morris. Salt loading abolishes osmotically stimulated vasopressin release within the supraoptic nucleus. *Neuroscience Letters*, 215(1):1–4, Aug, 30 1996.

[73] E. Marder and J.-M. Goaillard. Variability, compensation and homeostasis in neuron and network function. *Nature Reviews Neuroscience*, 7(7):563–74, Jul 2006.

[74] W. T. Mason. Supraoptic neurones of rat hypothalamus are osmosensitive. *Nature*, 287(5778):154–7, Sep, 11 1980.

[75] W. T. Mason. Electrical properties of neurons recorded from the rat supraoptic nucleus in vitro. *Proceedings of the Royal Society of London B Biological Sciences*, 217(1207):141–61, Jan, 22 1983.

[76] M. J. Mckinley, M. L. Mathai, R. M. Mcallen, R. C. Mcclear, R. R. Miselis, G. L. Pennington, L. Vivas, J. D. Wade, and B. J. Oldfield. Vasopressin secretion: osmotic and hormonal regulation by the lamina terminalis. *Journal of Neuroendocrinology*, 16(4):340–7, Apr 2004.

[77] A. E. Milne and Z. S. Chalabi. Control analysis of the Rose-Hindmarsh model for neural activity. *IMA Journal of Mathematics Applied in Medicine and Biology*, 18(1):53–75, Mar 2001.

[78] F. Moos, L. Gouzenes, D. Brown, G. Dayanithi, N. Sabatier, L. Boissin, A. Rabie, and P. Richard. New aspects of firing pattern autocontrol in oxytocin and vasopressin neurones. *Adv Exp Med Biol.*, 449:153–62, 1998.

[79] M. Muschol and B. M. Salzberg. Dependence of transient and residual calcium dynamics on action-potential patterning during neuropeptide secretion. *Journal of Neuroscience*, 20(18):6773–80, Sep, 15 2000.

[80] S. H. Oliet and C. W. Bourque. Steady-state osmotic modulation of cationic conductance in neurons of rat supraoptic nucleus. *American Journal of Physiology*, 265(6 Pt 2):R1475–9, Dec 1993.

[81] S. H. Oliet and C. W. Bourque. Osmoreception in magnocellular neurosecretory cells: from single channels to secretion. *Trends in Neurosciences*, 17(8):340–4, Aug 1994.

[82] S. H. Oliet and D. A. Poulain. Adenosine-induced presynaptic inhibition of IPSCs and EPSCs in rat hypothalamic supraoptic nucleus neurones. *J Physiol*, 520 Pt 3:815–25, Nov, 1 1999.

[83] M. A. Pitt, I. J. Myung, and S. Zhang. Toward a method of selecting among computational models of cognition. *Psychological Review*, 109(3):472–91, Jul 2002.

[84] T. A. Ponzio and G. I. Hatton. Adenosine postsynaptically modulates supraoptic neuronal excitability. *Journal Of Neurophysiology*, 93(1):535–47, Jan 2005.

[85] T. A. Ponzio, Y. F. Wang, and G. I. Hatton. Activation of Adenosine A2A Receptors Alters Postsynaptic Currents and Depolarizes Neurons of the Supraoptic Nucleus. *Am J Physiol Regul Integr Comp Physiol*, pages –, Apr, 27 2006.

[86] D. A. Poulain, D. Brown, and J. B. Wakerley. Statistical analysis of patterns of electrical activity in vasopressin and oxytocin-secreting neurones. In G. Leng, editor, *Pulsatility in neuroendocrine systems*, pages 119–154. CRC Press, 1988.

[87] D. A. Poulain and J. B. Wakerley. Electrophysiology of hypothalamic magnocellular neurones secreting oxytocin and vasopressin. *Neuroscience*, 7(4):773–808, Apr 1982.

[88] D. V. Pow and J. F. Morris. Dendrites of hypothalamic magnocellular neurons release neurohypophysial peptides by exocytosis. *Neuroscience*, 32(2):435–9, 1989. unread: don't have.

[89] A. A. Prinz, D. Bucher, and E. Marder. Similar network activity from disparate circuit parameters. *Nature Neuroscience*, 7(12):1345–52, Dec 2004.

[90] W. G. Regehr, K. R. Delaney, and D. W. Tank. The role of presynaptic calcium in short-term enhancement at the hippocampal mossy fiber synapse. *Journal of Neuroscience*, 14(2):523–37, Feb 1994.

[91] L. P. Renaud. Magnocellular neuroendocrine neurons: update on intrinsic properties, synaptic inputs and neuropharmacology. *Trends in Neurosciences*, 10:498–501, 1987.

[92] D. Richard and C. W. Bourque. Synaptic control of rat supraoptic neurones during osmotic stimulation of the organum vasculosum lamina terminalis in vitro. *J Physiol*, 489 (Pt 2):567–77, Dec, 1 1995.

[93] G. L. Robertson. Antidiuretic hormone. Normal and disordered function. *Endocrinol Metab Clin North Am*, 30(3):671–94, vii, Sep 2001.

[94] P. Roper. Frequency-dependent depletion of secretory vesicle pools modulates bursting in vasopressin neurones of the rat supraoptic nucleus. *Neurocomputing*, 65-66:485–491, 2005.

[95] P. Roper, J. Callaway, and W. Armstrong. Burst initiation and termination in phasic vasopressin cells of the rat supraoptic nucleus: a combined mathematical, electrical, and calcium fluorescence study. *Journal of Neuroscience*, 24(20):4818–31, May, 19 2004.

[96] P. Roper, J. Callaway, T. Shevchenko, R. Teruyama, and W. Armstrong. AHP's, HAP's and DAP's: how potassium currents regulate the excitability of rat supraoptic neurones. *Journal of Computational Neuroscience*, 15(3):367–89, 2003.

[97] N. Sabatier, C. H. Brown, M. Ludwig, and G. Leng. Phasic spike patterning in rat supraoptic neurones in vivo and in vitro. *J Physiol*, 558(Pt 1):161–80, Jul, 1 2004.

[98] N. Sabatier and G. Leng. Bistability with hysteresis in the activity of vasopressin cells. *Journal of Neuroendocrinology*, 19(2):95–101, 2007.

[99] N. Sabatier, I. Shibuya, and G. Dayanithi. Intracellular calcium increase and somatodendritic vasopressin release by vasopressin receptor agonists in the rat supraoptic nucleus: involvement of multiple intracellular transduction signals. *Journal of Neuroendocinology*, 16(3):221–36, Jun 1999.

[100] E. P. Seward, N. I. Chernevskaya, and M. C. Nowycky. Exocytosis in peptidergic nerve terminals exhibits two calcium-sensitive phases during pulsatile calcium entry. *Journal of Neuroscience*, 15(5 Pt 1):3390–9, May 1995.

[101] F. D. Shaw, R. J. Bicknell, and R. E. Dyball. Facilitation of vasopressin release from the neurohypophysis by application of electrical stimuli in bursts. Relevant stimulation parameters. *Neuroendocrinology*, 39(4):371–6, Oct 1984.

[102] S. J. Shuster, M. Riedl, X. Li, L. Vulchanova, and R. Elde. The kappa opioid receptor and dynorphin co-localize in vasopressin magnocellular neurosecretory neurons in guinea-pig hypothalamus. *Neuroscience*, 96(2):373–83, 2000.

[103] C. D. Sladek and J. R. Kapoor. Neurotransmitter/neuropeptide interactions in the regulation of neurohypophyseal hormone release. *Experimental Neurology*, 171(2):200–9, Oct 2001.

[104] B. L. Soldo, D. R. Giovannucci, E. L. Stuenkel, and H. C. Moises. Ca(2+) and frequency dependence of exocytosis in isolated somata of magnocellular supraoptic neurones of the rat hypothalamus. *J Physiol*, 555(Pt 3):699–711, Mar, 16 2004.

[105] J. E. Stern and W. E. Armstrong. Changes in the electrical properties of supraoptic nucleus oxytocin and vasopressin neurons during lactation. *Journal of Neuroscience*, 16(16):4861–71, Aug, 15 1996.

[106] J. E. Stern and M. Ludwig. NO inhibits supraoptic oxytocin and vasopressin neurons via activation of GABAergic synaptic inputs. *Am J Physiol Regul Integr Comp Physiol*, 280(6):R1815–22, Jun 2001.

[107] E. M. Stricker and A. F. Sved. Controls of vasopressin secretion and thirst: similarities and dissimilarities in signals. *Physiology And Behavior*, 77(4-5):731–6, Dec 2002.

[108] P. Thomas, J. G. Wong, and W. Almers. Millisecond studies of secretion in single rat pituitary cells stimulated by flash photolysis of caged Ca2+. *Embo Journal*, 12(1):303–6, Jan 1993.

[109] A. J. Vander. *Renal Physiology*. McGraw-Hill, third edition, 1985.

[110] T. Voets, E. Neher, and T. Moser. Mechanisms underlying phasic and sustained secretion in chromaffin cells from mouse adrenal slices. *Neuron*, 23(3):607–15, Jul 1999.

[111] D. L. Voisin and C. W. Bourque. Integration of sodium and osmosensory signals in vasopressin neurons. *Trends in Neurosciences*, 25(4):199–205, Apr 2002.

[112] J. B. Wakerley, D. A. Poulain, and D. Brown. Comparison of firing patterns in oxytocin- and vasopressin-releasing neurones during progressive dehydration. *Brain Research*, 148(2):425–40, Jun, 16 1978.

[113] S. Watanabe, T. Kunitake, K. Kato, C.-P. Chu, H. Nakao, D.-L. Qiu, and H. Kannan. Single-unit activity of paraventricular nucleus neurons in response to intero- and exteroceptive stressors in conscious, freely moving rats. *Brain Research*, 995(1):97–108, Jan, 2 2004.

[114] Z. Zhang and C. W. Bourque. Calcium permeability and flux through osmosensory transduction channels of isolated rat supraoptic nucleus neurons. *European Journal of Neuroscience*, 23(6):1491–500, Mar 2006.